

QE
350.2
P48

ATES
T OF
ICE
ON



NOAA Technical Report ERL 226-AOML 6

U.S. DEPARTMENT OF COMMERCE
National Oceanic and Atmospheric Administration
Environmental Research Laboratories

Geology and Geophysics of the Venezuelan Continental Margin Between Blanquilla and Orchilla Islands

GEORGE PETER

BOULDER, COLO.
FEBRUARY 1972



U.S. DEPARTMENT OF COMMERCE

Peter G. Peterson, Secretary

NATIONAL OCEANIC AND ATMOSPHERIC ADMINISTRATION

Robert M. White, Administrator

ENVIRONMENTAL RESEARCH LABORATORIES

Wilmot N. Hess, Director

NOAA TECHNICAL REPORT ERL 226-AOML 6

Geology and Geophysics of the Venezuelan Continental Margin Between Blanquilla and Orchilla Islands

GEORGE PETER

BOULDER, COLO.
February 1972

For sale by the Superintendent of Documents, U. S. Government Printing Office, Washington, D. C. 20402
Price 75 cents

TABLE OF CONTENTS

	Page
ABSTRACT	vi
1. INTRODUCTION	1
1.1 Location and planning	1
1.2 Field and laboratory methods	2
1.2.1 Navigation	2
1.2.2 Depth survey	3
1.2.3 Gravity survey	3
1.2.4 Magnetic survey	5
1.2.5 Seismic reflection survey	5
1.2.6 Rock sampling	6
1.3 Previous marine work	6
2. PHYSIOGRAPHY AND SUBMARINE GEOMORPHOLOGY	7
2.1 Caribbean physiography	7
2.2 Geomorphology of the Venezuelan margin	8
2.3 Coastal physiography	11
3. GEOPHYSICAL OBSERVATIONS	12
3.1 Seismic reflection profiles	12
3.1.1 The continental shelf	13
3.1.2 Island platforms - Los Roques Canyon	19
3.1.3 Venezuelan Basin - Curacao Ridge	27
3.1.4 Venezuelan Basin - Aves Ridge	28
3.2 Geomagnetic measurements	31
3.3 Gravity measurements	31
4. GEOLOGICAL INTERPRETATION AND DISCUSSION	35
4.1 The continental shelf	35
4.1.1 Regional geology	35
4.1.2 Discussion	41
4.2 Island platforms - Los Roques Canyon	46
4.2.1 Regional geology	46
4.2.2 Discussion	48
4.3 Southeast margin of the Venezuelan Basin	50
4.3.1 Regional geology	50
4.3.2 Discussion	51
4.4 Crustal structure of the Venezuelan continental margin	52
4.4.1 Evidence from seismic refraction data	52
4.4.2 Crustal thickness of the Venezuelan continental margin	53
4.5 Tectonic elements of the island arc	55
4.6 Regional history and development	57
4.6.1 Origin of the Caribbean Sea	57
4.6.2 Paleozoic	58
4.6.3 Mesozoic	58
4.6.4 Cenozoic	59

	Page
5. SUMMARY	59
6. ACKNOWLEDGEMENTS	61
7. REFERENCES	62
APPENDIX I	67
APPENDIX II	75
APPENDIX III	79

LIST OF FIGURES

Figure	Page
1. Location chart of study area	2
2. Survey tracklines	4
3. Physiography of the Caribbean area	7
4. Physiographic features of the north-central Venezuelan margin	9
5. Bathymetric chart of survey area	9
6. Slopes at 10:1 and 5:1 vertical exaggerations	13
7. Location of north-south profiles	14
8. Line drawing of seismic reflection profiles across continental shelf	15
9. Original seismic section of Cubagua high (Profile 7)	16
10. Original seismic section of buried terraces southwest of Margarita (Profile 5)	17
11. Copy of original seismic section of the southern part of the sill between the two deeps of the Cariaco Basin (Profile 3)	18
12. Copy of seismic section showing the central part of the western deep of the Cariaco Basin (Profile 2)	19
13. Location of east-west profiles	21
14. Line drawing of seismic reflection Profile 2 between the Los Roques Canyon and the Tortuga-Margarita Bank	21
15. Line drawing of seismic reflection Profiles 3 and 14 between the Blanquilla platform and the Tortuga-Margarita Bank	22
16. Line drawing of seismic reflection Profile 13	23
17. Copy of original seismic section showing the two different types of basements on Orchilla platform (Profile 13)	24
18. Line drawing of seismic reflection Profiles 1 and 11	24
19. Copy of original seismic section along $65^{\circ}45'W$, made by R/V CONRAD-9 (See fig. 2 for location)	25
20. Line drawing of profile 3 across the Blanquilla platform	25

	Page
21. Copy of original seismic section normal to the trends of the Blanquilla platform (See fig. 2 for location)	27
22. Line drawing of seismic reflection Profiles 12 and 10	28
23. Copy of original seismic section over the northwestern part of the Los Roques Canyon (Profile 10)	29
24. Line drawing of seismic reflection Profiles 1,2, and 3, over the southern margin of the Venezuelan Basin	29
25. Original seismic section of Profile 1, southern margin, Venezuelan Basin	30
26. Line drawings of seismic reflection Profile 8	30
27. Magnetic total intensity contour chart of the study area	32
28. Determination of the dipole field from the values of the total intensity chart along 65°00'W and 65°30'W	33
29. Magnetic total intensity anomaly map of the continental shelf off north-central Venezuela	33
30. Free-air gravity anomaly map of the study area	34
31. Bouguer gravity anomaly map of the study area	34
32. Location of two-dimensional Bouguer anomaly profiles and the regional Bouguer anomaly map	36
33. Comparison of "simple" and "two-dimensional" Bouguer corrections	36
34. Tectonic belts of the Caribbean mountains west of the Bay of Barcelona	37
35. Structural elements in northeastern Venezuela	39
36. Geologic map of the Araya Peninsula	40
37. Comparison of gravity anomalies across the eastern and western halves of the Cariaco Basin	42
38. Principal faults of the Venezuelan continental margin in the study area	44
39. Geologic map of Orchilla Island	47
40. Geologic map of Blanquilla Island	49
41. Residual Bouguer anomaly map	49
42. Composite seismic refraction section across the Venezuelan continental margin	52
43. Crustal thickness profile of the Venezuelan continental margin	54
44. Contour map of the depth below sea level to the top of the mantle	56
45. Reconstruction of Pangea at the end of Permian 225 m.y. ago	57

ABSTRACT

A study of the geology of the continental margin of northeast Venezuela was conducted by marine magnetic, gravity, seismic reflection, and bathymetric investigations, and by a program of dredging of submarine rock outcrops.

Previous surveys have established that geophysical anomalies associated with discrete tectonic elements of the Lesser Antilles Island Arc continue southwestward onto the continental shelf of Trinidad and Venezuela. This study demonstrates the extension of these tectonic elements westward to 65°W, where they either truncated or are interrupted by a major northwest-southeast trending fault system. The bordering faults of the Los Roques Canyon and the Urica and possibly the San Francisco faults form a continuous, northwest-southeast trending discontinuity, whose existence since Cretaceous time mitigates against large east-west displacements along the northeast Venezuelan margin during the Cenozoic.

Geophysical measurements indicate that west of the Urica fault the Bay of Barcelona is underlain by rocks that probably belong to the seaward extension of the tectonic belts of the western Serranía del Interior mountains. Over the island platforms these measurements indicate the presence of igneous rocks. Sampling of basement outcrops on Blanquilla platform yielded granites, granodiorites, quartz monzonites, and metabasalts. A potassium-argon age of 81 m.y. was obtained from the biotites of one granite sample, which is consistent with the ages of similar rocks dated on Curacao, Aruba, and the southern part of the Aves Ridge.

The major fault systems and the numerous minor faults offsetting the sea floor along the continental margin attest to Late Tertiary to Holocene tectonic activity, that most likely was responsible for the subsidence of several basins on the continental shelf.

GEOLOGY AND GEOPHYSICS OF THE VENEZUELAN CONTINENTAL MARGIN
BETWEEN BLANQUILLA AND ORCHILLA ISLANDS

George Peter

1. INTRODUCTION

This paper presents the results of one of a series of research projects that were initiated in 1968 by the Marine Geology and Geophysics Laboratory of the NOAA Atlantic Oceanographic and Meteorological Laboratories. The general purpose of these projects is to study the marine geology in key areas of the Caribbean through the use of systematic geo-physical surveys.

One of the most important geologic problems in the Caribbean is the nature of junction between the Lesser Antilles Island Arc and the South American continent. The acceptance of the new global tectonics hypothesis (Morgan, 1968; Le Pichon, 1968; Isacks *et al.*, 1968) as well as current studies of the Lesser Antilles Island Arc (Chase and Bunce, 1969) seem to give strength to an earlier hypothesis of Hess and Maxwell (1953) that a major east-west strike-slip (or transform) fault must exist between the island arc and the continent.

On the other hand, geophysical studies of the area of junction between the island arc and the continent (Talwani, 1966; Weeks *et al.*, 1969, 1971; Bassinger *et al.*, 1971; Lattimore *et al.*, 1971) indicate that the major tectonic elements of the arc, such as the Barbados anti-clinorium, the Tobago Trough, and the volcanic arc of the Lesser Antilles extend into the continental shelves of northeast Venezuela and Trinidad without noticeable interruption.

Tracing the structural elements of the Lesser Antilles Island Arc farther westward and establishing the relationship of these structures to the Cordillera de la Costa of Venezuela comprise the major part of the present study. In addition, the boundary of the Venezuelan Basin with the Curacao and Aves ridges, the structure of the Los Roques Canyon, the extent of the plutonic basement rock complex around the Aruba-Orchilla-Blanquilla island chain, and the extension of the major faults of the continent into the offshore area are investigated.

1.1 Location and Planning

The area selected for this study lies north of the Gulf of Barcelona, off north-central Venezuela (fig. 1). The approximate eastern and western limits are along 64°W and 66°W longitudes respectively; to the north the 13°N parallel is the approximate border.

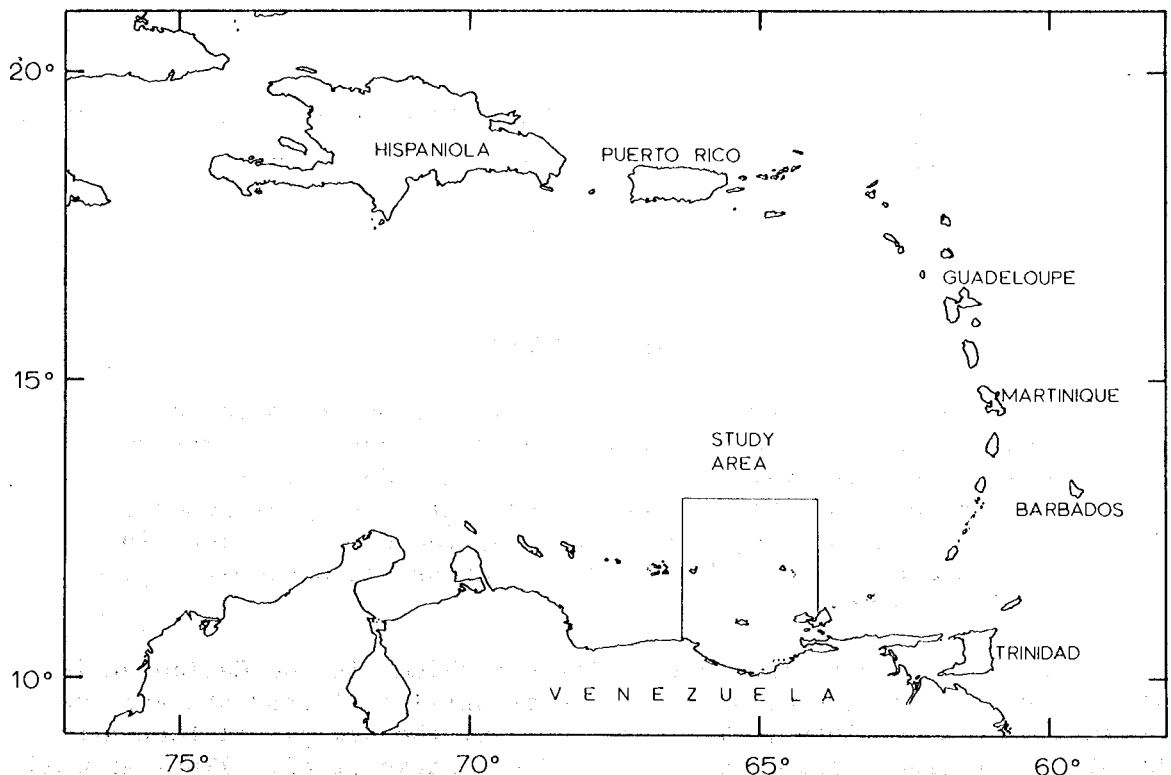


Figure 1. Location chart of study area.

Six north-south geophysical lines were laid out to cover the essentially east-west geologic trends in the southern half of the area; four north-south and four east-west lines were chosen to cover the geologic trends in the northern half.

The geological sampling program was concentrated on six potential sites, which looked promising for dredging or coring operations according to the available bathymetric information.

1.2 Field and Laboratory Methods

1.2.1 Navigation

The position of the U.S.C. & G.S. Ship *DISCOVERER* when near the islands was controlled by visual bearings during daylight and by radar range and bearings during the nights. OMEGA and star. fixes were utilized when the ship was outside radar range of the islands.

The effect of surface currents was very pronounced during seismic profiling because the speed of the ship was only 5 to 7 knots (9 to 13 km/hr). Because the strongest currents were felt in the northern half of the survey area where navigational control was marginal, the planned east-west and north-south tracklines in that area could not be followed.

The navigation was rechecked in the laboratory, and the tracklines were adjusted on the basis of the original navigation information and the repeated geophysical measurements at trackline crossings. It is estimated that the corrected position of the tracklines in the southern half of the survey is better than ± 3 km, in the northern half ± 5 km. The track between Julian Day 222, 0700 hour and Julian Day 223, 0300 hour may be in error by as much as ± 10 km (fig. 2).

1.2.2 Depth Survey

Depth soundings were taken continuously along all the tracklines with a "narrow beam echo-sounding system" that utilizes an electronically stabilized beam with an effective cone-width of approximately 3° .

The sounding records were read to the nearest fathom ($1 \text{ fm} = 1.83 \text{ m}$) at even 5 min intervals and at intermediate points where peaks, troughs, or inflection points occurred. These data were digitized, merged with the magnetic and gravity information, and were plotted by an electronic computer using the program developed by Grim (1970). The soundings are based on an assumed sound velocity of 800 fm/sec. Corrections for sea water density variations were not applied to facilitate the comparison of these profiles with the seismic sections and to make data compatible with sounding lines run by other ships.

As the sounding coverage obtained during the field survey is clearly insufficient to describe the bottom physiography, the bathymetric chart of Maloney (1966) was adopted as a base map for the area. Corrections, additions, and reinterpretations to this map were made on the basis of HO charts 6572, 6573, and 2319, BC chart 0703N, unpublished U.S. Navy charts (USOC), and the sounding data of the present survey.

1.2.3 Gravity Survey

Gravity measurements were made continuously along most of the survey lines by an Askania-Graf seagravimeter mounted on an Anschütz gyro-stabilized platform.

The gravity analog records were read to the nearest dial unit at even 5 min intervals. These data were digitized and then reduced to free-air anomalies with the aid of an electronic computer. This involved the multiplication of dial units with the instrument constant to obtain the gravity variation in milligals (mgals), the addition of the Base Gravity value (Barbados Seawell Airport $\bar{g} = 978.2997$ Gals), the correction for instrument drift (3.2 mgals in 20 days) and for the speed and heading of the ship (Eötvös correction). From the corrected data, the theoretical gravity values were subtracted to obtain the free-air anomalies. The free-air anomalies were merged with magnetic and bathymetric data and plotted in a profile form, as described previously.

The survey has twelve trackline crossings with gravity data. At five crossings the discrepancy is ± 2 mgals or less; eight are within ± 3 mgals. The other four crossings (± 11 mgals, ± 12 mgals, ± 14 mgals, and ± 17 mgals) are over areas of large gravity gradient or directly .

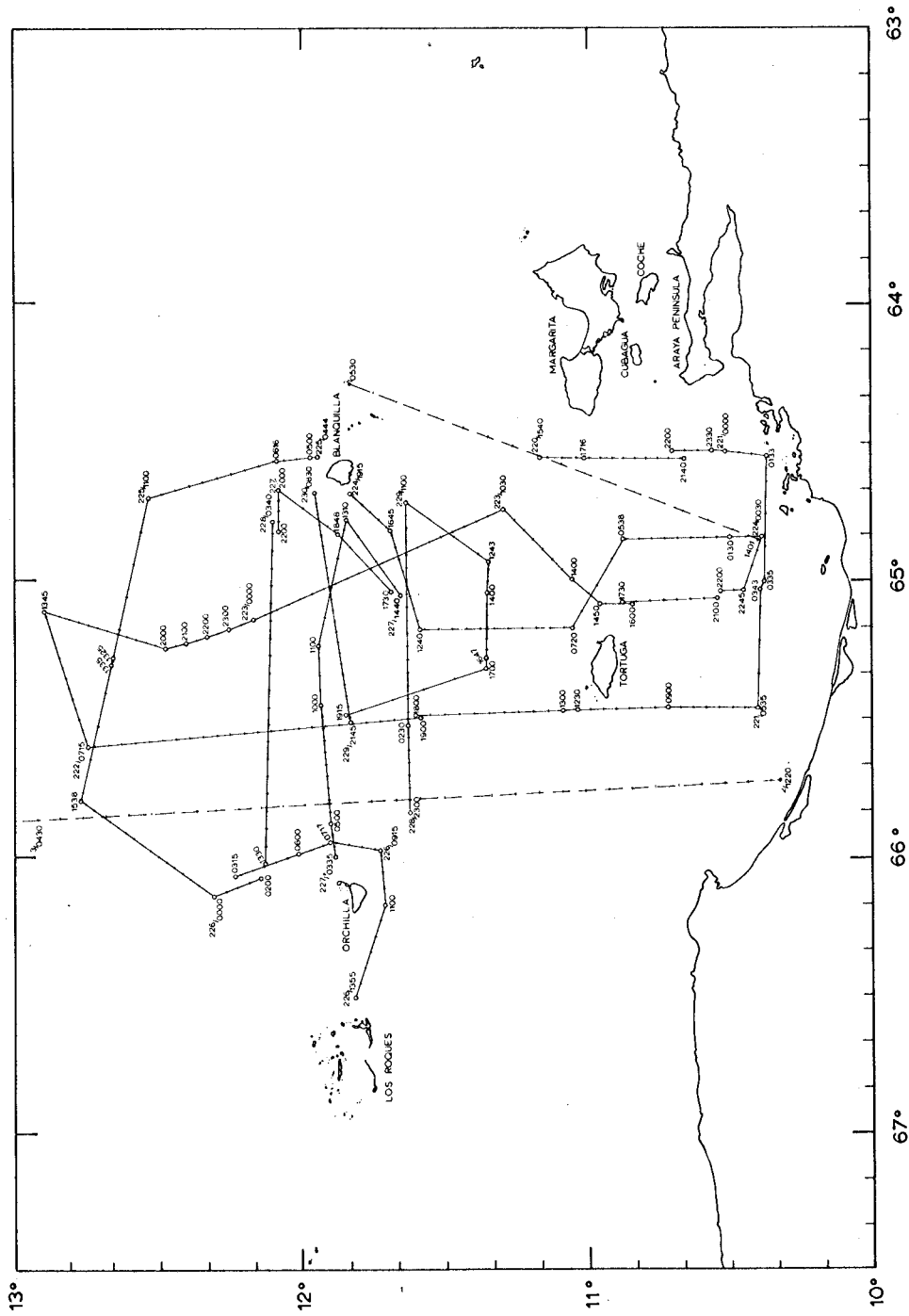


Figure 2 Survey tracklines. Solid line = ship DISCOVERER, dashed line = ship CONRAD - 9. Julian Day, hour, and minutes indicated at points of major course and speed changes. Cross-dashes are at every half-hour intervals.

involve tracklines with uncertain navigation or both. On this basis the accuracy of the gravity data is estimated to be better than \pm 3 mgals. A similar estimate is indicated from comparisons with previous data obtained by Ewing *et al.* (1957), Wollard and Rose (1963), and Ball *et al.* (1971).

1.2.4 Magnetic Survey

Continuous measurements of the Earth's total magnetic field were obtained along all the tracklines with a Varian direct-reading proton precession magnetometer, whose sensor was towed approximately 150 m behind the ship.

The total field values were read from the analog records to the nearest gamma (10^{-5} Oe.) at 5 min intervals and at intermediate points where peaks, troughs, or abrupt changes in slope occurred.

The data were digitized with the aid of an electronic computer, and the core field was removed using the International Geomagnetic Reference Field (IGRF) with a constant correction (-160 gammas) added to it. The anomalies were plotted together with the bathymetric and gravity data.

It was assumed that the magnetic influence of the survey ship on the sensor is negligible when compared to the error caused by the diurnal variation of the Earth's magnetic field. As the survey was not detailed enough to warrant it, corrections were not made for the diurnal variations. From repeated observations at trackline crossings, it is estimated that the accuracy of the magnetic data is better than \pm 25 gammas.

1.2.5 Seismic Reflection Survey

Continuous seismic reflection profiling data were obtained along the majority of the tracklines with a 40 cubic inch (656 cm^3) Bolt air gun as a sound source. An array of 10 variable-reluctance hydrophones towed approximately 30 m behind the ship served as the sensor. The gun was fired at variable intervals between 2 and 5 sec and the return signal filtered through a 20 - 320 Hz variable filter that was adjusted periodically to obtain optimum signal-to-noise ratio. The filtered signal was recorded on an Alpine wet-paper recorder at either 2 sec or 5 sec full scale.

To present a clear picture of the subbottom structures, without the inherent noise and multiple reflections, an interpretive line drawing of the seismic sections was prepared. Although it is impossible to present the true quality of the original records of these compressed scale drawings, care was taken to imitate the original records through emphasizing the reflective characteristics of the various strata. In this manner, double continuous lines represent the strongest continuous reflectors that can be traced usually for several tens of kilometers; single continuous lines, weaker but continuous reflectors; and dashed and dotted lines, either weak or discontinuous reflecting horizons. Short unoriented dashes were used for chaotic, indescernable reflections.

The seismic reflection sections were plotted against latitude or longitude, depending on the ship's heading. The vertical scale is two-way reflection time in seconds. The records are readily comparable to the other geophysical profiles in which the depths are plotted in fathoms (each interval of 400 fathoms is approximately equal to 1-sec two-way reflection time in the water column).

The capability of the seismic equipment may be judged by the fact that approximately 2 sec of subbottom penetration was obtained in 2000 fathoms of water.

1.2.6 Rock Sampling

Twelve attempts were made to retrieve bottom samples in the study area. It was considered first priority to obtain samples from outcrops of the basement (believed to be part of the plutonic rock complex known from the islands). After two successful chain bag dredge samples were obtained on the Blanquilla Island platform, six chain bag and one pipe dredge attempts on the Orchilla Island platform were unsuccessful. Similarly no rocks were recovered off the southeast tip of Los Roques Islands during another chain bag dredging attempt.

One chain bag dredge in the Blanquilla canyon brought up only hard clay. A boomerang core aimed at the outcrop of a major reflector at the eastern wall of Los Roques canyon returned empty, suggesting that the material penetrated may have been too coarse and washed out during the ascent of the sampling tube. Another boomerang core from the floor of the Los Roques canyon returned with dark layered clay.

A large unaltered sample of granitic rock from the second dredge haul west of Blanquilla canyon was dated (see Appendix III).*

The two sediment samples obtained are not described because of their locations are too far apart, and the samples lack pertinent information. A cursory examination of the hard clay sample from the chain bag dredge from Blanquilla canyon (where it was hoped to recover older sediments) indicates only shallow water reworked Foraminifera and Brachiopoda assemblages of Pleistocene and Recent age (J. Holden, personal communication).

1.3 Previous Marine Work

The geomorphology of the Venezuelan coast and margin has been studied by Maloney (1965, 1966). Heezen *et al.* (1959) and Lidz *et al.* (1969) described the regional bathymetry and sediment pattern in the Cariaco Basin and vicinity.

*Ten thin sections were prepared from the representative rock samples by the University of Miami, Rosenstiel School of Marine and Atmospheric Sciences, through the courtesy of Dr. E. Bonatti. A general identification of the rock specimens and the thin sections were made by the writer; detailed description of the thin sections were made by Mr. P. Kirch of the University of Miami, Rosenstiel School of Marine and Atmospheric Sciences (Appendix III).

The first gravity measurements were made by submarines in 1936-1937 (Ewing et al., 1957). More recent gravity data were summarized by Talwani (1966), and Bush and Bush (1969).

Results of combined geophysical studies over the southern part of the study area are published by Lidz et al. (1968) and Ball et al. (1971). Magnetic data presented by these latter authors were incorporated with those obtained during this study. Two unpublished seismic reflection profiles received through the courtesy of J. I. Ewing, Lamont-Doherty Geological Observatory, were also utilized in the interpretation.

The first seismic refraction studies of the area were made by Officer et al. (1957); summary of more recent seismic refraction and reflection results in the Caribbean is given in Edgar (1968). The seismicity of the area is described by Sykes and Ewing (1965) and Molnar and Sykes (1969).

2. PHYSIOGRAPHY AND SUBMARINE GEOMORPHOLOGY

2.1 Caribbean Physiography

The Caribbean Sea consists of three major basins; from west to east, these are the Yucatan Basin, the Colombian Basin, and the Venezuelan Basin (fig. 3). The Yucatan Basin lies between the island of Cuba

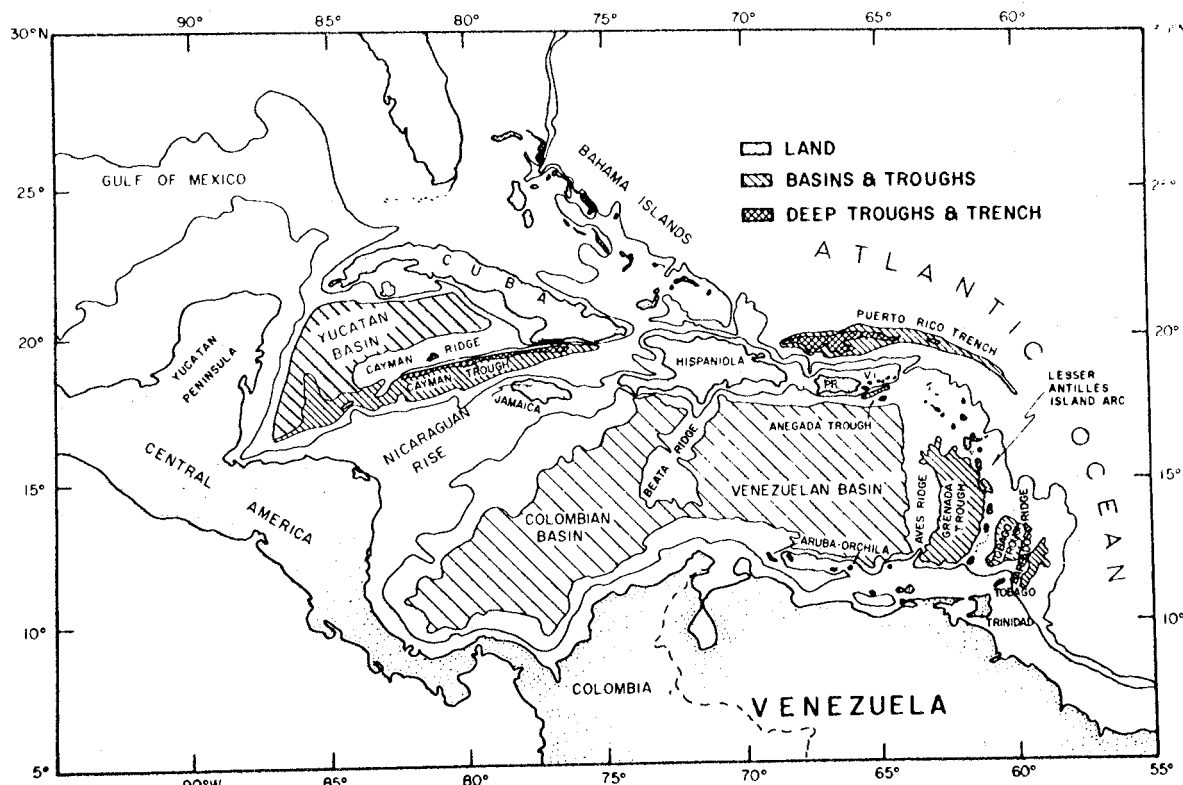


Figure 3. Physiography of the Caribbean area
(after Fink, 1968).

on the north and the Yucatan Peninsula on the west; its southern margin is formed by the Cayman Ridge and the Cayman Trough complex, which is considered to be the trace of a major fault zone (Hess and Maxwell, 1953).

South of the Cayman Trough lies the broad Nicaraguan Rise, which connects Central America with the islands of Jamaica and Hispaniola. East of this rise, the Colombian Basin extends between Panama and Hispaniola. Its eastern margin is formed by the South American continent (Colombia) and a narrow submarine ridge, the Beata Ridge.

The Venezuelan Basin is bounded by the Beata Ridge on the west and the Aves Ridge on the east; the Aves Ridge is separated from the Lesser Antilles Island Arc by the Grenada Trough.

The study area includes only the southeastern corner of the Venezuelan Basin, where the floor of the basin is essentially flat at a depth of 2630 fm. The sea floor rises gently toward the east to about 1500 fm, where an abrupt increase in gradient marks the physiographic border of the Aves Ridge.

2.2 Geomorphology of the Venezuelan Margin

The area between the shore line of the South American continent and the Venezuelan Basin is occupied by a complex system of ridges, basins, canyons, and island platforms (fig. 4).

Starting on the north, the Venezuelan Basin has a sharp southern border against the Curacao Ridge and its narrow eastward extension. This ridge is much more pronounced west of 67°W; in the study area it is only about 35 km wide and rises some 460 m over the Venezuelan Basin. Toward the east it merges with a spur of the Blanquilla Island platform (fig. 5).

The Los Roques Trench and the Los Roques Canyon lie to the south of the Curacao Ridge. The Los Roques Canyon has a flat base of 2180 fm that joins the Los Roques Trench just north of Orchilla (fig. 5). On its southern part the canyon bifurcates into narrow "V" shaped valleys that suggest active erosional processes in this area. The canyon head is not connected to any river or drainage pattern; it terminates against the Tortuga-Margarita Bank.

West of the Los Roques Canyon and south of the Los Roques Trench lie the islands of the Aruba-Orchilla chain. The southern half of Orchilla Island is flat and covered with limestone. On the northern side of the island the mountains consist of the more resistant rocks of the igneous-metamorphic complex (Schubert, 1969b). There is a north-south trending shoal east of Orchilla (Burgana Bank); between the shoal and Orchilla a northeast-southwest trending canyon parallels the trend of the northern islands.

Depth contours of the Orchilla platform are tentative; data available were inadequate to show the intricate details, especially on the eastern and southern parts of the platform where there may be other isolated highs.

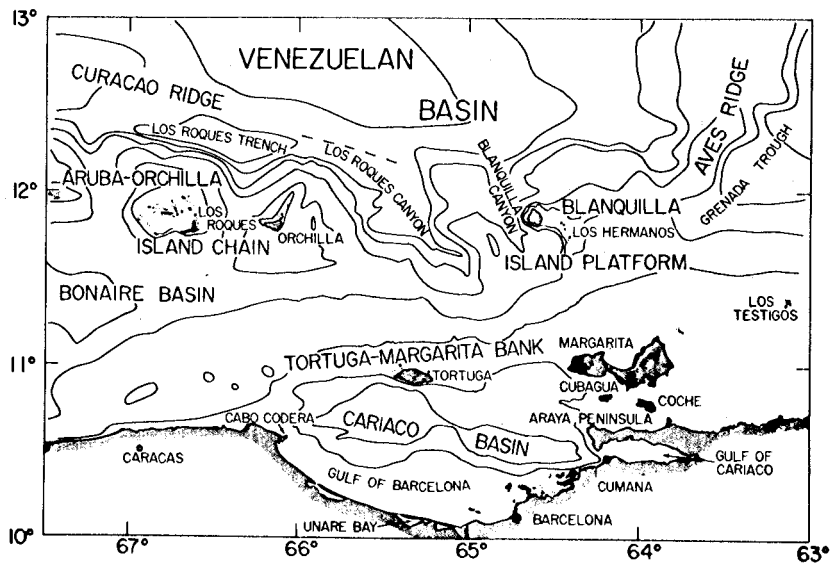


Figure 4. Physiographic features of the north-central Venezuelan margin (after Lidez et al., 1969; Maloney 1966).

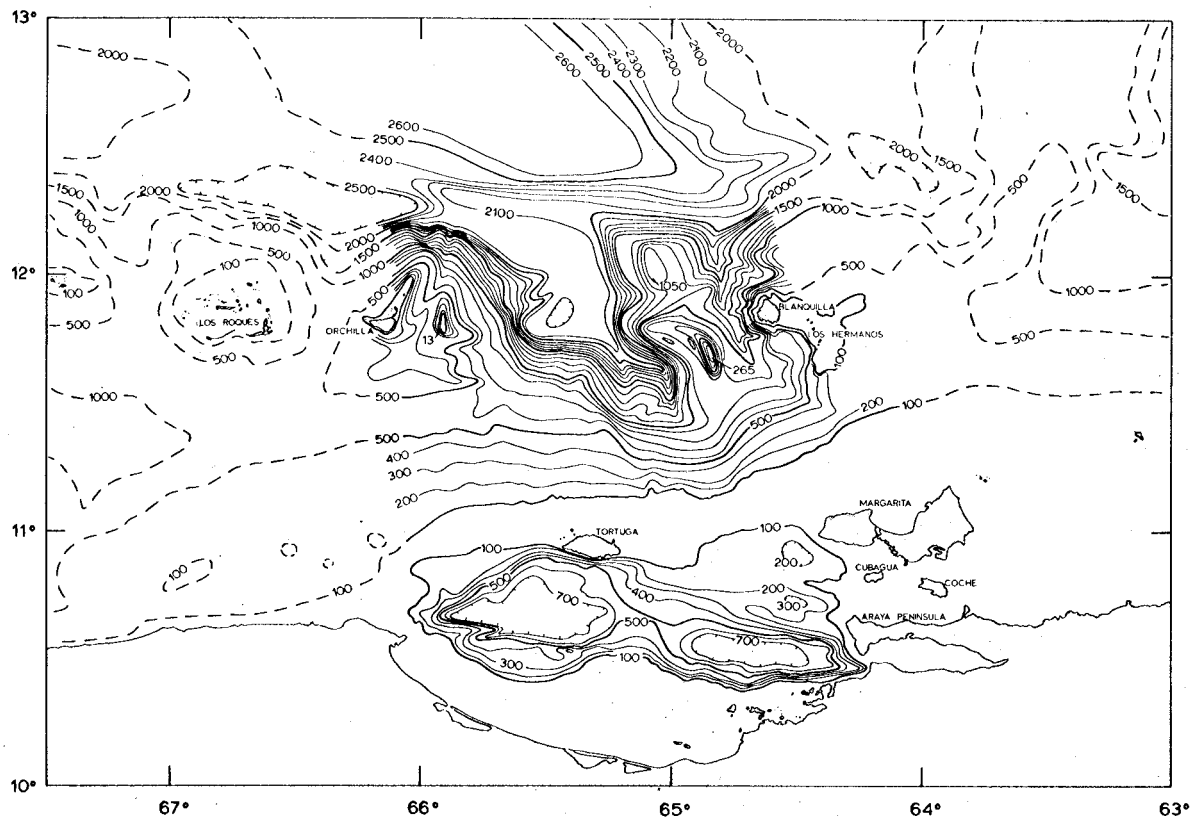


Figure 5. Bathymetric chart of survey area (revised after Maloney, 1966). Dashed contours outside of the immediate area of interest are only approximate. Contour interval 100 fm.

East of Los Roques Canyon lies the Blanquilla Island platform. The Venezuelan Basin and the west flank of the Aves Ridge form its northern border; toward the northeast it merges with the Aves Ridge. East of the Blanquilla platform the Grenada Trough extends southwestward and separates the platform from the Venezuelan shelf.

The Blanquilla platform is divided by a northwest-southeast trending canyon, here named the Blanquilla Canyon. In the western half of the platform the highest elevation is a northwest-southeast trending ridge that rises to 265 fm (fig. 5). It has a west-northwest trending spur that projects into the wall of the Los Roques Trench. A gentle depression separates this ridge from a broad topographic high on the north that reaches only to 1050 fm.

The northern half of Blanquilla Canyon is "V" shaped suggesting erosion, while the center part has a basin-like appearance (Maloney, 1966); farther south the head of the canyon is once again narrow and "V" shaped. It gently curves southeast into the depression between the Venezuelan shelf and the Blanquilla platform.

The major island on the platform is Blanquilla, which is a flat island covered mostly by limestone (Maloney, 1968). A string of islands southeast of Blanquilla, called the Los Hermanos, are sharp peaks of protruding basement rocks (Schubert, 1969a).

The 100-fm line representing the edge of the Venezuelan shelf is 95 km north of the Araya Peninsula (fig. 5). The shelf break has an overall west-southwest trend and comes within 5 km of the shore line west of Cabo Cordera (see fig. 4). West of Cabo Codera to 68°20'W, the shore line of Venezuela reflects the same west-southwest trend. As the Aruba-Orchilla island chain trends west-northwest, the distance between the shore and the island chain increases westward. The space created by the diverging trends of these two topographic elements is occupied by the Bonaire Basin.

Southwest of Margarita, the broad shelf is depressed into a major, deep basin, the Cariaco Basin. It is divided by a sill into two deeps of almost equal length and depth (fig. 4). The width of the western deep is nearly twice that of the eastern deep; however, with two smaller basins to the north, the eastern deep matches the width of the western deep. One of the small basins is located northwest of the Araya Peninsula, and the other is southwest of Margarita. The two basins are separated by a small ridge that appears to be in alignment with the Island of Cubagua. To the south, another ridge that appears to be in alignment with the Araya Peninsula separates these basins from the eastern deep (fig. 5).

An 100 fm line encloses the three basins and forms the southern boundary of a flat-topped ridge between Cabo Codera and Margarita. Following the definition of Ball *et al.* (1971), this ridge is referred to as the Tortuga-Margarita Bank (see fig. 4).

Shepard and Emery (1941), Maloney (1966), and Lidz *et al.* (1969) described the Venezuelan shelf between Margarita and Curacao as a continental borderland. The writer believes that the Los Roques Trench and the Aruba-Orchilla island chain are independent of the structural

framework of Venezuela and should not be termed a part of a continental borderland.

As the present study suggests, the geologic trends of the continent extend into the area south of the Tortuga-Margarita Bank which, therefore, may be termed a borderland; however, the Tortuga-Margarita Bank is a simple feature and forms an uninterrupted part of the shelf both to the east of Margarita and to the west of Cabo Codera. For these reasons the writer prefers to call the northern border of the Tortuga-Margarita Bank a "shelf edge" and the Cariaco and other basins of the area "depressions" within the continental shelf.

The area south of the Cariaco Basin is occupied by the Gulf of Barcelona (fig. 4). Between the two deeps of the Cariaco Basin this part of the shelf is approximately 40 km wide and has a gentle northward gradient with water depths ranging between 20 and 50 fm.

To the west, the distance between the shore line and the basin narrows to 20 km; to the east, the basin nearly merges with the shore line at Cumana (Maloney, 1966).

2.3 Coastal Physiography

Following the description of Maloney (1965), the Venezuelan coast in the study area can be divided into mountain front, lagoonal, and ria coasts. The best example of the mountain front coast lies west of Cabo Codera, where the Cordillera de la Costa mountain range reaches a height of 2765 m north of Caracas (fig. 4). Elevations are much more subdued along the Cordillera de la Costa Oriental on the Araya-Paria Peninsula, where at the western end of the peninsula mountains reach only 300 m. Toward the east along the peninsula the mountains rise as high as 600 m, and exposures of the more resistant rocks of the Carupano Formation are present (Schubert, 1971).

The coastline along the Cordillera de la Costa is quite straight and probably controlled by a system of normal faults (Dengo, 1953; Morgan, 1967; Lattimore *et al.*, 1971). There are numerous raised terraces and beaches that suggest Holocene tectonic activity of these regions (Maloney, 1965).

A lagoonal coast exists between Cabo Codera and Barcelona and around Cumana (fig. 4). In both areas large rivers enter the Caribbean Sea, transporting sediments to the coast. There are sand beaches, lagoons, and mangrove swamps along the coast with occasional sand bars and tombolos.

The ria coast lies between Barcelona and Cumana (fig. 4). In this area numerous offshore islands lie along east-west structural trends that are traceable onshore (Von der Osten, 1955, 1957). Steeply dipping Lower Cretaceous limestones form sharp cliffs on several of the islands (Rod and Maync, 1954). The drowning of the ria coast was mainly the result of the Holocene rise of sea level, but Recent tectonic uplift and subsidence could also have played an important role in forming the topography (Von der Osten, 1955).

East of Cumana, between the mainland and the Araya Peninsula, lies the Gulf of Cariaco. It is another structural depression lying at the eastern extension of the Cariaco Basin. According to Maloney (1965), the coastal landforms of the gulf are mostly of the drowned river type.

3. GEOPHYSICAL OBSERVATIONS

3.1 Seismic Reflection Profiles

Seismic reflections indicate a change in the acoustic impedance of the rocks caused by variations of lithology, density, porosity, and other factors. The depth of penetration and the resolution of individual horizons are functions of the output energy and frequency of the sound source and the acoustic impedance of the underlying rocks.

The seismic equipment used for this survey can distinguish only those impedance changes, which involve strata that are at least 10 to 20 m thick. Portions of the seismic records that are characterized by numerous conformable reflectors, therefore, are interpreted as "well stratified" or "massively stratified" sediments. Those parts of the seismic record that are devoid of discernible reflectors are interpreted as "acoustically transparent" sediments and may possess fine scale stratification.

The major faults are indicated on the line tracings with solid lines. The direction of motion along the faults can be inferred from the attitude of the displaced beds, the dip changes, and the direction of offsets of the sea floor.

As the effective speed of the ship varied along each seismic reflection line, the vertical exaggeration of each tracing is different. On the average it is between 10:1 and 5:1. This gives a false impression of the actual relief, angle of slopes, and subbottom penetration (fig. 6).

The vertical exaggeration of the topographic relief which is given on the tracings of the seismic records is based on the assumption that the velocity of sound in sea water is 800 fm/sec (1460 m/sec). The vertical exaggeration for subbottom slopes is approximately 30% less, because of the higher velocity of the sound in the sediments. As a first approximation, each second of penetration can be equated with 1 km of depth below the sea floor, based on the range of 1.9 km/sec to 3.0 km/sec velocities measured in the sediments of this area (Officer et al., 1957; Edgar, 1968).

Dip of reflectors always means "apparent dip", that is dip related to the plane of the seismic section discussed. The true dip of the sedimentary beds cannot be determined without additional control lines, which in most cases are not available.

Side echoes commonly occur when flat parts of the sea floor join steep slopes. The reflector that in this case may extend the slope below the flat surface may not be real, because the reflection could be from the side instead of the buried part of the slope. Cross-over reflections and parabolic echoes are good indicators of side echoes, but

these are not always present. Reflections from features on either side of the seismic line often appear as if these were directly under the profile; these also rarely can be identified without additional information.

The seismic records are discussed in relation to four key morphologic areas: (1) the continental shelf; (2) the island platforms and the Los Roques Canyon; (3) the Venezuelan Basin and the Curacao Ridge; and (4) the Venezuelan Basin and the Aves Ridge. A brief description of the salient features of the line tracings is given for each area.

3.1.1 The Continental Shelf

Seismic reflection records discussed in this section cover the area between the Tortuga-Margarita Bank and the Gulf of Barcelona: Profiles 7 and 5 cross the eastern deep of the Cariaco Basin and the adjacent basins to the north; Profile 3 is across the sill that separates the eastern and western Cariaco Basin deeps, and Profile 2 is across the western deep (fig. 7).

Profile 7 is located near the islands of Margarita and Cubagua and the Araya Peninsula (fig. 8). The westward extension of these features is clearly visible on this record. South of Margarita, sediments on the flank of a buried anticline (at $10^{\circ}55'N$), the Punta Arenas High (Ball et al., 1971), dip toward the north. These are overlain unconformably by younger, southward dipping sediments derived from the Tortuga-Margarita Bank.

The westward extension of Cubagua at $10^{\circ}50'N$ appears as an anticline on Profile 7, although the north dipping normal faults separating it from the Punta Arenas High might indicate a fault origin of this

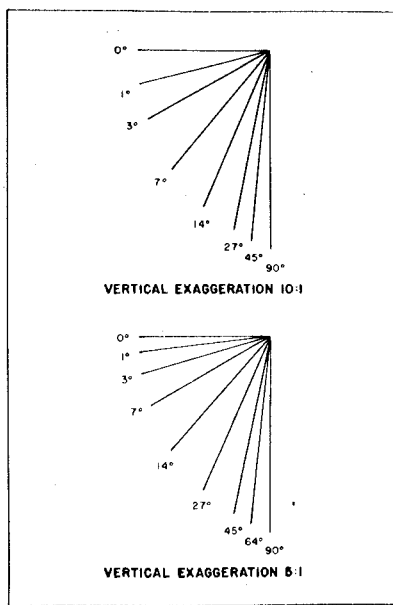


Figure 6. Slopes at 10:1 and 5:1 vertical exaggerations.

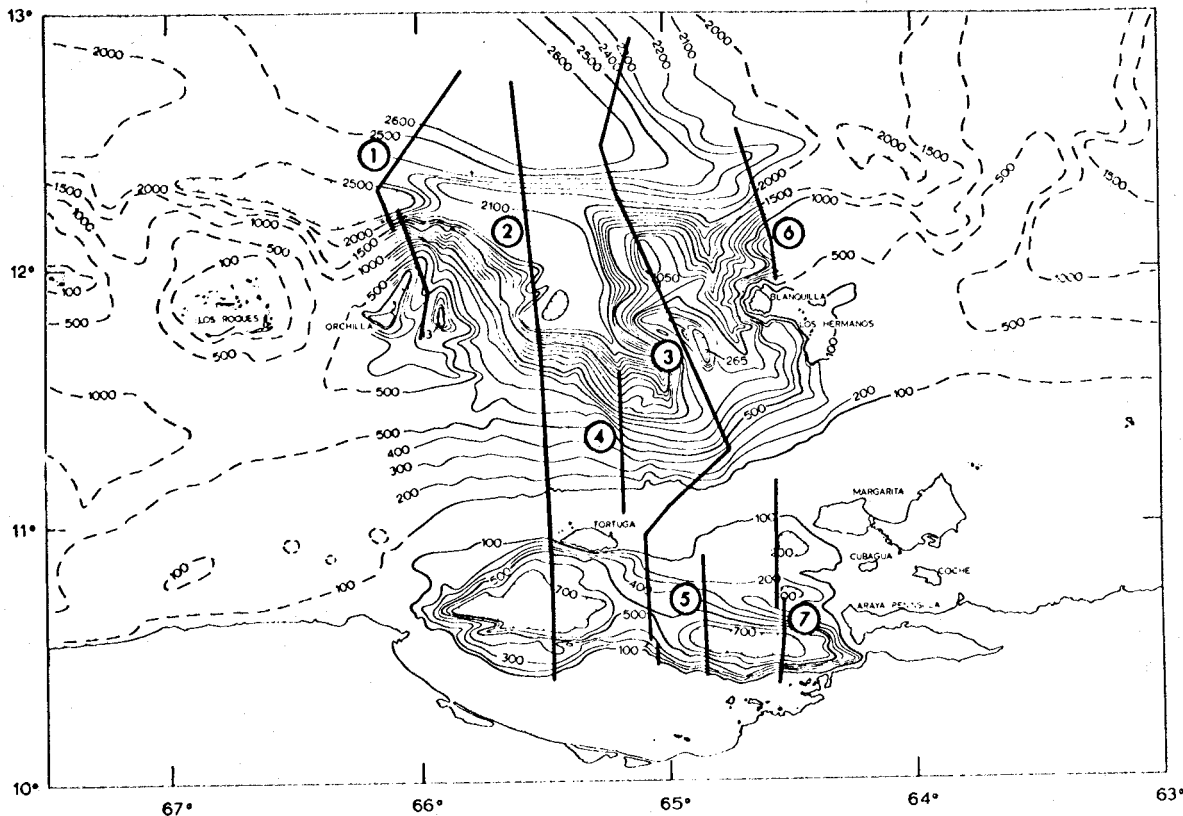


Figure 7. Location of north-south profiles.

feature (Ball *et al.*, 1971). Some of the beds near the crest of the Cubagua anticline are tightly folded and possibly thrust-faulted (fig. 9). These beds can be traced southward into a basin, and then up and across several faults on the northern flank of a horst block ($10^{\circ}40'N$), here named the Araya block.

Beds dip southward on the top of the Araya block, but down on its southern flank reflections become chaotic with no indication of bedding until the base of the block is reached. A major fault contact may be traced beneath the sediments of the southern flank.

The Cariaco Basin south of the Araya block can be divided into a northern half that is underlain by the downfaulted sediments (or metamorphics) of the Araya block and a southern half, which is a deep trough, filled with at least 700 m of sediments. The sediments of the southern half thicken northward and are ponded against a fault contact that separates the two halves indicating that subsidence has been greater along this fault than along the southern border of the basin.

The seaward extension of the El Pilar fault coincides with the southern wall of the Cariaco Basin (Ball *et al.*, 1971). On this seismic section (Profile 7) the El Pilar fault appears as a steep slope (near 30°). The lack of penetration may suggest that this slope is underlain by dense rocks, although some of the energy could have been dissipated because of the steepness of the slope.

Profile 5 is located 35 km west of Profile 7. On the north it terminates on a broad terrace that lies at the westward extension of the basin southwest of Margarita. Below the sediments of the terrace, several nearly horizontal reflectors mark prograded scarps, the deepest of which is located 300 m below the sea floor. If these at one time were at surf-base, they suggest a 600 m subsidence of the area (fig. 10).

The terrace terminates at a normal fault, that with the other faults immediately to the south suggest recent tectonic activity. The beds of the downthrown blocks dip into the fault plane and thicken with depth, indicating that sediment deposition was concurrent with the motion along the faults.

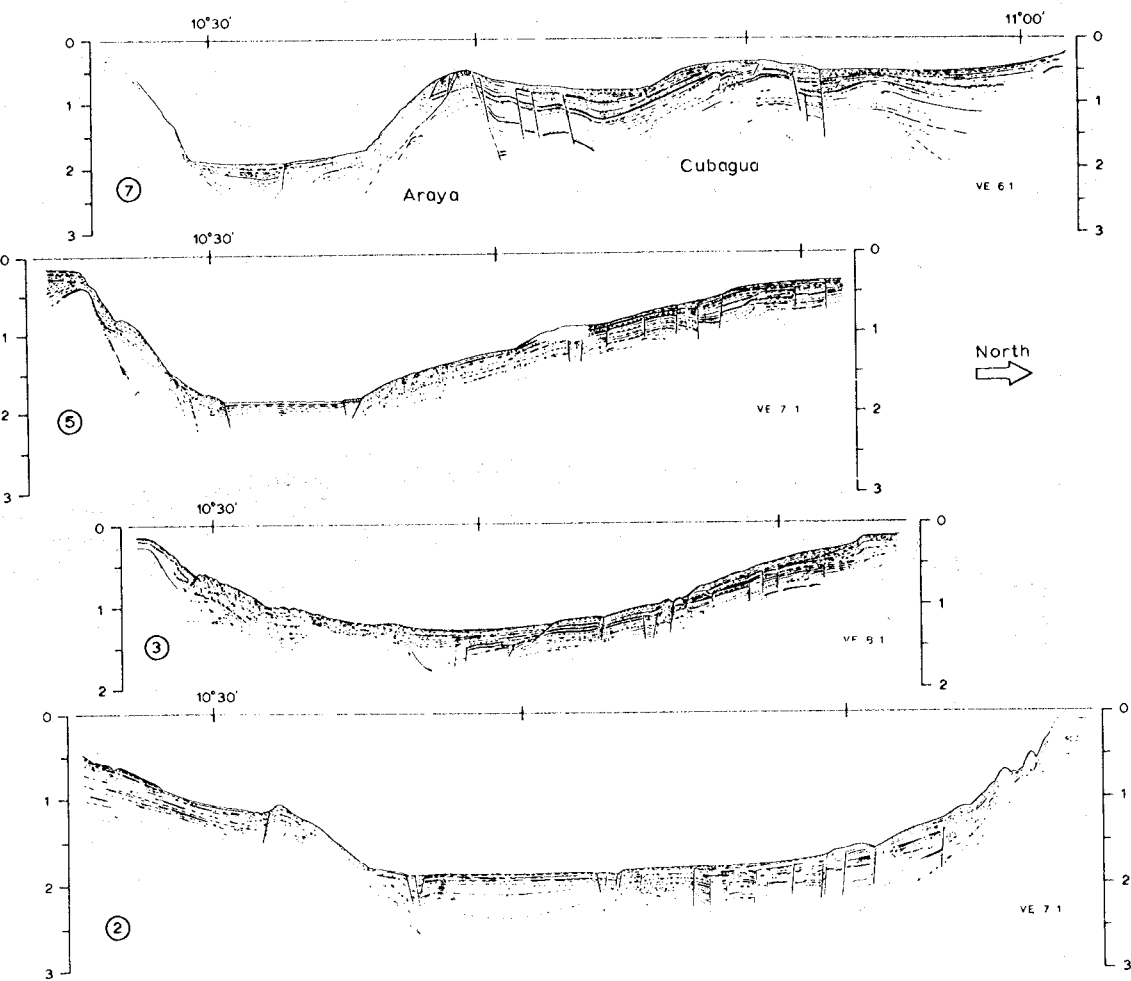


Figure 8. Line drawings of seismic reflection profiles across the continental shelf.

At $10^{\circ}42'N$ the upper part of the record is missing, but 200 m below the sea floor two faults are seen that border a zone of incoherent reflections. Based on the extension of trends from Profile 7, this fault zone may mark a near-surface expression of the faults associated with the northern border of the Araya Block; the fault contact between the Cariaco Basin sediments and the incoherent reflectors at $10^{\circ}36'N$ (Profile 5) may represent its southern margin.

In Profile 5, only about 150 m of well stratified sediments are detected in the Cariaco Basin; below these the sediments are acoustically transparent. There is a small reverse fault at the northern edge of the basin, and the sediments, instead of forming a pond (as to the east in Profile 7), are arched upward in the middle of the basin. This could be caused by compression, or the sediments may be thickening into the boundary faults and form a broad fault anticline, as suggested by Ball et al. (1971).

Beyond the southern boundary fault there is a gentle rise underlain by at least 300 m of sediments. There is some indication of stratification within these sediments, but it is discontinuous and suggestive of slumping. The slope becomes steeper at another fault contact, and the sediments that lie below this part of the slope (at least 200 m) also appear to be broken up by slumping. Just below the shelf break

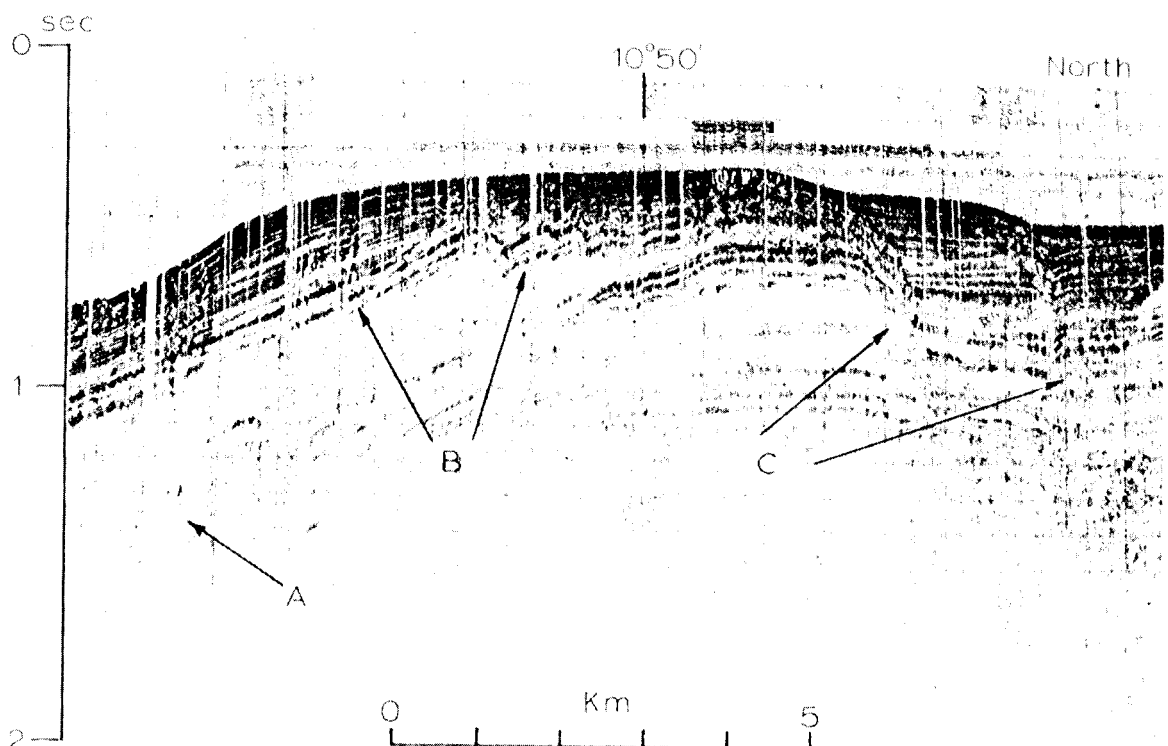


Figure 9. Copy of original seismic section of the Cubagua anticline (Profile 7). Arrows: A, multiples; B, thrust faulted (?) and folded strata; C, major normal faults.

there is a strong reflector that parallels the slope, but at the shelf break it dips to the south under the flat shelf. It is covered conformably with layered sediments to about 150 m below the shelf. At this depth there is an unconformity, followed by a sequence of horizontally bedded sediments.

Profile 3 (fig. 8) is across the sill that separates the eastern and western deeps of the Cariaco Basin. On the northern half of the profile approximately 350 m well-stratified sediments were penetrated, with major disconformities at 70 m and 150 m. Below 350 m there is a possible unconformity, beneath which steeper, southward dipping reflectors are seen. The upper 150 m of the sediments south of the shelf break show foreset bedding; below 150 m, there are several faults with small vertical displacements. At $10^{\circ}47'N$ there is a major fault along which the sediments of the slope are downfaulted by 150 m. Minor folding or slumping is associated with this fault.

At $10^{\circ}37'N$ the well stratified sediments of the northern slope abut against broad folded rocks that are characterized by mostly incoherent internal reflectors (fig. 11). South of the folded rocks, the

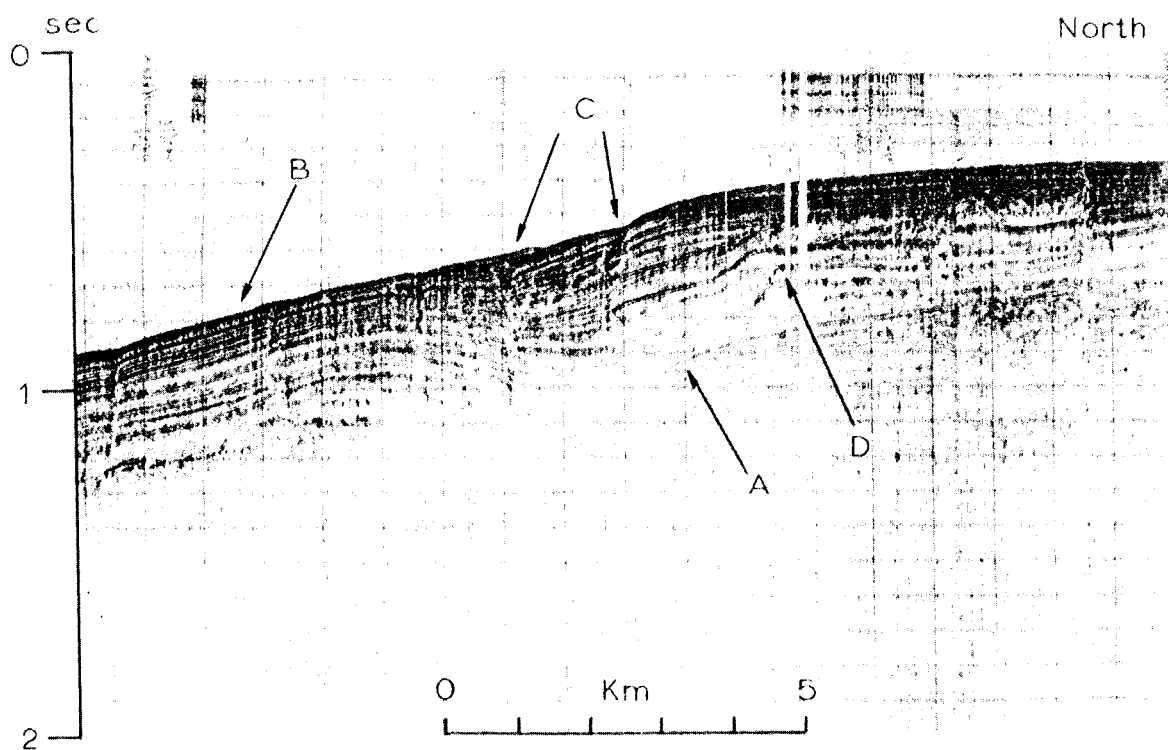


Figure 10. Copy of original seismic section of buried terraces southwest of Margarita (Profile 5). Arrows: A, multiples; B, stratified sediments; C, faults related to the Cubagua high (?); D, prograded scarps.

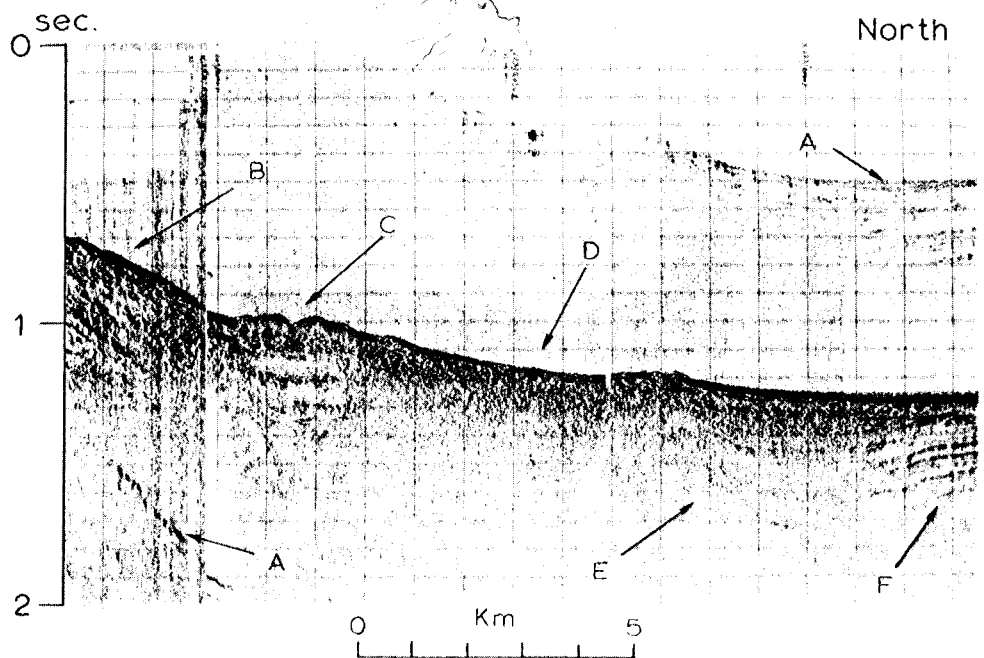


Figure 11. Copy of original seismic section of the southern part of the sill between the two deeps of the Cariaco Basin (Profile 3). Arrows: A, multiplies; B, stratified slope sediments; C, buried canyon with small channel on top; D, competent rocks; E, arch; F, stratified sediments.

southern slope of the sill is underlain by the rocks with similar reflective characteristics. At $10^{\circ}33'N$ there may be a 600 m deep filled-in canyon. Its top is occupied by either sediment slumps, or a small leveed channel.

The southern slope is underlain by approximately 300 m of well stratified sediments with large slumps at $10^{\circ}30'N$. About 600 m below the surface of the slope in this area a horizontal reflector indicates a major unconformity. To the south, sediments on the slope return only incoherent reflections that may also be the result of slumping. There is a major acoustic basement type reflector 150–200 m below these sediments.

Profile 2 crosses the western deep of the Cariaco Basin. South of the sharp shelf break of the Tortuga-Margarita Bank, the hummocky bottom and the incoherent reflections may indicate large slump blocks, although it is equally possible that these reflections represent more competent rocks that plunge below the softer sediments to the south.

From near the base of the slope to approximately $10^{\circ}45'N$, several normal faults of small displacement offset the well stratified sediments. The faults at $10^{\circ}45'N$ appear to be related to a broad arch, centered at $10^{\circ}43'N$ (fig. 12), which divides the western deep of the Cariaco Basin into two halves. The northern half of the western deep is characterized by a sequence of well stratified and faulted sediments. Recent uplift of the arch is suggested by the approximately 40 m higher elevation of

the sea floor over the arch and by a graben located directly to the south of it. The elevation is obscured, because the fault scarp north of the arch (also 40 m high) is buried by sediments that ponded behind it.

In the southern half of the western deep the sediments are not as well stratified and are devoid of internal faults. The only faults in this half of the deep are near $10^{\circ}37'N$, where they form a small graben and a fault anticline near the southern wall of the deep. Below 500 fm, reflections under the southern wall are incoherent, most likely because of the reflective characteristic of the rocks, and not because of slumping. Above 500 fm the slope is underlain by well stratified sediments with numerous large slump blocks at $10^{\circ}28'N$. The promontory at $10^{\circ}32'N$ is the result of faulting and relative uplift of the more competent rocks of the lower slope.

3.1.2 Island Platforms - Los Roques Canyon

Seismic reflection profiles of this area are discussed in relation to the major physiographic provinces. For the identification and location of the seismic sections figure 7 and figure 13 are used.

Profile 14 and segments of Profile 2 and Profile 3 illustrate the subbottom structure between the Tortuga-Margarita Bank and the island platforms.

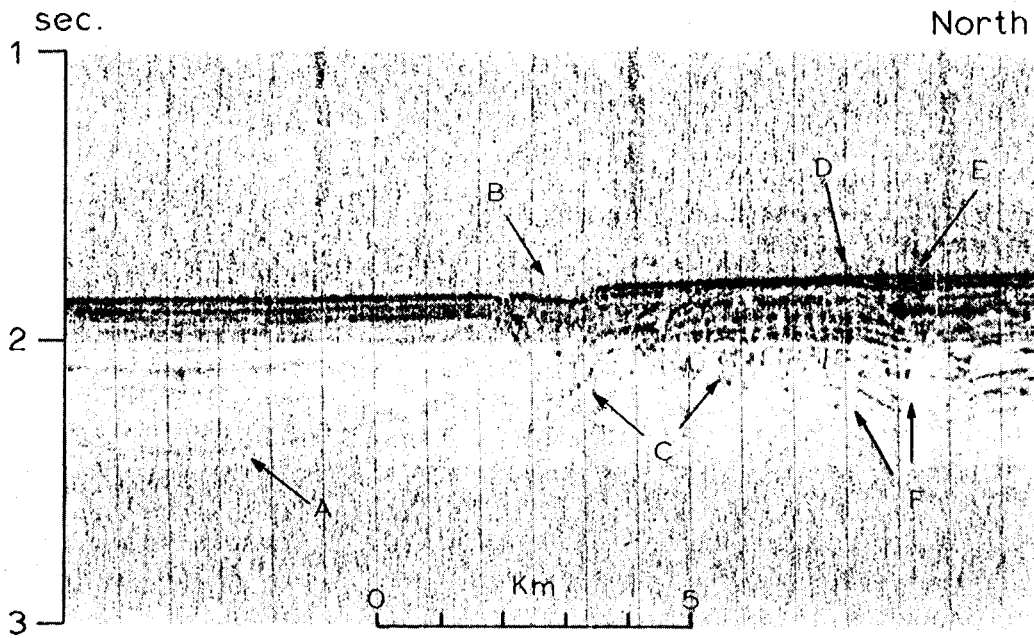


Figure 12. Copy of seismic section showing the central part of the western deep of the Cariaco Basin (Profile 2). Arrows: A, southern half of basin; B, graben; C, arch; D, buried northern scarp; E, sediment pond; F, faults north of the arch.

The sediments on the northern slope of the Tortuga-Margarita Bank are well-stratified (Profile 2) and are virtually undisturbed by faults (fig. 14). The only faulting in the section is related to a buried ridge at $11^{\circ}13'N$ that arched the lower half of the stratified sediments. The upper 300 m of the well-stratified sequence in the middle of the shelf appears to pinch out near this ridge on the south, and near to another high at $11^{\circ}36'N$, next to the southern wall of the Los Roques Canyon. Reflectors that characterize this second high have crescent-shaped side echoes and incoherent internal reflections. For convenience of presentation these reflectors are described as "acoustic basement", because of their wide distribution throughout the area of the platforms and the canyon. These can be distinguished from the smooth, coherent basement reflectors that usually form dome-shaped structures and are referred to as "granitic" basement.

In the southern end of Profile 3 (fig. 15) there are several sequences of foreset bedding near the shelf break of the Tortuga-Margarita Bank. These overlie a gently northward dipping unconformity 200 m below the sea floor. Below the unconformity the dip of the beds is steeper and increases northward to $11^{\circ}15'N$, where a major fault uplifted the section to the north. Although the deeper beds are not seen in the immediate area of the major fault, the sense of displacement is clearly indicated by the offsets of the sea floor and by the sense of displacement and drag of the upper 300 m sediments along some of the auxiliary faults. These faults lie along the extension of the eastern wall of the Los Roques Canyon and strongly suggest that recent motions took place along this wall.

Approximately 400 m of well stratified sediments cover an unconformity directly north of the major fault and continue down-slope and over the Blanquilla platform. The numerous small faults within the well stratified sequence seem to be related to basement highs, indicated by the arched sediments below the well stratified group.

Profile 14 (fig. 15) is oriented east-west, parallel to the slope of the Tortuga-Margarita Bank. The eastern half of the section shows a 700 m thick, well stratified sequence that becomes gently folded west of $65^{\circ}02'W$, and faulted at $65^{\circ}06'W$. The fault contact lies at the extension of the western branch of the Los Roques Canyon, suggesting again recent motions and tectonic control for the formation of the canyon.

Profile 13 crosses the southern part of the Los Roques Canyon and the Orchilla and Blanquilla platforms (fig. 16). West of the canyon on the Orchilla platform two "granitic" basement domes are shown: One is at $65^{\circ}53'W$, the other at $65^{\circ}38'W$. This section crossed only the northern flank of the first dome; it appears as a prominent feature, forming an 80 fm high outcrop on the sea floor on a north-south seismic reflection line. The second dome is flanked on the east by the rough acoustic basement (fig. 17) that was noted in this area also on the north-south crossing of Profile 2. Between the two domes approximately 600 m of well stratified sediments overlay acoustically transparent sediments that are at least that thick.

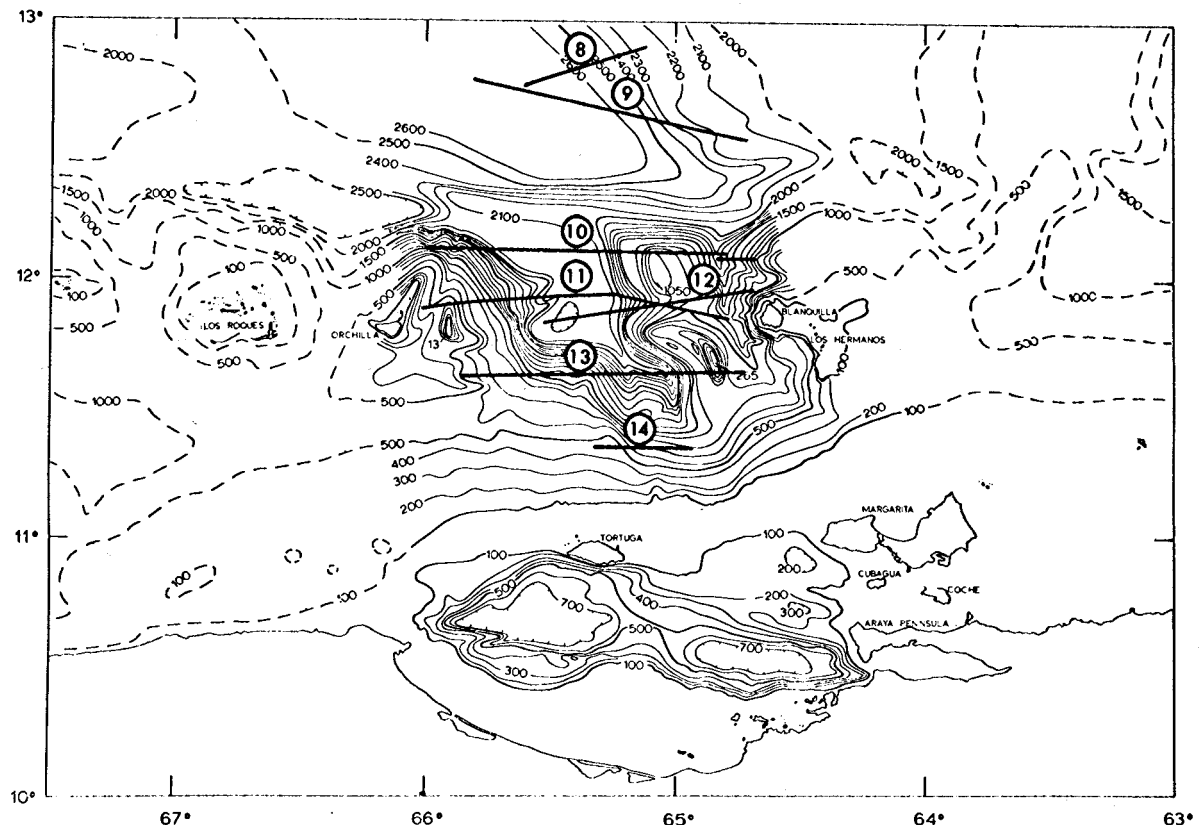


Figure 13. Location of east-west profiles.

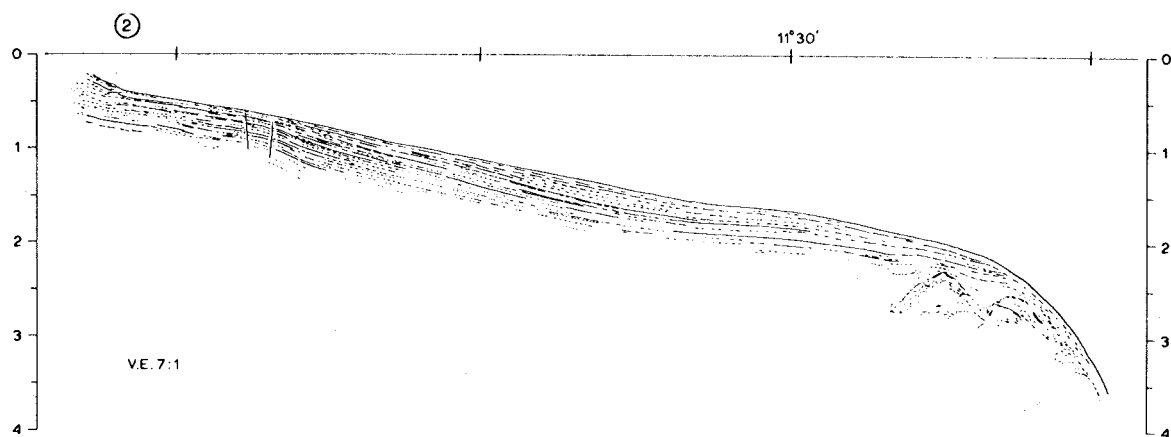


Figure 14. Line drawing of seismic reflection Profile 2 between the Los Roques Canyon and the Tortuga-Margarita Bank.

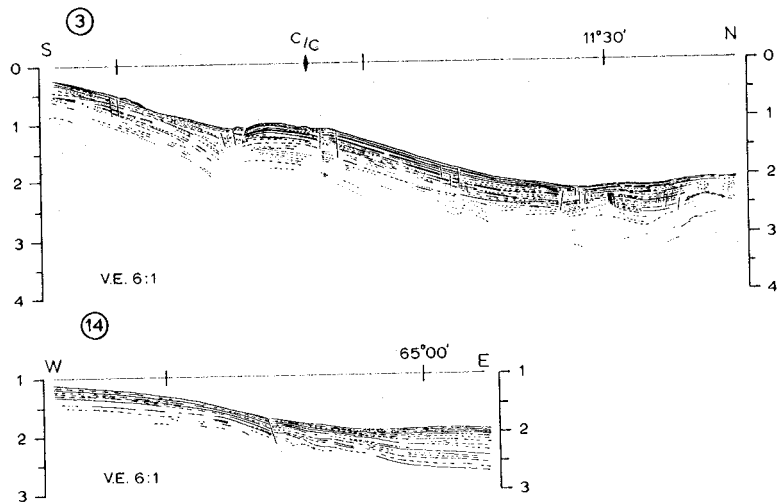


Figure 15. Line drawing of seismic reflection Profiles 3 and 14 between the Blanquilla platform and the Tortuga-Margarita Bank.

To the east at 65°30'W the acoustic basement is only 150 m below the sea floor, and the stratified sequence is missing. East of 65°25'W approximately 250 m of acoustically transparent sediments cover the basement that outcrops in the wall of the Los Roques Canyon.

Both branches of the Los Roques Canyon are carved into the unit that comprises the rough acoustic basement; on the eastern wall of the canyon these rocks outcrop at depths greater than 1,100 fm. Between 1,100 fm and 800 fm the well stratified sequence of the Blanquilla platform is truncated at the canyon wall. At 64°50'W the granitic basement rises above the surrounding sea floor and forms a major ridge.

The topography of the sea floor is closely controlled by the basement west of the canyon. Although clear fault contacts are not seen, one may infer that the step-like changes of the sea floor at 65°35'W and at 65°25'W, and the western branch of the canyon may represent faulting.

Profile 11 and Profile 1 illustrate the subbottom structure of the Orchilla platform (fig. 18). The western end of Profile 11 is over a depression east of Orchilla Island, where more than 600 m of acoustically transparent sediments and 300 m of well stratified sediments cover the "granitic" basement. This basement outcrops at 65°55'W along the northern extension of the Burgana Bank. Basement type reflectors underlie the entire platform. The eastern limit of the "granitic" type

basement is $65^{\circ}46'W$; farther to the east the character of the reflectors suggest the presence of the acoustic basement. The scarps at $65^{\circ}40'W$ and $65^{\circ}35'W$ and the sediment-basement contact at $65^{\circ}30'$ most likely represent the fault borders of the Los Roques Canyon.

Another seismic reflection line over the eastern Orchilla platform was made by the R/V CONRAD-9 (fig. 19). Some of the features that were discussed in connection with Profile 2, Profile 13, and Profile 11 are shown better on that north-south crossing (see also p. and fig. 14 and fig. 16).

The structure of the central and northern parts of the Orchilla platform is shown on Profile 1. A major "granitic" basement outcrop dominates this section at $12^{\circ}00'N$, at the extension of the trend of the islands north of Orchilla. The basement high directly to the south of this outcrop is probably another "granitic" dome, but further south the acoustic basement type reflectors probably represent lower density rocks.

At $11^{\circ}45'N$ the broad subbottom arch exhibits internal stratification suggestive of sedimentary rocks. To the north, the acoustic basement outcrops at $12^{\circ}07'N$ and apparently forms the northern slope of the Orchilla platform.

A part of Profile 3 crosses the western half of the Blanquilla platform (fig. 20). The dominant feature here is the "granitic" basement ridge whose western spur is crossed by this section. Approximately 600 m of stratified sediments are present on both sides of the "granitic" ridge; rough, acoustic basement-type reflectors are seen at the edges of the broad high to the north. On the top of the high, about 300 m of stratified sediments are present that seem to pinch out farther to the north as the rocks of the acoustic basement approach the northern slope.

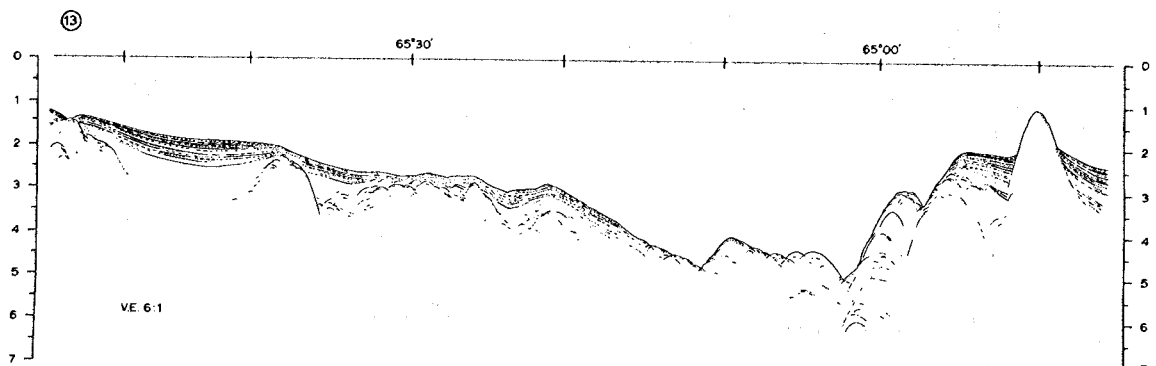


Figure 16. Line drawing of seismic reflection Profile 13.

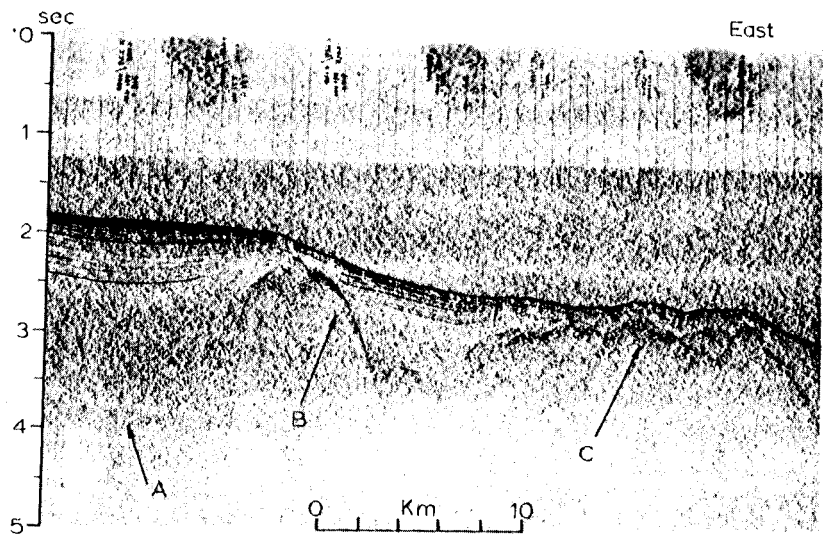


Figure 17. Copy of original seismic section showing the two different type of basements on Orchilla platform (Profile 13). Arrows: A, multiples; B, "granitic" basement; C, rough, acoustic basement.

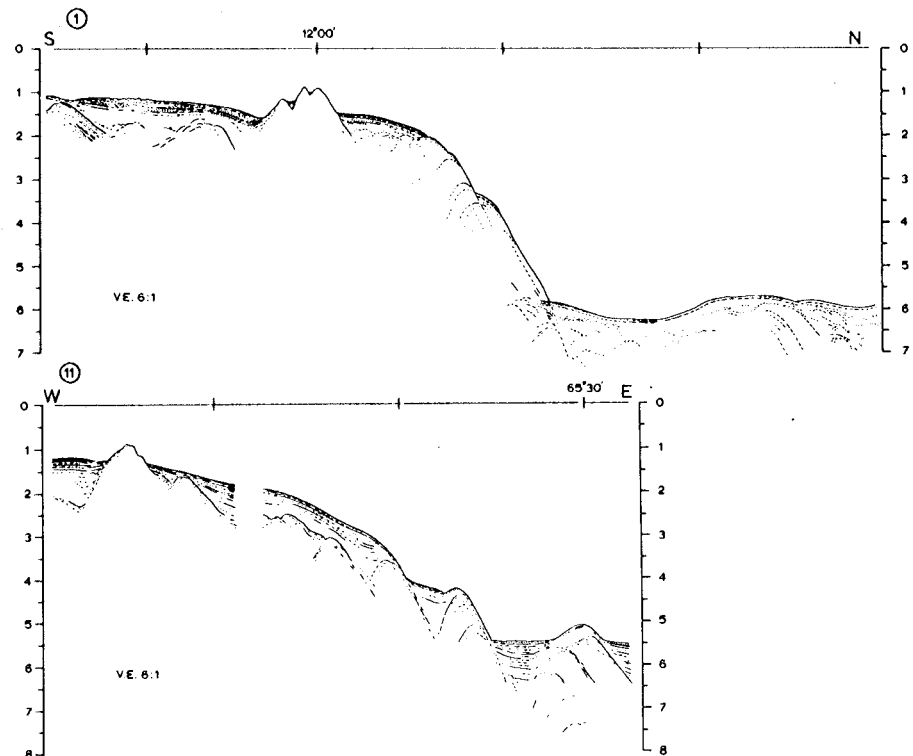


Figure 18. Line drawing of seismic reflection Profiles 1 and 11.

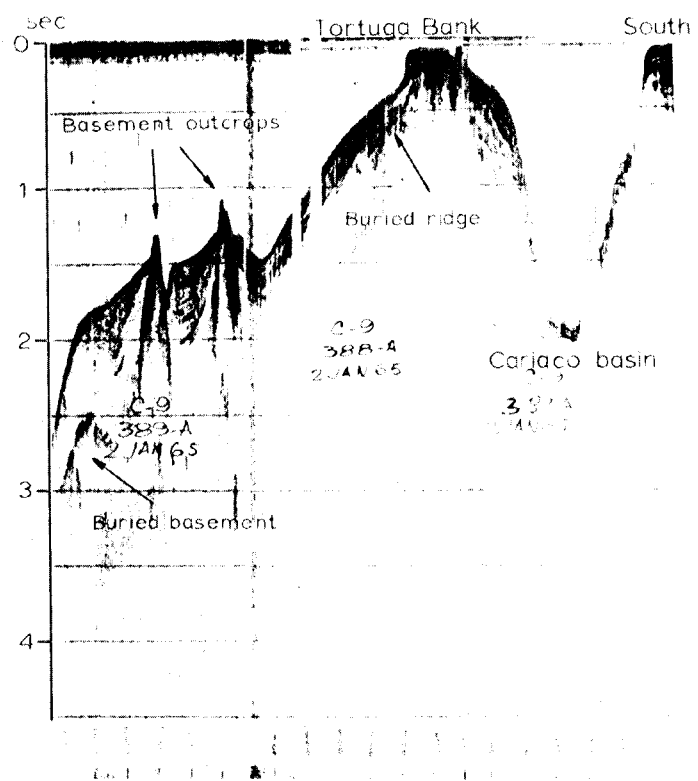


Figure 19. R/V CONRAD-9 seismic section along $65^{\circ}45'W$.
For location see figure 2.

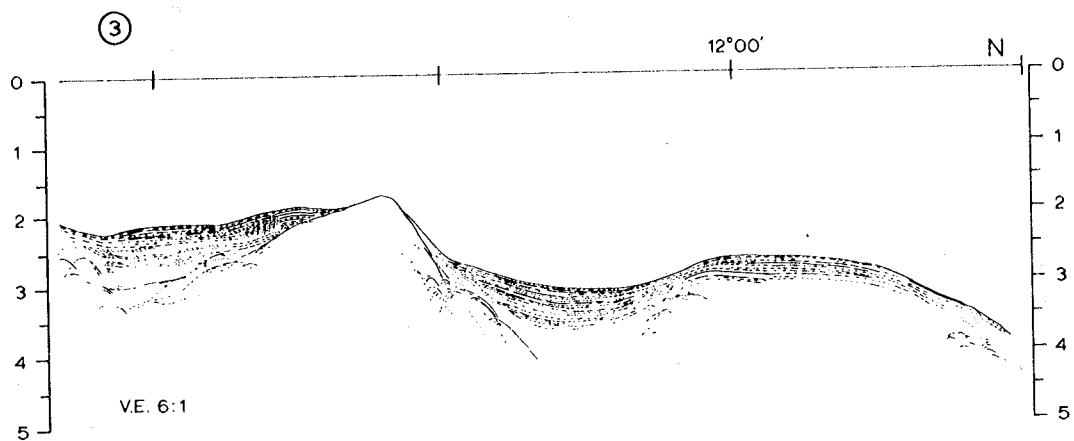


Figure 20. Line drawing of Profile 3 across the Blanquilla platform.

A short seismic section crosses the eastern half of Profile 13 and presents the structure of the southwestern part of the Blanquilla platform (fig. 21). The section is essentially the same as Profile 13 west of the "granitic" ridge (D). To the east it shows 600 m of stratified sediments covering the ridge becoming disturbed as they mix with the talus of the island and other sediments in the Blanquilla Canyon (E). A nonconformity or fault contact is indicated (F) at the base of Blanquilla Island and below the eastern wall of the Los Roques Canyon.

Profile 12 and Profile 10 cross the northwestern part of the Blanquilla platform and the Los Roques Canyon (fig. 22). In Profile 12 over 700 m of well stratified sediments cover the western part of the Blanquilla platform. Blanquilla Canyon at $64^{\circ}48'W$ has been cut into this strata, but its eastern wall in this profile appears to be a slump block. The canyon is underlain by westward dipping reflectors, probably related to the island on the east. Farther north in Profile 10 the canyon walls are apparently cut into more competent rocks of the platform that show no stratification. Some incoherent reflectors underlying the western wall represent either rocks derived by slumping or the acoustic basement.

At $64^{\circ}56'W$ (Profile 10) stratified sediments may indicate a former channel of the canyon, which is now filled. In this profile acoustic basement type reflectors are present between $64^{\circ}56'W$ and $65^{\circ}10'W$. At $65^{\circ}10'W$, a fault contact probably represents one of the two faults bordering the Los Roques Canyon on the east. The eastern wall of the canyon itself represents the other fault.

The acoustic basement is seen only under the western part of the platform in Profile 12 where it outcrops at the wall of the Los Roques Canyon at $65^{\circ}10'W$. This wall represents one of the faults associated with the eastern edge of the canyon; the other fault contact is seen at $65^{\circ}13'W$ where the more than 1000 m of well stratified sediments covering the floor of the Los Roques Canyon abut the acoustic basement rocks. The sediments thicken against this contact, suggesting relatively greater subsidence of the canyon floor on the east. Sediments on the west are in fault contact with the downfaulted acoustic basement rocks of the Orchilla platform at $65^{\circ}30'W$. This buried basement apparently extends northward from Profile 12 and forms the topographic high in Profile 11 (fig. 18). It becomes buried again farther north but appears below the stratified sediments at $65^{\circ}31'W$ in Profile 10 (fig. 23). In Profile 10 the division of the canyon floor into two halves is well illustrated; the western half is underlain by the buried acoustic basement; the eastern half, similar to Profile 12, contains well stratified sediments that thicken to the east.

Profile 10 crossed the northern tip of the Orchilla platform, where the lack of subbottom penetration suggests the presence of competent basement-type rocks. The steep western wall of the canyon probably represents its major fault border.

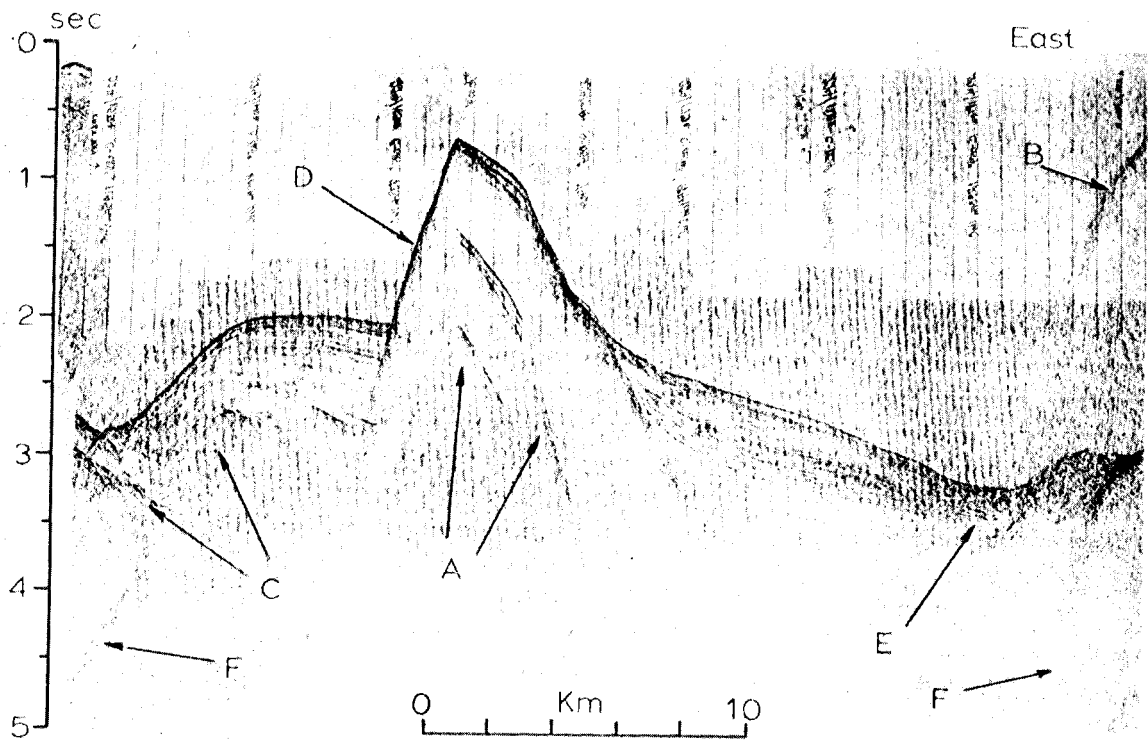


Figure 21. Copy of original seismic section normal to the trends of the Blanquilla platform. Illustration covers part of the track line made between $11^{\circ}40'N$, $46^{\circ}56'W$ and $11^{\circ}49'N$, $64^{\circ}42'W$, southwest of Blanquilla Island (fig. 2). Arrows: A, multiples; B, side echo from the slope of Blanquilla; C, acoustic basement; D, "granitic" ridge; E, Blanquilla Canyon; F, fault contact (?).

3.1.3 Venezuelan Basin - Curacao Ridge

Segments of Profile 1, Profile 2, and Profile 3 cross the southern margin of the Venezuelan Basin (fig. 24). Each profile shows approximately 900 m of well stratified sediments that abut the Curacao Ridge along a possible fault contact. These sediments are essentially horizontal and contain several reflectors that can be identified on each profile (e.g. the reflectors 350 m below the sea floor). The large number of the reflecting horizons that dominate the upper part of the sediment column decrease with depth; the deepest reflectors coming from about 1800 m below the sea floor are separated from the well stratified near-surface sequence by a 600-700 m thick acoustically transparent layer. In Profiles 1 and 2 the lowest reflector has a definite upward curve near its contact with the Curacao Ridge that may suggest drag as a result of relative uplift of the ridge.

The Curacao Ridge in Profile 1 has a rough surface topography that is conformable with the folded subsurface sediments. The strong parabolic reflectors (fig. 25) most likely represent side echoes from the

large buried arches, characteristic of this part of the ridge. In Profile 2 the extension of the Curacao Ridge has a much smoother surface, and it is covered by 250 m of well stratified sediments. Folded sediments similar to those observed in Profile 1 appear approximately 600 m below the northern slope of the ridge.

South of $12^{\circ}10'N$ Profile 2 crosses the northwestern part of the Los Roques Canyon. It shows the stratified sediments, ponded between the Curacao Ridge and the Orchilla platform and the acoustic basement near the southern edge of the profile.

Profile 3 shows the contact between the well stratified sediment sequence of the Venezuelan Basin and the competent acoustic basement-type rocks of the Blanquilla platform. On the northern end of this section the sea floor gently rises as the profile crosses the flank of the Aves Ridge. Numerous layers of the well stratified sequence pinch out at the beginning of the rise until only 300 m remains over the flank. Beneath the well stratified sequence on the flank of the Aves Ridge, there is a 500 m thick, acoustically transparent layer, which terminates at the bottom at a 150-200 m wide reflector, characterized by incoherent returns on the original records.

3.1.4 Venezuelan Basin - Aves Ridge

Profile 8 (fig. 26) crosses the transition area from the Venezuelan Basin to the western flank of the Aves Ridge. Most of the well stratified sediments that cover the southern margin of the Venezuelan Basin pinch out near the edge of the flank of the Aves Ridge ($65^{\circ}29'W$) until only about 300 m of the sequence remains. There are two down-to-basin normal faults near $65^{\circ}29'W$; another similar fault is at $65^{\circ}21'W$. The well stratified sequence is underlain by a 600 m thick acoustically transparent layer that ends at a 150-200 m thick incoherent reflector, noted also in this area on Profile 3. There are two other reflectors

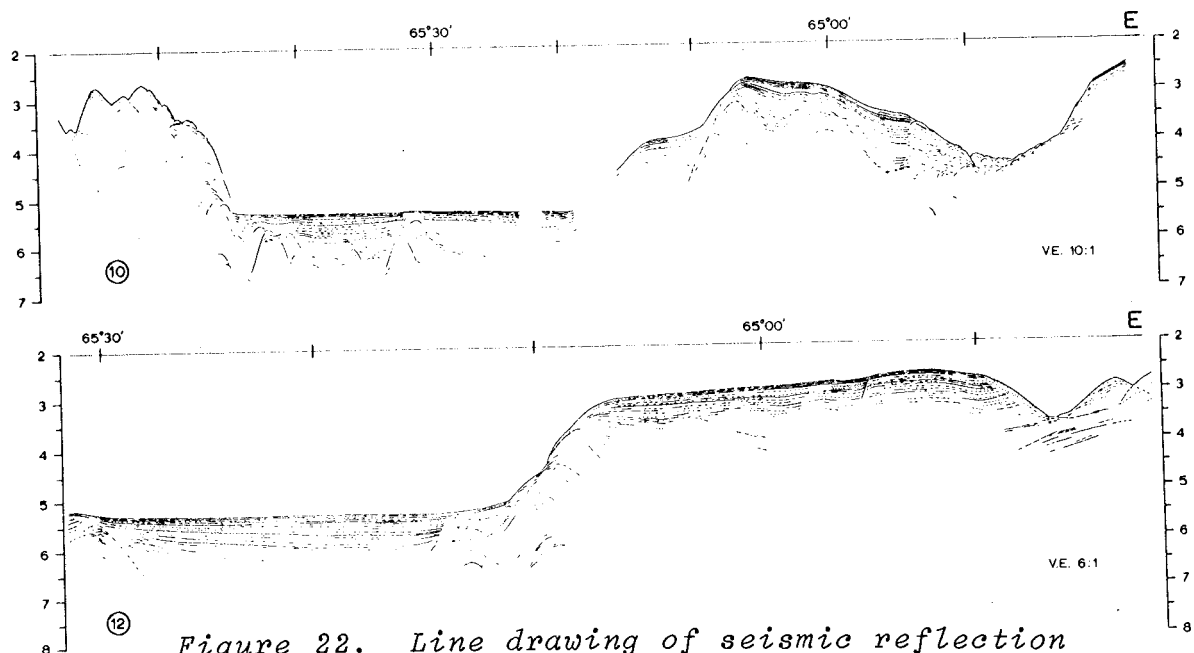


Figure 22. Line drawing of seismic reflection Profiles 12 and 10.

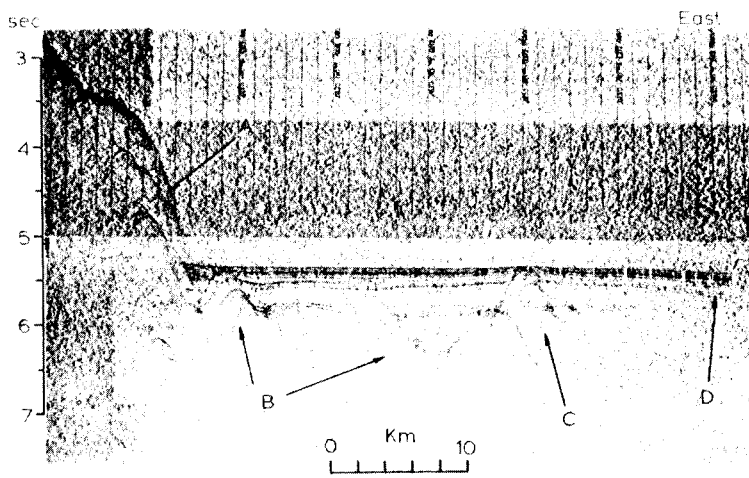


Figure 23. Copy of original seismic section over the north-western part of the Los Roques Canyon (Profile 10). Arrows: A, western wall of canyon; B, acoustic basement; C, buried basement ridge; D, thickening strata toward the east.

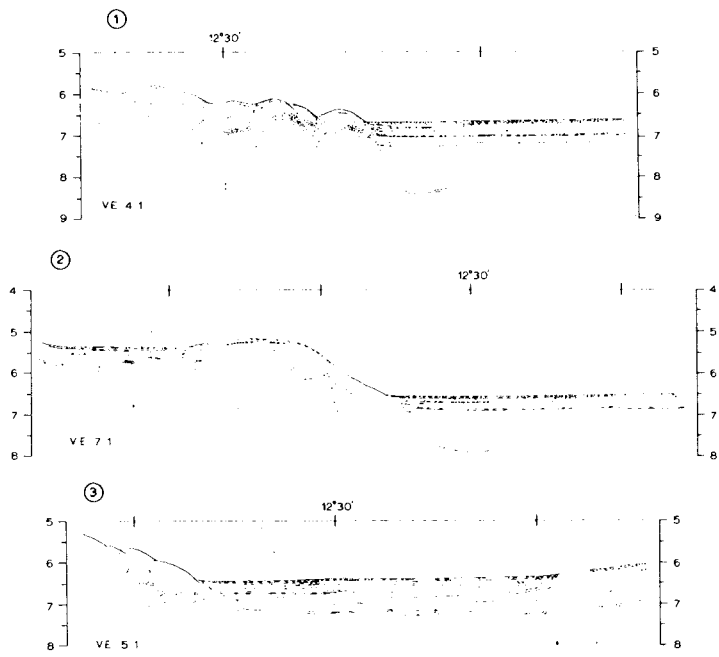


Figure 24. Line drawing of seismic reflection Profiles 1, 2, and 3 over the southern margin of the Venezuelan Basin.

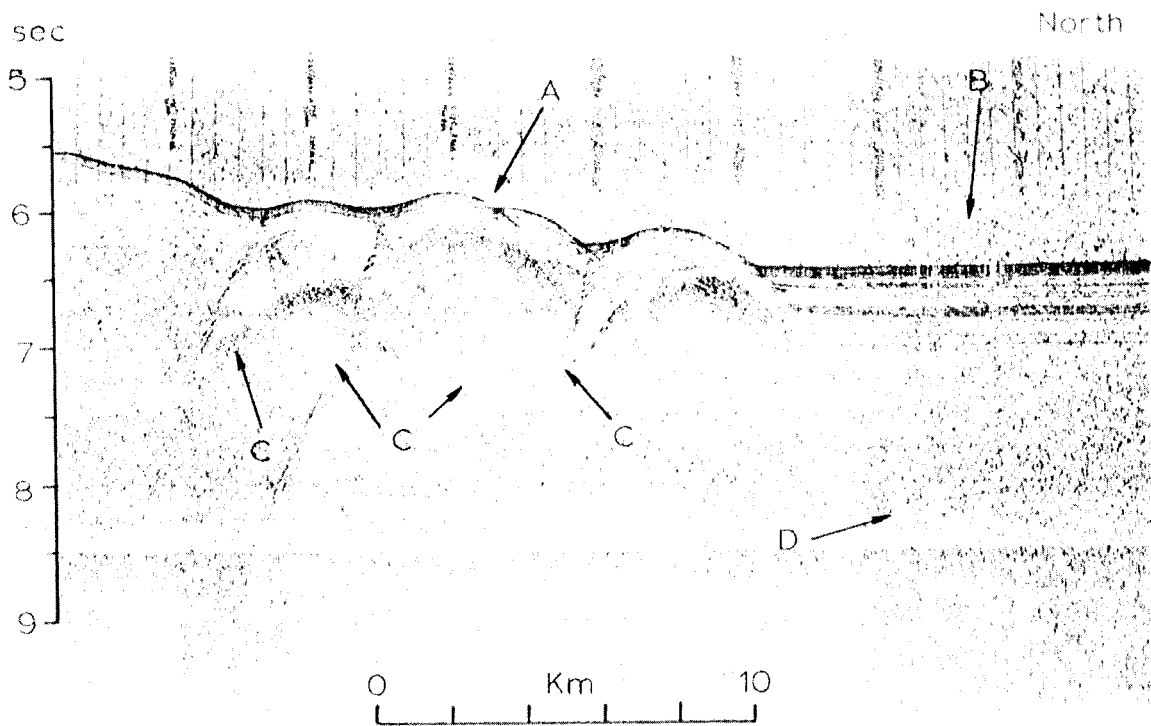


Figure 25. Copy of original seismic section of Profile 1 over the southern margin of the Venezuelan Basin. Arrows: A, eastward extension of Curaçao Ridge; B, Venezuelan Basin turbidite sequence; C, parabolic reflectors; D, deepest reflector.

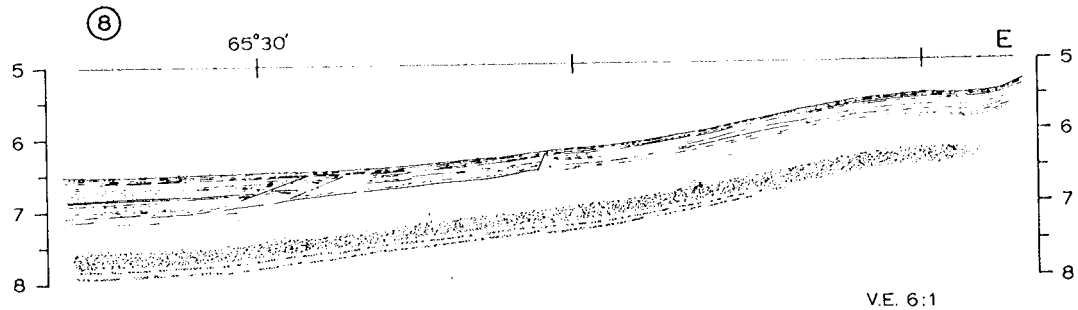


Figure 26. Line drawing of seismic reflection Profile 8.

approximately 100 m apart that underlie the band of incoherent returns and with it extend to the west toward the Venezuelan Basin.

3.2 Geomagnetic Measurements

Geomagnetic data obtained during this investigation are presented in the form of a magnetic total intensity contour chart (fig. 27) and as a series of magnetic total intensity anomaly profiles, plotted together with the profiles of the bottom topography and the free-air gravity anomaly (see Appendix I). Data collected along all the tracklines were utilized in the preparation of the total intensity contour map, but Appendix I contains only the key sections shown in figures 7 and 13.

Additional geomagnetic data obtained along north-south tracklines in the area south of $11^{\circ}00'N$ by Ball *et al.* (1971) were also incorporated in the total intensity contour map. A correction of -150γ was added to these data to eliminate the effect of the secular variation that occurred during the two-year interval separating the two sets of measurements.

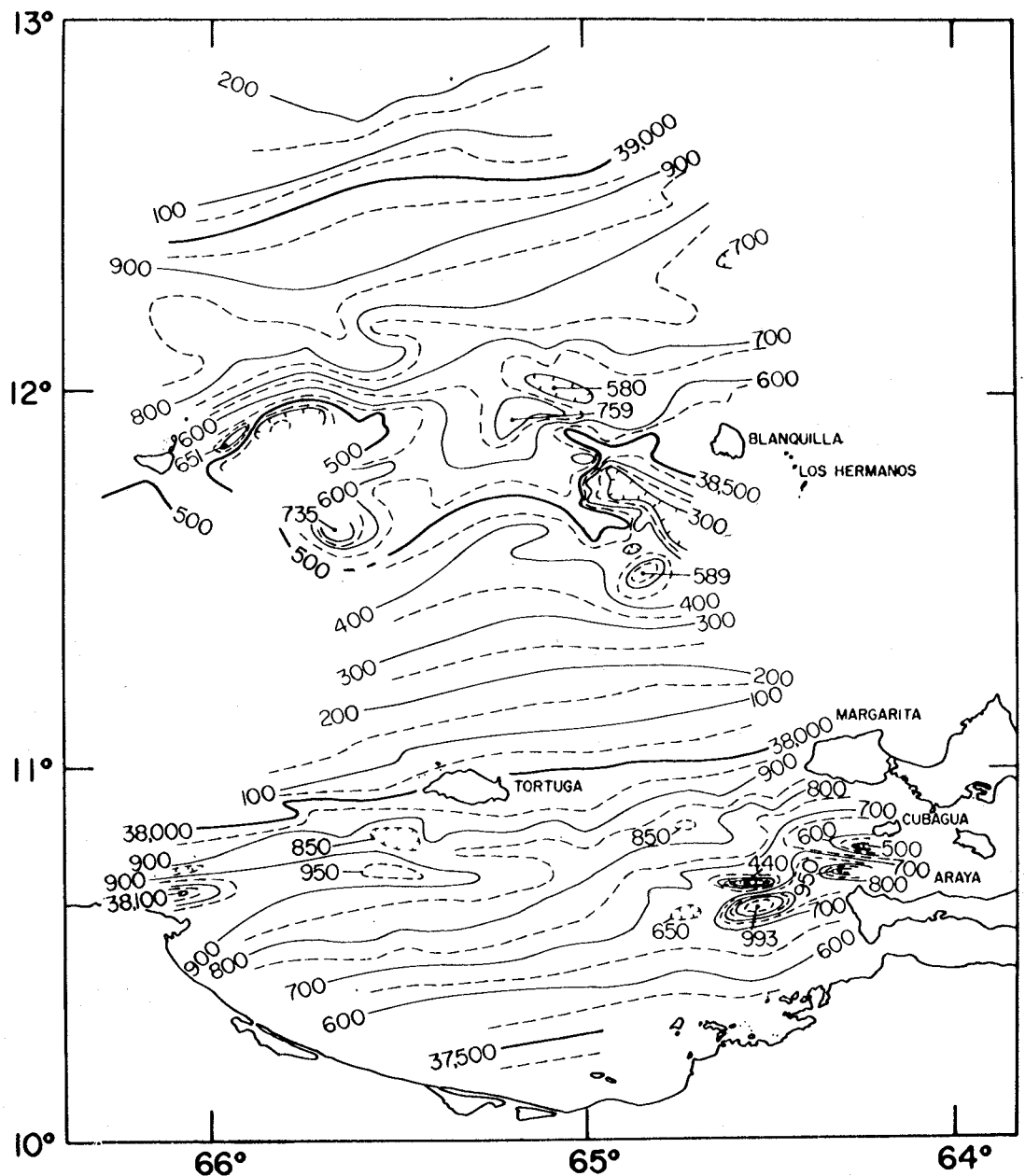
An essentially smooth magnetic field characterizes the northern part of the study area which overlies the Venezuelan Basin, the northern slope of the Tortuga-Margarita Bank, and, in the south, the Bay of Barcelona. Anomalies up to $\pm 300 \gamma$ were observed over the Orchilla and Blanquilla platforms, where the tracklines were too widely spaced for the accurate presentation of the magnetic field variations. The magnetic data in these areas serve only to indicate the presence of igneous rocks in various parts of the platform.

Over the continental shelf south of $11^{\circ}00'N$ the density of the trackline coverage permits a much more accurate presentation of the magnetic field. In order to see the magnetic anomalies of this area more clearly, the earth's main magnetic field was removed by using a grid, constructed from the values of the total intensity chart along $65^{\circ}00'W$ and $65^{\circ}30'W$ (fig. 28). The magnetic anomaly map (fig. 29) reveals two $600-\gamma$ (peak-to-trough) anomalies off the Araya Peninsula, and a number of smaller, short-wavelength (<10 km) anomalies southwest of Margarita. The Bay of Barcelona and large parts of the Cariaco Basin are essentially free of short-wavelength magnetic anomalies, although a $300-\gamma$ positive anomaly off Cabo Codera extends into the western deep of the Cariaco Basin, and a small minimum seems to follow the southern margin of the Tortuga-Margarita Bank west of $65^{\circ}00'W$.

3.3 Gravity Measurements

Gravity free-air anomaly values are presented in the form of a contour map (fig. 30) and as a series of profiles, plotted together with the magnetic anomalies and the bottom topography (Appendix I).

The largest free-air anomalies are associated with the area of the island platforms and the extension of the Curacao Ridge. A -194 mgal minimum is associated with the Curacao Ridge at $66^{\circ}00'W$, which diminishes eastward to about -120 mgals at the point where the ridge merges



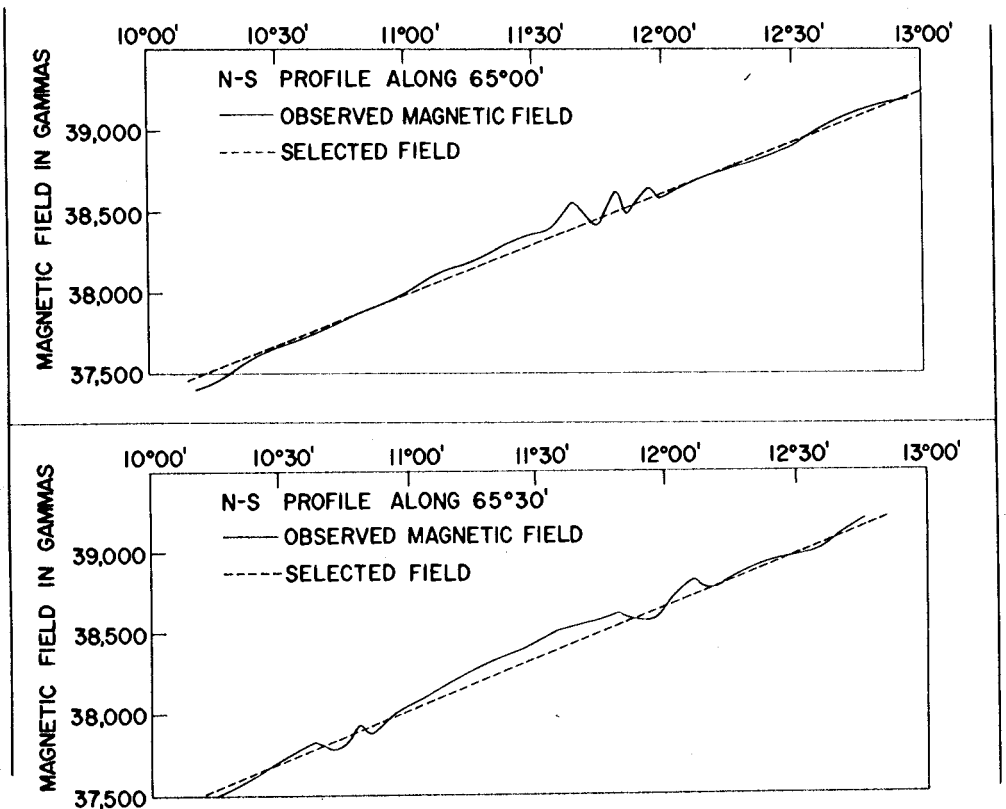


Figure 28. Determination of the regional magnetic field from the values of the total intensity chart along $65^{\circ}00'W$ and $65^{\circ}30'W$.

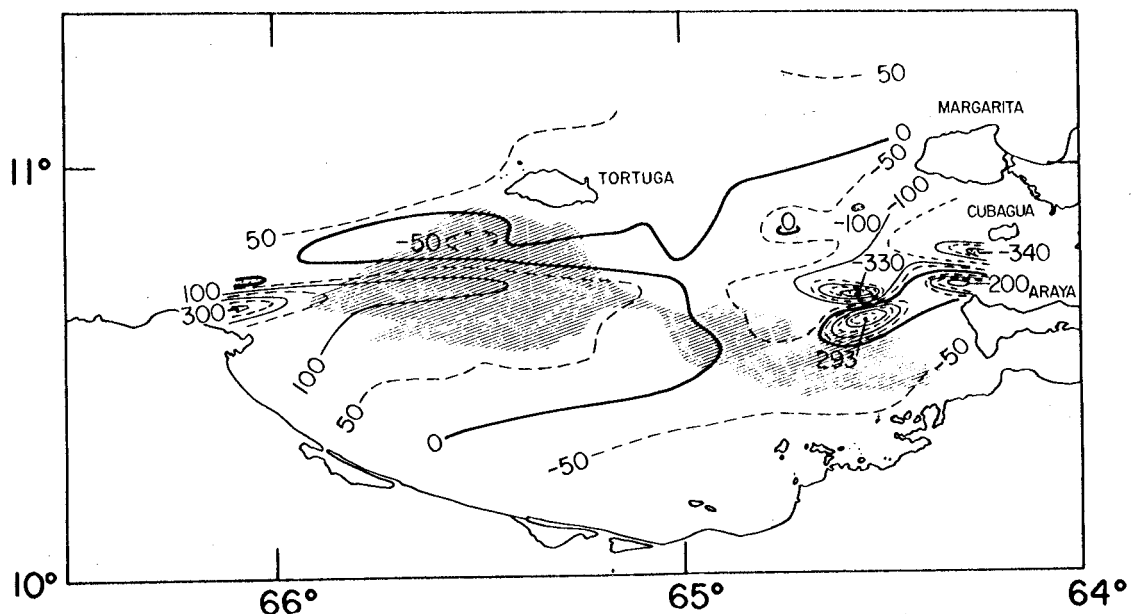
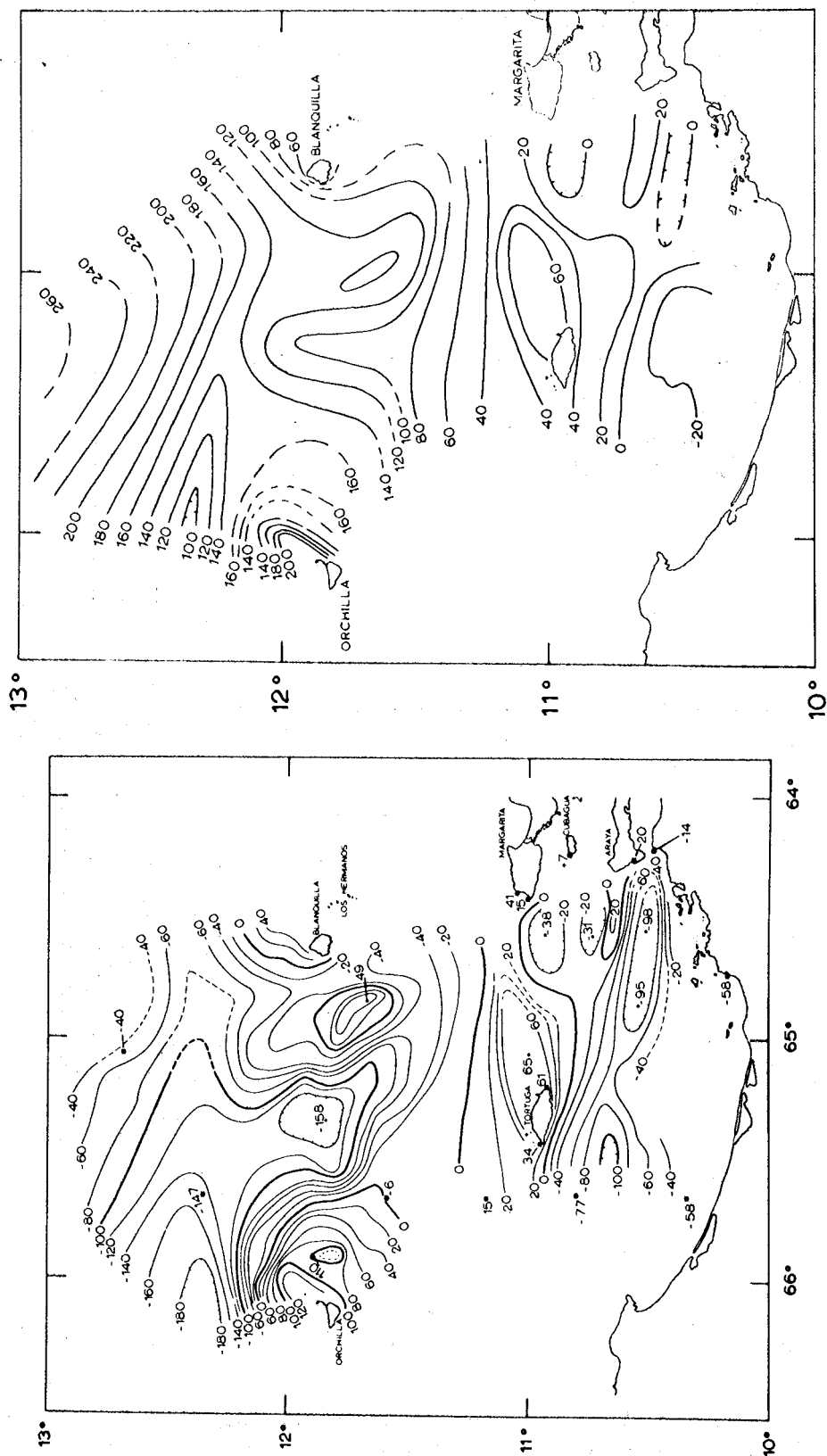


Figure 29. Magnetic total intensity anomaly map of the continental shelf off north-central Venezuela. Shaded area: Cariaco Basin below 500 fm.



34

Figure 30. Free-air gravity anomaly map of the study area. Contour interval 20 mgals. Values with stars: Marine measurements, Ewing et al., 1957; Land measurements, Ball et al., 1971.

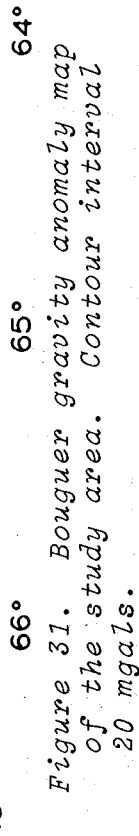


Figure 31. Bouguer gravity anomaly map of the study area. Contour interval 20 mgals.

with the Blanquilla platform. Farther to the east the axis of this minimum shifts northward, and follows the topographic depression north of the platform.

There is a -158 mgal minimum in the Los Roques Canyon, and positive anomalies of 125 mgals and 49 mgals were observed over the Orchilla and Blanquilla platforms, respectively.

The Tortuga-Margarita Bank is characterized by small amplitude positive free-air anomalies that range up to 65 mgals in the area immediately east of Tortuga. Farther south, over the depressions of the shelf negative anomalies predominate, with approximately -100 mgal values in the Cariaco Basin. Positive anomalies are associated with the westward extension of Cubagua Island and the Araya Peninsula.

In order to eliminate the effect of the topography on the gravity anomalies and to study the subbottom density distribution, a Bouguer anomaly map was prepared (fig. 31). Instead of computing the commonly used "simple Bouguer anomaly" (Free-air anomaly + depth x constant x density difference between sea water and underlying rocks), "two-dimensional Bouguer anomaly" computations (Talwani *et al.*, 1959) were performed along eight profiles (fig. 32) that were selected in areas where the sea floor had no appreciable variations transverse to the section (see Appendix II). A comparison of the "simple Bouguer" correction and the "two-dimensional Bouguer" correction (fig. 33) shows that the latter in essence contains a terrain correction also that can amount to 40 mgals in areas of rough topography. The Bouguer anomaly map was prepared on the basis of the eight two-dimensional Bouguer anomaly profiles (Appendix II) that were computed with an assumed subbottom density of 2.67 g/cm³. The density value chosen is representative of granitic rocks that were sampled through dredging and described in the literature as outcrops on several islands.

The Bouguer anomaly map is dominated by a strong regional gradient reflecting the dip of the mantle beneath the continental margin. There are positive Bouguer anomalies over the Tortuga-Margarita Bank, but the large negative free-air anomalies over the Cariaco Basin have been eliminated. A local low of approximately 40 mgals characterizes the Los Roques Canyon, and a 100 mgal local low identifies with the Curacao Ridge north of Orchilla.

4. GEOLOGICAL INTERPRETATION AND DISCUSSION

4.1 The Continental Shelf

4.1.1 Regional Geology

Northern Venezuela is dominated by a complexly folded and faulted mountain system, the Caribbean ranges. These mountains trend in a general east-west ($N75^{\circ}E$) direction and are separated into an eastern and western region by the Bay of Barcelona. The topographic lows associated with the Gulf of Cariaco on the east and the Tuy River - Valencia Lake depression on the west further divide the mountains into the

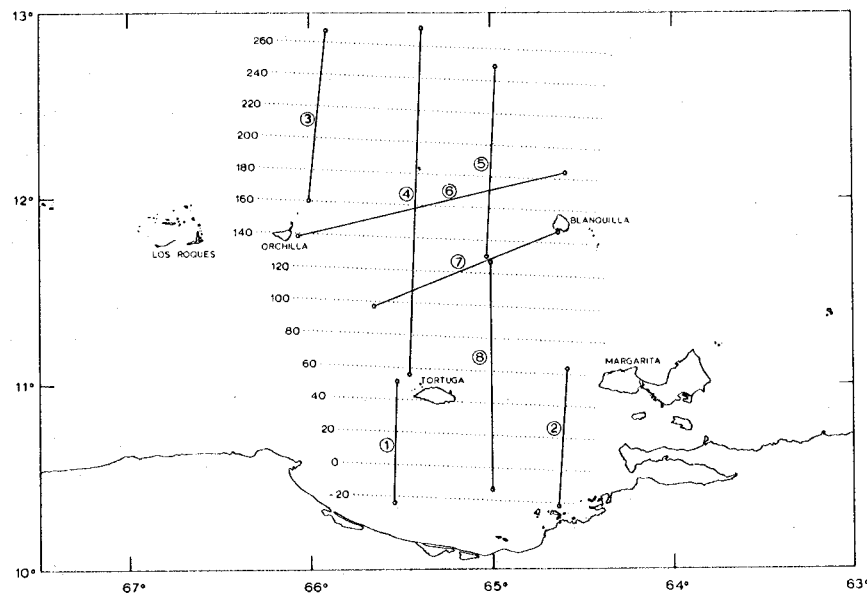


Figure 32. Location of two-dimensional Bouguer anomaly profiles, and the regional Bouguer anomaly map. Contour interval 20 mgals.

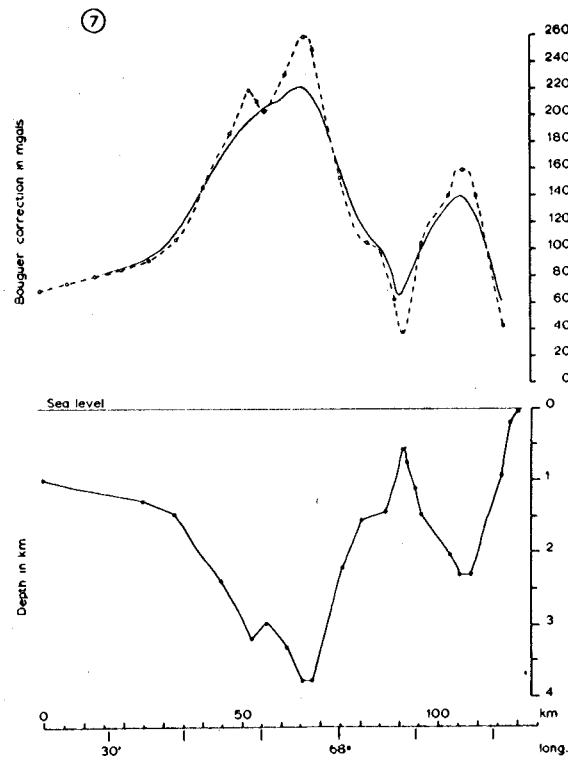


Figure 33. Comparison of "simple" (dashed line) and "two-dimensional" (solid line) Bouguer corrections.

Cordillera de la Costa on the north and the Serrania del Interior on the South.

Summaries of the geology of the area west of Barcelona Bay are contained in the works of Bell (1967), Dengo (1953), Menendez (1962, 1967), Morgan (1967), and Oxburgh (1966). Sources used for the geology of the eastern region are Mencher *et al.* (1953), Metz (1968a, 1968b), Rod (1956, 1959), Rod and Maync (1954), Salvador and Stainforth (1968), Schubert (1971), and Von der Osten (1955, 1957). The geology of Cubagua, Margarita, and Tortuga is from Kugler (1957), Taylor (1960), and Maloney and Macsotay (1967), respectively.

Bell (1967) distinguished eight tectonic belts in the Caribbean mountains west of the Bay of Barcelona (fig. 34). Although their ages are subject to debate, the basement rocks are considered pre-Mesozoic, and represented by the Sebastopol granitic gneiss complex and the Peña de Mora gneiss in the Cordillera de la Costa belt. These are overlain unconformably by the quartz-mica schists of the Las Brisas and Las Mercedes formations, generally believed to be Upper Jurassic to Lower Cretaceous in age (Menendez, 1967; Salvador and Stainforth, 1968). There are several amphibolite layers in the Las Mercedes formation which probably were emplaced originally as basic igneous intrusions; serpentinites occur along the contact of the two formations in the northern part of the belt (Dengo, 1953).

The El Tinaco gneisses and schists represent the pre-Mesozoic (?) basement complex in the Caucagua-El Tinaco belt. This basement is overlain by varied groups of sedimentary and metasedimentary units, ranging in age from Lower to Upper Cretaceous (Menendez, 1962, 1967).

These two tectonic belts form the Cordillera de la Costa mountains west of the Bay of Barcelona. They contain the oldest rocks exposed and a complex sequence of metasedimentary rocks that generally are called

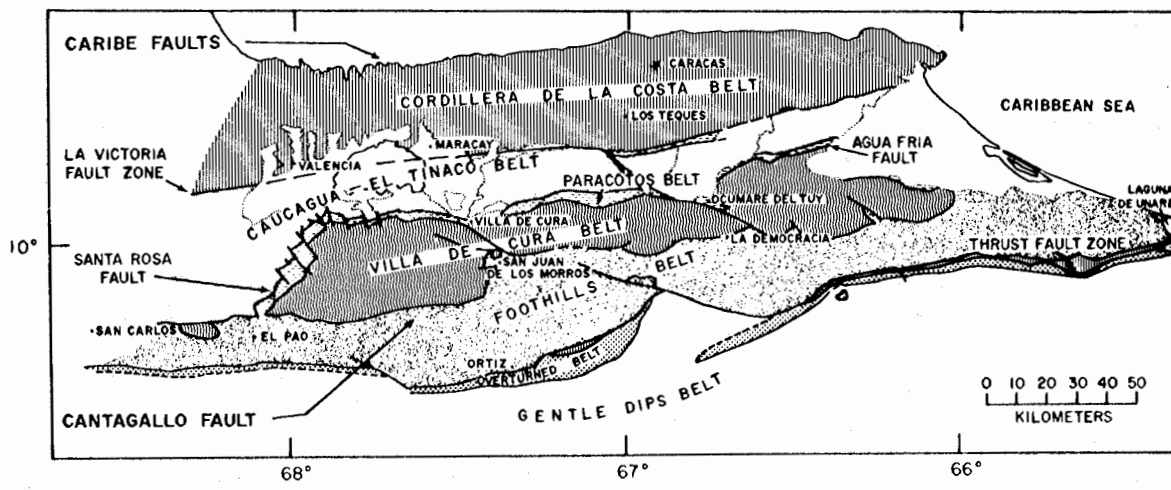


Figure 34. Tectonic belts of the Caribbean mountains west of the Bay of Barcelona (from Bell, 1967).

the Caracas group (Aguerrevere and Zuloaga, 1937). The Caracas group is believed to represent a thick, largely clastic sequence of marine shelf deposits that were metamorphosed in the Upper Cretaceous (Dengo, 1953; Oxburgh, 1966). The regional metamorphism of the Caracas group increases from south to north: In the southern part of the Cordillera de la Costa it is in the greenschist facies, while in the northern part the metamorphism of the Caracas group is in the epidote-amphibolite facies.

Major longitudinal fault systems border the two tectonic belts just described. These are the Caribe fault systems that terminate the Cordillera de la Costa on the north; the La Victoria fault zone that separates the two tectonic belts; and the Santa Rosa fault that borders the Caucagua-El Tinaco belt on the south. Based on the prominence and length of the linear fault traces, these have been considered primarily strike-slip faults (Smith, 1953; Rod, 1956; Alberding, 1957), but more recent interpretations emphasize that the dominant motions along these faults were vertical, and continued from the Upper Cretaceous to Holocene time (Menendez, 1967; Morgan, 1967). Cross-faults along northwest-southeast trends cut the longitudinal faults in many places. Morgan (1967) suggests that the persistence of formations along the strike direction, despite the consistent 5° to 25° plunge of fold axes, is caused by uplift along a series of repetitive high-angle cross faults.

The two major tectonic elements of the Serrania del Interior to the south of this area are the Villa de Cura belt and the Foothills belt (fig. 34). The Villa de Cura belt is a 3 to 6 km thick sequence of low grade metavolcanic rocks, that are believed to represent former submarine volcanic deposits (Bell, 1967; Menende, 1967). The sequence consists of quartz-albite-chlorite-epidote schists, quartz-albite-granulites with smaller amounts of volcanic conglomerates, metatuffs, metalavas, and metacherts (Bell, 1967). Along its southern margin it is overlain by the weakly metamorphosed basalts and gabbros of the Tiara volcanic formation.

Menendez (1962, 1967) and Bell (1967) suggest that the Villa de Cura belt is an allochthon block, deposited in the Lower Cretaceous over the Caracas group, metamorphosed, and then moved southward during the Maestrichtian and Paleocene time across the narrow Paracotos belt, located now on its northern border. The Agua Fria and the Cantagalio faults dip under the Villa de Cura belt and represent the sole thrust of the block.

The Foothills belt south of the Villa de Cura belt contains Middle Cretaceous conglomerates, lithic wackes, siltstones and shales, with pyroxene-breccia sills and serpentinites (Garrapata formation). The major part of the belt is occupied by the Paleocene sandstones, siltstones, and shales of the Guarico formation.

The Foothills belt, in essence, consists of a series of "tectonic slices", separated by north-sipping thrust faults, that were formed as the result of renewed southward gravity sliding of the Villa de Cura block in Late Tertiary time (Bell, 1967). Cross-faulting with both horizontal and vertical movements is common along northwest-southeast trends, just as it was noted in the Cordillera de la Costa.

The western part of the Eastern Venezuelan Basin, known as the Guarico sub-basin, lies south of the frontal thrust zone of the western Serrania del Interior. It contains Late Tertiary shales, mudstones, and sandstones that reach 6000 m in thickness. That the basin was overridden on the north by the southward thrusts of the Foothills belt is suggested by the numerous outcrops of the Late Eocene Roblecito formation within the Foothills belt and within the Overturned belt and thrust fault zone (Bell, 1967).

The Tertiary basin ends abruptly to the northeast at the Urica Fault (fig. 35). East of this fault extend the eastern Caribbean ranges. The eastern Serrania del Interior lies between the El Pilar fault on the north and the frontal thrust faults on the south; to the north of the El Pilar fault the eastern Cordillera de la Costa occupies the narrow coastal region.

The eastern Serrania del Interior and the small offshore islands between Barcelona and the mouth of the Gulf of Cariaco are dominated by Lower Cretaceous quartzose sandstones (Barranquin formation), massive biostromal limestones (El Cantil formation), and alternating sandstones,

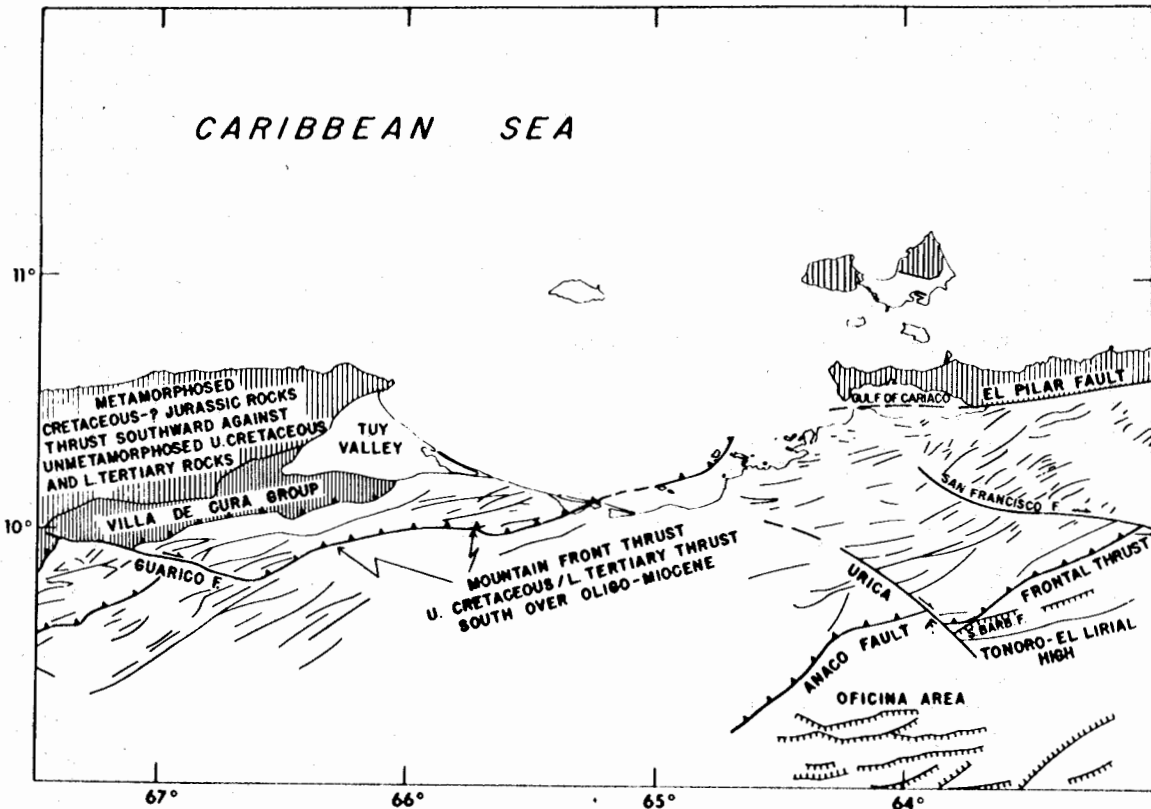


Figure 35. Structural elements in northeastern Venezuela (from Salvador and Stainforth, 1968).

limestones, and shales (Chimana formation) (Metz, 1968b). Early Upper Cretaceous limestones and cherts (Querecual formation) were almost entirely stripped during an intra-Senonian folding and erosion. Maestrichtian and Paleocene massive sandstones (San Juan formation) and shales and marls (Vidño formation) were subjected to erosion together with the earlier Cretaceous rocks since Late Eocene or Early Oligocene time (Metz, 1968b).

The eastern Cordillera de la Costa is an anticlinorium which consists of Lower Cretaceous garnet-epidote schists, quartz-mica schists, and calcareous schists that are similar in many respects to the Caracas group of the western Cordillera de la Costa (Christensen, 1961; Schubert, 1971). In the Araya Peninsula the Guamache formation (fig. 36) represents the oldest and most metamorphosed rocks (epidote-amphibolite facies; Schubert, 1971); the Carupano and Tunapui formations represent greenschist facies metamorphism and were compared to the Las Mercedes and the Las Brisas formations by Christensen (1961). Serpentinites and serpentinized peridotites are found in numerous localities near the contact of the Laguna Chica and Carupano formations (Schubert, 1971).

The regional strike of the folding is east-northeast in both the Cordillera de la Costa and the Serranía del Interior, suggesting compression and thrusts from the north-northwest. While the motion along the longitudinal fault system that separates the metamorphic formations of the Araya Peninsula was essentially vertical (Schubert, 1971), Christensen (1961), Salvador and Stainforth (1968), and Metz (1968a) believe that a large southward thrust placed the metamorphic rocks of the Araya and Paria Peninsula in contact with the Cretaceous sedimentary rocks of the Serranía del Interior in Late Eocene time.

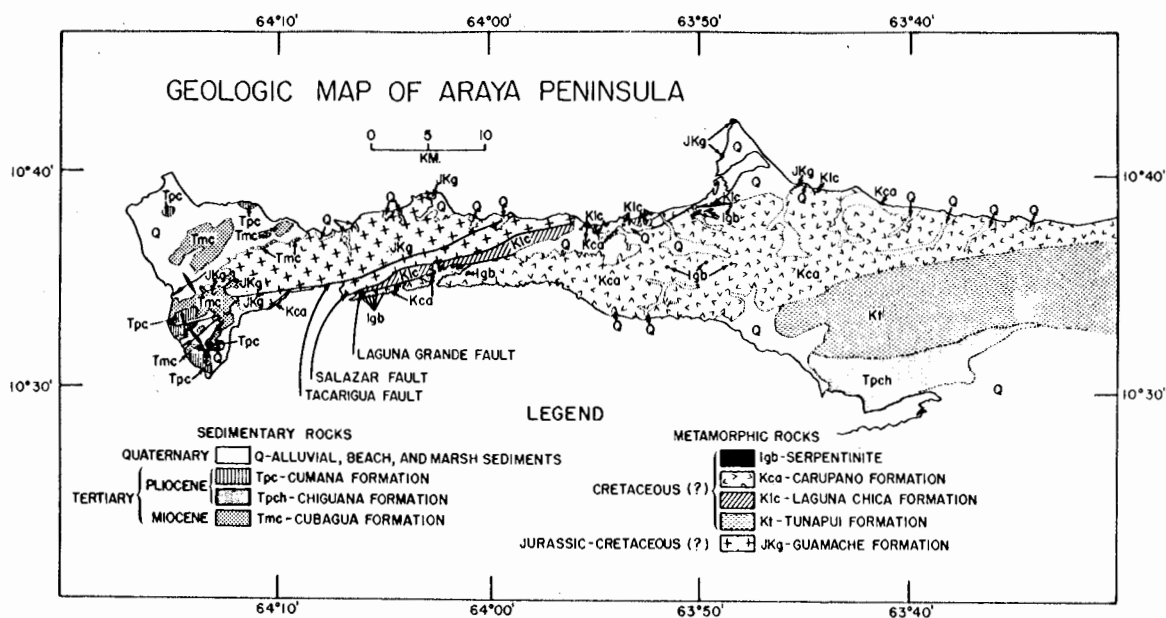


Figure 36. Geologic map of the Araya Peninsula (from Schubert, 1971).

Contrary to earlier interpretations suggesting large right-lateral motions along the El Pilar fault system (Liddle, 1946; Rod, 1956; Alberding, 1957), it may have originated as part of the southward thrust (Salvador and Stainforth, 1968). According to Metz (1968a), however, the motions were essentially vertical along the El Pilar fault system (less than 15 km right-lateral component) and related to Late Tertiary orogenic processes.

Crossfaulting along a northwest-southeast trend is common also in the eastern Caribbean ranges. Motion along the two major cross-faults of the area, the Urica and San Francisco faults, has been dominantly right-lateral, and related to the orogenic episodes (folding and uplift) between the Cretaceous and Miocene times (Rod, 1959). Salvador and Stainforth (1968) report that significant right lateral motions took place along the Urica fault during the Late Miocene and Pliocene, while no post-Eocene motions are noted along the San Francisco fault.

North of the Araya Peninsula the island of Cubagua represents the exposed part of an anticline composed of several thousand meters of Tertiary sediments (Kugler, 1957).

North of Cubagua, the northern part of the eastern island of Margarita and most of the western island (also called Macanao) are underlain by a metasedimentary and metavolcanic sequence that was intruded by both granitic and ultramafic rocks (Taylor, 1960). The oldest rocks belong to the presumably Upper Jurassic to Lower Cretaceous Juan Griego group that, although more metamorphosed than the Caracas group of the western Cordillera de la Costa, may represent its equivalent on Margarita. Major orogenic deformation, metamorphism, and the intrusion of the ultramafic rocks occurred in mid-Upper Cretaceous (?), followed in mid-Maestrichtian time by another deformation and milder metamorphism (Los Robles group). Paleocene and Lower Eocene sediments were mostly eroded during a Middle Eocene uplift that was followed by rapid subsidence and the accumulation of at least 2000 m of Upper Eocene limestones, conglomerates, and shales (Punta Carnero formation). A milder deformation folded these rocks during mid-Miocene, but sediment accumulation continued throughout the remainder of the Tertiary. Uplift and faulting reoccurred during the Pleistocene and Holocene times (Taylor, 1960).

The trend of the fold axes in Margarita is generally southwest-northeast. Northwest-southeast trending faults are commonly normal faults, whereas many of the east-west faults are high angle reverse faults (Kugler, 1957; Taylor, 1960).

West of Margarita, on the island of Tortuga only Pliocene marls and Pleistocene coral reefs and associated clastic limestones are exposed. The available structural data suggest a possible northward tilting of the island during Late Pleistocene time (Maloney and Macsotay, 1967).

4.1.2 Discussion

Geologic units of the continental shelf are tentatively identified on the basis of the relationship of their apparent physical characteristics to those of the known rock formations exposed on the adjacent land

areas. Where possible, a more direct correlation is made through the extension of the exposed geologic units along trends of topography or structure or both.

The best examples for the extension of the land geology to the shelf are seen east of 65° W. The El Pilar fault, located near the contact of the metamorphic rocks of the Araya Peninsula and the more competent rocks of the eastern Serrania del Interior (Metz, 1968a), extends westward from Cumana and forms the southern boundary of the eastern deep of the Cariaco Basin. The offshore portion of the El Pilar fault resembles a north dipping normal fault (Profiles 5 and 7, fig. 8), as suggested by Ball *et al.* (1971). The presence of the competent Lower Cretaceous sedimentary rocks (Barranquin and El Cantil formations) south of the El Pilar fault is indicated by the lack of reflectors below the southern wall of the Cariaco Basin on Profile 7, the presence of a strong "basement type" reflector on Profile 5, the absence of magnetic anomalies, and by the small positive Bouguer anomalies (figs. 29, 31, and 37).

The writer believes that the metamorphic rocks of the Araya Peninsula, like the Caracas and Juan Griego groups, have igneous intrusives associated with them. These underlie the northern edge of the peninsula and are responsible for its westward topographic extension on the shelf.

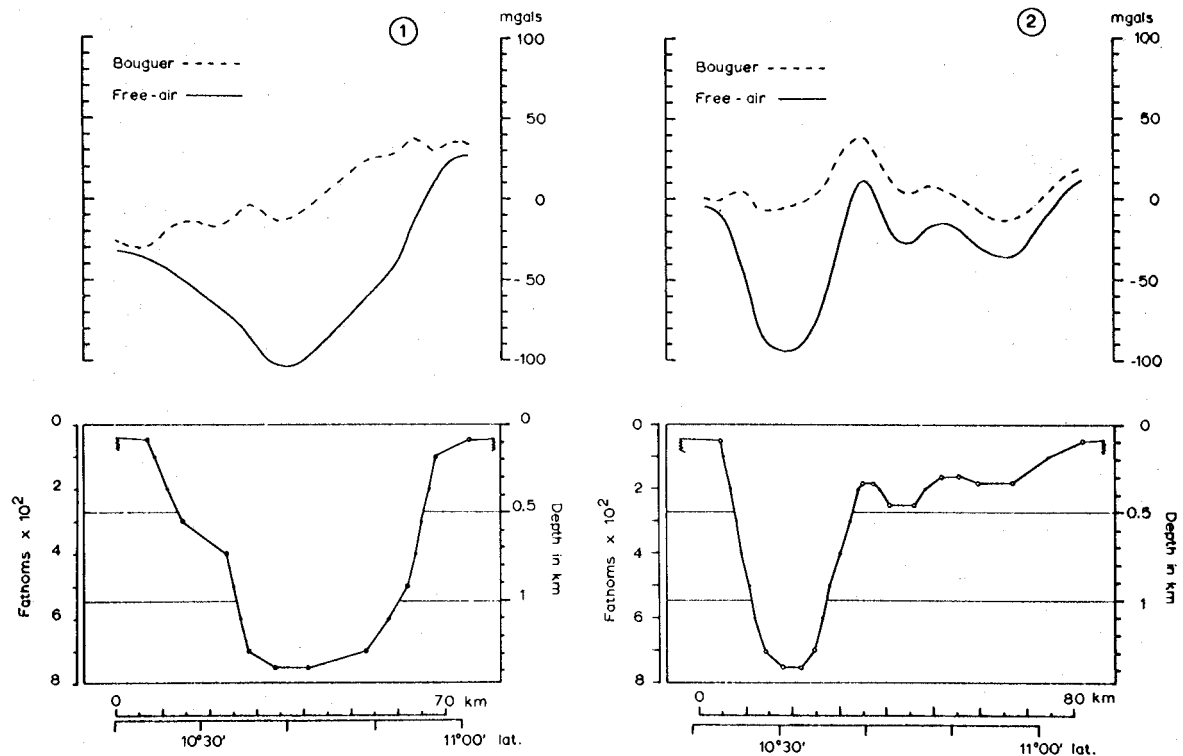


Figure 37. Comparison of gravity anomalies across the eastern and western deeps of the Cariaco Basin (see fig. 32 for location).

This conclusion is supported by the fact that a topographic high extending from the northern edge of the peninsula (fig. 5) is associated with a +38 mgal Bouguer anomaly and two of the largest magnetic anomalies (one approximately 600 γ, the other 550 γ) observed in the area of the shelf (fig. 29).

From model studies of the magnetic anomaly west of the Araya Peninsula, Ball *et al.* (1971) concluded that the magnetic effect of a 5 km wide, 15 km long igneous body located 2 km below the surface gives the best fit of the observed anomalies. The close similarity of this anomaly to the one directly north of the tip of the Araya Peninsula (fig. 29) suggests a similar interpretation for that area. Ball *et al.* (1971) suggest that the two structures responsible for the magnetic anomalies might have been offset by a left-lateral fault. The relatively low magnetic values between the two major anomalies may suggest, however, that the anomalies belong to two separate intrusions, emplaced along a same east-northeast structural trend that characterizes the peninsula.

The igneous basement cannot be detected on Profile 7 because of inadequate penetration. The massive well-bedded strata overlying the Araya block most likely represent the Tertiary and Quarternary sediment cover. The 300 m thick layer on the southern slope of the Araya block characterized by mostly incoherent internal reflectors may represent the westward extension of the metamorphic schists of the Guamache formation (fig. 36). The fault contact between the inferred metamorphic rocks and the younger sediments in the eastern deep of the Cariaco Basin could be the extension of the Salazar or Laguna Grande faults. The Carupano formation, which is located south of this fault contact on the Araya Peninsula, has been apparently downfaulted along a cross-fault between Profile 7 and the eastern slope of the basin (location of this fault must be west of Line 2, fig. 6 of Ball *et al.*, 1971, where the entire metamorphic {?} sequence of the Araya Peninsula abuts the El Pilar fault).

Another cross-fault is suggested between Profile 7 and Profile 5 (fig. 8). On Profile 7 the seismic reflectors indicate a sinking basin with over 700 m of well stratified sediments south of the inferred Salazar fault, whereas on Profile 5 there is no indication of the "Salazar fault", and the reflectors show gently arched sediments below the floor of the basin, with no reflectors below 150 m. A cross-fault with a down-to-west displacement could explain the different tectonic conditions in the two halves of the eastern deep as well as the disappearance of the metamorphic rocks under the basin floor, and the elimination of the Araya block as a topographic high. The faults at the northern margin of the basin floor ($10^{\circ}35'N$) and at $10^{\circ}43'N$ on Profile 5, however, are probably still related to the Araya block.

Profile 3 (fig. 8) across the saddle between the two deeps of the Cariaco Basin shows no indication of either the El Pilar fault or the faults that were seen associated with the edges of the Araya block in Profile 5. The Bouguer anomaly is -38 mgal near the southern end of this profile (Line 8, Appendix II), as opposed to the small but positive values measured to the east.

This fact suggests that the relatively dense, competent Lower Cretaceous rocks do not extend this far west. The writer suggests that the Urica fault that forms the border between the eastern Serranía del Interior and the Eastern Venezuelan Basin southwest of Cumana extends northwestward from the area of Cumana and forms the western limit of the El Pilar fault and the Araya block. The Urica fault also cuts the Cariaco Basin into two halves, and may be responsible for the relative right lateral offset of the eastern and western deeps (fig. 38).

The series of north-dipping normal faults north of the Araya block (Profile 7, fig. 8) are probably part of the "coastline fault system", noted farther to the east by Lattimore *et al.* (1971). To the north of these faults the Cubagua and Punta Arenas highs appear to have a complex structure: Profile 7 and the seismic reflection work of Ball *et al.* (1971) suggest that either the Tertiary sediments of Cubagua were uplifted by a basement fault block, or these sediments were draped over the basement horst. A westward plunge of the Cubagua basement block with greater uplift along its northern bordering faults (southward tilting) could explain the more faulted appearance of the Cubagua high to the east (on Line 2, Ball *et al.*, 1971), and the existence of the faults between the Cubagua and Punta Arenas highs on Profile 7. Southward tilt-

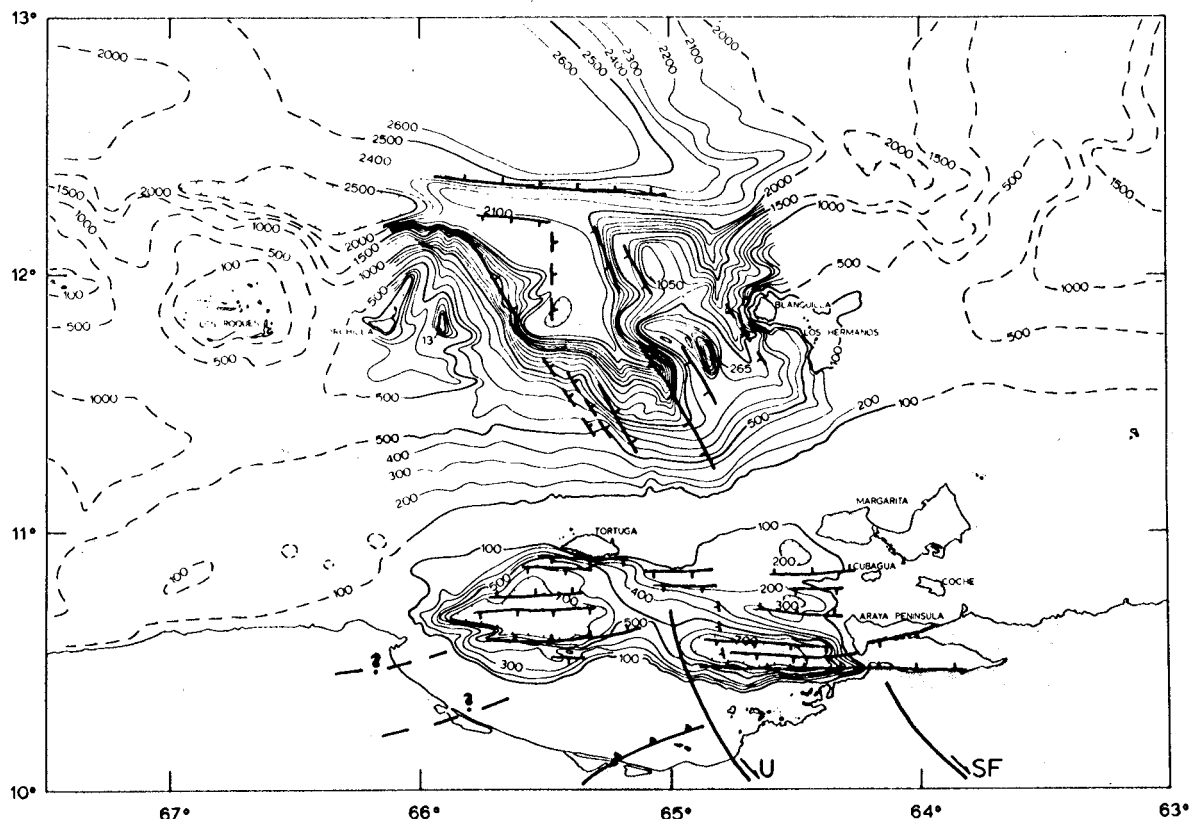


Figure 38. Principal faults of the Venezuelan continental margin in the study area.

ing was suggested not only for the Cubagua high but also for the Araya block because of the apparent southward dip of the overlying sediments (Ball et al., 1971).

The 80 γ magnetic anomaly associated with the Cubagua high may be related to this proposed basement fault block. The wavelength of this anomaly is similar to that of the Araya block, suggesting same depth to source, but its smaller amplitude indicates a much weaker magnetic material, possibly one that consists of metamorphic rather than basic igneous rocks.

Although numerous faults occur on the shelf directly south of the Tortuga-Margarita Bank, none of those in Profile 5 can be correlated with certainty with faults on Profile 7 (fig. 8). Also, with the exception of the faults at 10°47'N and 10°50'N, the faults on Profile 5 cannot be correlated with those on Profile 3; however, the character of the reflectors is very similar in each profile in this area of the shelf and closely resemble the reflectors around the Cubagua high. It is suggested, therefore, that these massive stratified sediments represent a Late Tertiary sequence, similar to that drilled on Cubagua Island (Kugler, 1957).

The resemblance of the reflective characteristics and faulting of the sediments on the gentle slope south of the Tortuga-Margarita Bank (Profile 3, fig. 8) and in the northern half of the western deep of the Cariaco Basin (Profile 2, fig. 8) is also striking. The writer concurs with the interpretation of Maloney and Macsotay (1967) that the relatively steep submarine slope south and southwest of Tortuga is a faultscarp and proposes that along this fault part of the former shelf of this area has been subsided. This former shelf now underlies the northern half of the western deep of the Cariaco Basin and is responsible for its anomalous width.

The southern edge of the down-faulted shelf is underlain by a basement ridge at 10°43'N that extends westward from Profile 2 (fig. 8) to just north of Cabo Codera. This ridge probably consists of igneous rocks and is outlined by the +100 γ isogama line over the western deep and a +300 γ magnetic anomaly north of Cabo Codera (fig. 29). The suggested down-faulting of the shelf is supported by the reduced amplitude and broadened wavelength of the magnetic anomalies associated with the igneous ridge.

South of the subsided shelf lies the main graben of the western deep of the Cariaco Basin (Profile 2, fig. 8). The rocks that form the southern slope of the western deep between 10°32'N and its boundary fault (10°37'N), characterized by incoherent internal reflectors, may represent the eastward extension of more competent sedimentary or metamorphic rocks, possibly associated with the Villa de Cura belt. These rocks probably extend farther eastward to Profile 3 (fig. 8), where they abut the massive stratified sediments of the slope of the Tortuga-Margarita Bank at 10°37'N.

Direct interpretation of the seismic reflection data in terms of the geology of the western Caribbean mountains is difficult because the most useful aides in correlation, the known fault trends separating the major tectonic elements, cannot be traced from the continent into the shelf. With the aid of gravity and magnetic data, however, it is pos-

sible to suggest that certain elements of the major tectonic belts (Bell, 1967, fig. 34) do extend eastward into the Bay of Barcelona.

The best example is a -38 mgal Bouguer anomaly minimum (outlined by the -20 mgal isogal in fig. 31) southwest of the central sill of the Cariaco Basin. As this gravity minimum coincides with the projected trend of the Foothills belt (Bell, 1967, fig. 34), the writer suggests that it represents the extension of the thick Tertiary sedimentary sequence of the Foothills belt into the Bay of Barcelona. The lack of magnetic anomalies in this area also supports such an interpretation.

North of the Foothills belt the metavolcanic sequence of the Villa de Cura belt contains rocks with higher magnetization and susceptibility. The gentle northward increase of the regional magnetic anomaly west of 65°W could be related to this magnetic property of the underlying rocks. The magnetic data, and the small negative Bouguer anomaly values are consistent with an interpretation suggesting the seaward extension of the Villa de Cura belt. Short-wavelength magnetic anomalies that might be expected over the small flows and intrusions associated with the Villa de Cura sequence are probably not seen because of the burial of these rocks below the sea floor (rocks tentatively identified on the seismic profiles as metamorphics outcrop on the southern wall of the sill and the western deep below 750 m), although the small undulations of the 50 γ isogamma line could be related to them.

4.2 Island Platforms - Los Roques Canyon

4.2.1 Regional Geology

The Orchilla and the Blanquilla platforms, separated by the Los Roques Canyon, are the two eastern members of a series of island platforms located north of Venezuela between the continental shelf and the Venezuelan Basin. The geologic framework of the islands is similar in many respects: The oldest rocks dated are Cretaceous intrusives of intermediate composition which are associated with volcanic or metamorphic rocks, and overlain commonly by limestones of Quaternary age (Lagaay, 1969; Rutten, 1939, 1940).

The variety of igneous intrusive rocks which comprise these offshore platforms is illustrated by the reconnaissance of Orchilla by Schubert (1970), who found quartz-diorites associated with quartz-mica schists and diabase on the extreme northwestern edge of the island of Orchilla (fig. 39) and amphibole-schists, intruded by granite-gneiss, on the eastern part. In the central part of Orchilla an ultrabasic complex consisting of serpentinized gabbros and possibly peridotites was mapped. This igneous-metamorphic complex is covered by Quaternary sediments, among them numerous reefs elevated to 3-4 m (Schubert, 1970).

The oldest known rocks on the Blanquilla Island are the hornblende-quartz-diorites and biotite granodiorites of the Garanton Stock (Maloney, 1968), exposed near the western and southern margin of the island (fig. 40). Rutten (1931), Zuloaga (1953), Maloney (1968), and Schubert (1969a) described hornblende dioritic-gabbro, granitic pegmatite, diorite-hornblendite, amphibole-gneiss, schists and quartzites on the island of the Los Hermanos.

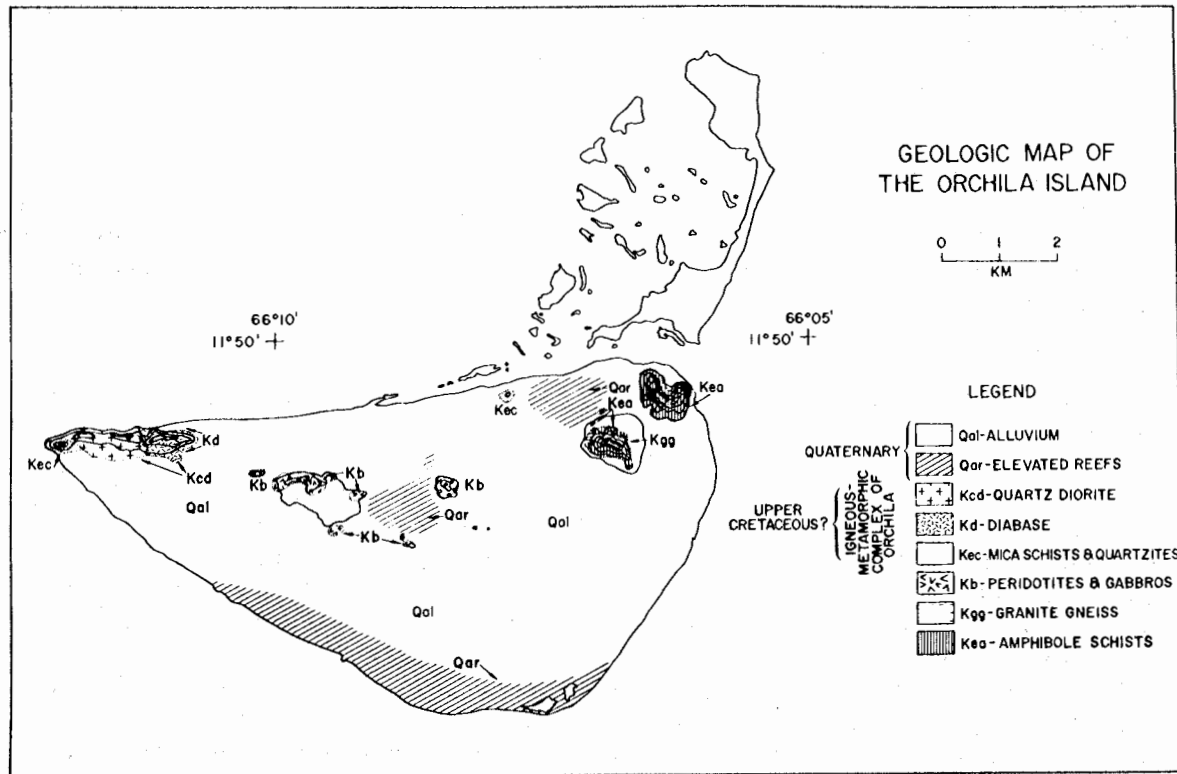


Figure 39. Geologic map of Orchilla Island (from Schubert, 1970).

On the basis of the similarity of the Garanton Stock and the quartz-diorites of Aruba, Rutten (1931) suggested that they are probably of the same age. Isotopic age determinations (Rb-Sr and K-Ar) made on the biotites of the quartz-diorites of Aruba gave 73 ± 3 m.y. for the formation of these rocks (Priem, et al., 1966). Whole-rock K-Ar age determinations on similar rocks in Curacao gave 72 ± 7 m.y. (Priem, 1967).

The central and eastern part of Blanquilla Island is covered by coralline limestones of Pleistocene and Recent age (Maloney, 1968). Based on the elevations of terraces in the southwestern part of Blanquilla Island and on their dip towards the northeast, Maloney (1968) suggested that the island was tilted to the northeast in the Pleistocene.

Although faults or folds were not reported from Blanquilla Island, there are numerous east-west and northwest-southeast trending faults on Los Hermanos islands (Maloney, 1968; Schubert, 1969a).

The writer dredged the talus material off the southwest tip of Blanquilla Island and recovered quartz-diorite, quartz-monzonite, meta-basalt, and marble. Another dredge haul from the western slope of the seamount southwest of Blanquilla Island ($11^{\circ}41'N$, $64^{\circ}54'W$) yielded graphic granite, amphibole-biotite granite, quartz-diorite, and granodiorite. An age of 81 m.y. was determined by K-Ar measurements on the

biotite of the granite (see Appendix III), which is in close agreement with the age of the other batholithic rocks of the island chain.

4.2.2 Discussion

An acoustic basement and a "granitic" basement have been tentatively identified in the presentation of the seismic reflection profiles of the Orchilla and Blanquilla platforms. Reflectors that characterize the acoustic basement were observed in many places on the island platforms below the well stratified and the acoustically transparent sediments. These reflectors appear to crop out also on the northern slope of the platforms and on the walls of the Los Roques Canyon. On the other hand, reflectors that were interpreted to represent the "granitic" basement appear to be restricted to individual dome-shaped structures on both platforms.

The identification of the dome-shaped structures as "granitic" basement is supported by the following data: (1) The outcrop of one such structure sampled on the Blanquilla platform yielded granitic rocks; (2) "granitic" plutons are known to exist on the adjacent islands; and (3) magnetic anomalies are generally restricted to those parts of the platforms where these structures are present (fig. 27).

The writer, therefore, suggests that not only the islands but also the submerged parts of the Orchilla and Blanquilla platforms are underlain by "granitic" intrusives of Upper Cretaceous age. The irregular acoustic basement probably represents the older, more competent sedimentary rocks that were affected by the emplacement of the igneous intrusions. The subdued surface of the acoustic basement and the plutonic rocks penetrating through it suggest that a major uplift and subaerial erosion followed the emplacement of the plutons. The massive stratified sediment overlying the acoustic basement and the plutonic rocks probably represent Late Tertiary sediments deposited after the subsidence of the platforms.

It has been shown on the seismic reflection profiles that the Los Roques Canyon, which separates the Orchilla and Blanquilla platforms, is a major graben whose bordering faults are still active. These faults strike northwest-southeast (fig. 38), the same as the principal cross-faults of the Caribbean mountain system to the south. The canyon is the only major structure that intersects the Aruba-Orchilla-Blanquilla island chain; that it is also located at the seaward extension of the most significant discontinuity of the Caribbean mountain system, the abrupt termination of the eastern Serrania del Interior along the Urica fault, suggests that its formation may be genetically related to this discontinuity.

Seismic Profiles 10 and 12 (fig. 22) and the residual Bouguer anomalies (fig. 41) indicate that the main graben of the canyon lies east of $65^{\circ}30'W$. The smooth floor of the canyon west of $65^{\circ}30'W$ is underlain by the downfaulted acoustic basement of the Orchilla platform.

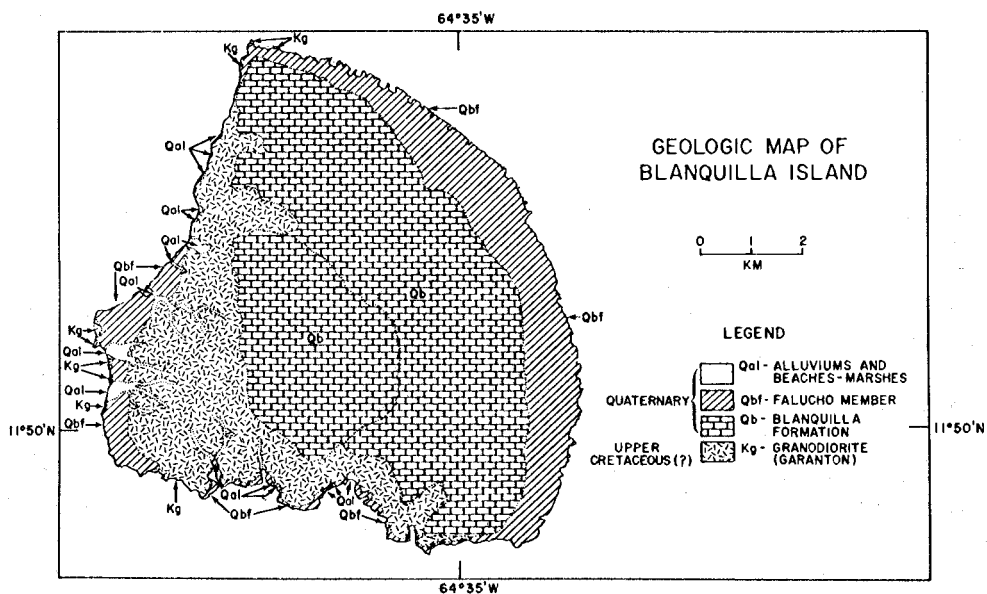


Figure 40. Geologic map of Blanquilla Island (after Maloney, 1968, and Schubert, 1969b).

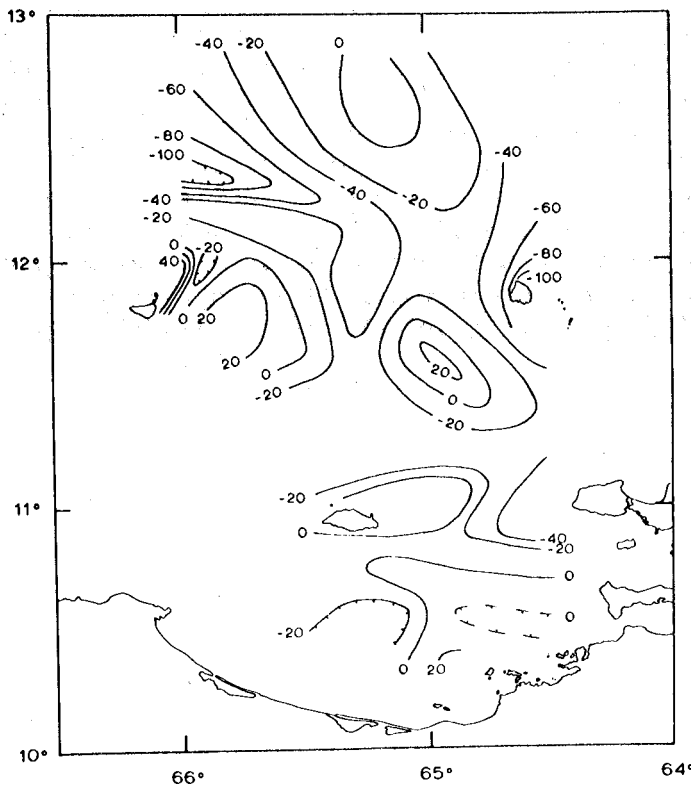


Figure 41. Residual Bouguer anomaly map of study area. Contour interval 20 mgals. Regional field removed from the Bouguer anomaly map (fig. 31) is shown on figure 32.

In the southern part of the Los Roques Canyon there are two narrow "V" shaped valleys within the main depression of the canyon. The lack of the well stratified Late Tertiary to Recent (?) sediments in this area suggests that erosional processes are currently active here. To the north, the floor of the canyon is flat because of sediment fill. The eastward extension of the Curacao Ridge apparently forms a dam against which the sediments carried down the canyon are ponded and restricted from flowing into the Venezuelan basin. Profile 1 (fig. 18) suggests that the downfaulted base of the Orchilla platform and the extension of the Curacao Ridge merge north of the platform and form a sill between the Los Roques Canyon and Los Roques Trench. This prevented also the sediment flow from the canyon into the trench, until the sediments filled the canyon floor and spilled over the sill.

Erosion and slumping are indicated in the northern part of Blanquilla Canyon (fig. 22), whereas the center part is being filled with sediments (fig. 21) derived from the Blanquilla platform as well as from the area of the head of the canyon.

4.3 Southeast Margin of the Venezuelan Basin

4.3.1 Regional Geology

The general structure and distribution of the sediments in the Caribbean Sea and the identification of the major reflecting horizons have been established through an extensive program of seismic reflection and refraction measurements (Ewing *et al.*, 1967; Edgar, 1968). Ewing *et al.* (1967) identified two prominent reflecting horizons that can be traced throughout most of the Caribbean Sea. The upper horizon was called A", the lower horizon B" because of their similarity to the prominent reflectors of A and B in the Atlantic (J. Ewing *et al.*, 1966), A' and B' in the Pacific Ocean (M. Ewing *et al.*, 1966).

Edgar (1968) noted that on the seismic system used during his survey, horizon A" in the Venezuelan Basin appears as the top reflector of a sequence of two or three closely spaced horizons, and horizon B" as a reflector with coherent, smooth surface, which was the deepest recorded in the basin. An approximately 500 m thick acoustically transparent layer is present above A", which together with a similar layer (approximately 400 m thick) between A" and B" are termed the Carib beds (Ewing *et al.*, 1967; Edgar, 1968).

From coring (Ewing *et al.*, 1967; Edgar, 1968) and deep sea drilling (JOIDES, 1969) A" has been identified as a chert or cherty limestone layer, overlain by Lower Eocene radiolarian ooze. Ewing *et al.* (1967) suggested that A" may represent the Mesozoic-Cenozoic boundary, and extrapolating the sedimentation rate established above A", they inferred that B" could represent the Paleozoic-Mesozoic boundary. The Carib beds were interpreted as pelagic sediments or very fine-layered turbidites, that would appear as acoustically transparent layers on the seismic reflection records.

The Carib beds and A" and B" were observed to dip under a thick sequence of well stratified turbidites on the northern and southern margin of the Venezuelan Basin; to the east these layers conformably overlap the lower flank of Aves Ridge (Ewing *et al.*, 1967).

4.3.2 Discussion

The three seismic reflection profiles (fig. 24) across the south-east margin of the Venezuelan Basin indicate an approximately 700 to 900 m thick sequence of massively stratified, horizontally bedded sediments that are similar to those identified as turbidites on a profile made by Ewing *et al.* (1967) to the west of this area. The turbidite sequence abuts sharply the Curacao Ridge to the south, while to the east it onlaps the lower flank of the Aves Ridge (see Profile 3, fig. 24; Profile 8, fig. 26).

Profile 8 and the northern portion of Profile 3 clearly show that below the turbidites there is an acoustically transparent layer, approximately 600 m (0.6 sec) thick, which is underlain by a prominent sequence of reflectors. The latter consists of a thick (150-200 m), irregular band, characterized by incoherent reflections, underlain by two sharp horizons, approximately 100 m apart. Based on the description of the character and general occurrence of the Carib beds and A" (Ewing *et al.*, 1967; Edgar, 1968), the writer suggests that the acoustically transparent layer below the well stratified sequence corresponds to the upper Carib bed, and the underlying prominent group of reflectors represent A".

Because the western end of Profile 8 joins the northern end of Profile 2 (see figs. 2, 7, and 14), the upper Carib bed and A" can be correlated and extended southward despite an apparent change in character of the seismic record, which is due mostly to the different noise conditions brought about by the new heading of the ship. The broad incoherent upper reflector of A" cannot be distinguished on the profiles of figure 23 because of the background noise of the record; but the acoustically transparent layer and the two sharp lower horizons of A" can be distinguished on Profile 2. The acoustically transparent layer is also evident on Profile 1 and Profile 3, and the reflectors that resemble the lower horizons of A" are present near the contact of the sedimentary sequence with the base of the Curacao Ridge and the Blanquilla platform.

Both Profile 1 and Profile 2 indicate that the eastward extension of the Curacao Ridge contains strongly folded sediments (fig. 24). The well stratified sediments on the top of the Curacao Ridge in Profile 2 suggest that the sediments have been carried directly to the Venezuelan Basin from the Los Roques Canyon before an uplift of the ridge took place. An apparent fault contact between the Curacao Ridge and the sediments of the Los Roques Canyon (Profile 2, fig. 24) and upward arching of A" and the upper Carib bed support the proposed uplift of the ridge.

Both the free-air (fig. 30) and the residual Bouguer (fig. 41) anomaly maps indicate that the major bulk of the sediments of the Curacao Ridge (Edgar, 1968) lies west of $65^{\circ}30'W$. The northward swing of the Bouguer anomaly isogal lines (fig. 31) northwest of Blanquilla may be attributed to the eastward plunge of the mantle under the flank of the Aves Ridge.

4.4 Crustal Structure of the Venezuelan Continental Margin

4.4.1 Evidence from Seismic Refraction Data

Refraction data in the area of the Venezuelan continental margin exhibit a large variation of seismic velocities (Edgar, 1968). Measurements in the Venezuelan Basin indicate a 1.9 km/sec velocity for the sediments above A" and 2.7 km/sec velocity for the sediments between A" and B". The velocity of the turbidites in the Bonaire Basin and elsewhere on the continental margin falls in the 1.9 - 2.1 km/sec range. A layer of sediments with a velocity range of 3.9 - 4.2 km/sec underlies the low velocity sediments of the Venezuelan Basin and forms the bulk of the sediments under the Curacao Ridge (fig. 42). The large negative gravity anomalies could, in large part, be attributed to these sediments on the Curacao Ridge. The presence of 5 km thick, combined low and high velocity sediments north of the Blanquilla platform (Edgar, 1968) can explain the gravity minimum in that area.

In the area of the island platforms the seismic velocities of the rocks underlying the surface sediments range between 5.1 - 5.8 km/sec, which is expected for the "granitic" rocks that were dredged on the Blanquilla platform, and were indicated under the platforms by the magnetic, gravity, and seismic reflection data.

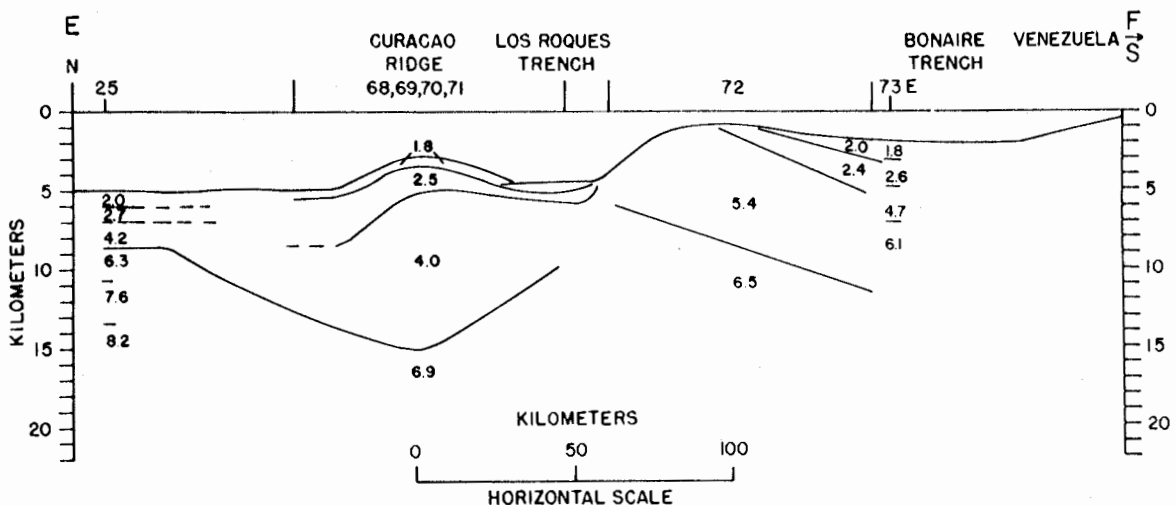


Figure 42. Composite seismic refraction section across the Venezuelan continental margin (from Edgar, 1968).

A velocity of 5.8 km/sec was recorded 1 km below the surface sediments on a refraction profile run directly east of Tortuga Island (Officer *et al.*, 1957). The absence of a major magnetic anomaly over the Tortuga-Margarita Bank does not allow an interpretation that would assign an igneous basement to this seismic velocity 1 km below the surface of the bank. The reflector may indicate a small acidic igneous intrusion, a very competent limestone, or metamorphic rocks.

The crustal velocities under the continental margin range from 6.1 to 6.9 km/sec (fig. 42), while under the Venezuelan Basin there is a two layered crust: The upper crustal layer has an average velocity of 6.3 km/sec, the lower crustal layer, of 7.6 km/sec (Edgar, 1968). A mantle velocity of 8.2 km/sec was measured on a refraction profile run in the southeastern Venezuelan Basin; under the continental margin mantle arrivals were not recorded (Edgar, 1968).

4.4.2 Crustal Thickness of the Venezuelan Continental Margin

A first approximation of the thickness of the crust was made along a section normal to the shoreline by matching a Bouguer anomaly profile with a crust-mantle interface, determined at one end of the section by a seismic refraction line located approximately 170 km northwest of the study area (station 25; fig. 42). The technique follows that of Woppard (1959) and Talwani *et al.* (1959).

For the computation of the crustal section (fig. 43) a two-dimensional Bouguer anomaly profile was used (combined from Profile 1 and Profile 4; fig. 32 and Appendix II). For the area of the seismic section a simple Bouguer anomaly was computed ($\rho_{\text{crust}} = 2.67 \text{ g/cm}^3$) by using an assumed free air anomaly value of -20 mgal (reported as an average for the Venezuelan Basin: Edgar, 1968). The regional Bouguer anomaly was determined by inspection (see dashed line in fig. 43), and was extrapolated along the same gradient northward until it matched the Bouguer anomaly computed for the area of the seismic refraction profile. It is assumed that the crust-mantle interface at the continental margin is a simple dipping surface whose angle of dip can be determined, if the crust-mantle density contrast is known, by computing the gravitational attraction of various mantle surfaces until a match with the regional Bouguer anomaly is obtained. A key assumption of this technique is that no lateral density variations exist either within the crust or the mantle.

The densities used for the computation were determined on the basis of the crustal and mantle velocities determined at the seismic section (Nafe and Drake, 1963), and are shown in figure 43. Alternates are given there also to illustrate the change in mantle depth in response to different crust-mantle density contrasts.

The results indicate that if the assumptions used in the computation are valid then the mantle is at a depth of 28 km under the Tortuga-Margarita Bank and at 37 km under the shoreline (fig. 43).

If it is assumed that the Bouguer anomalies, with the exception of the short-wavelength variations (< 10 km), reflect only the depths of

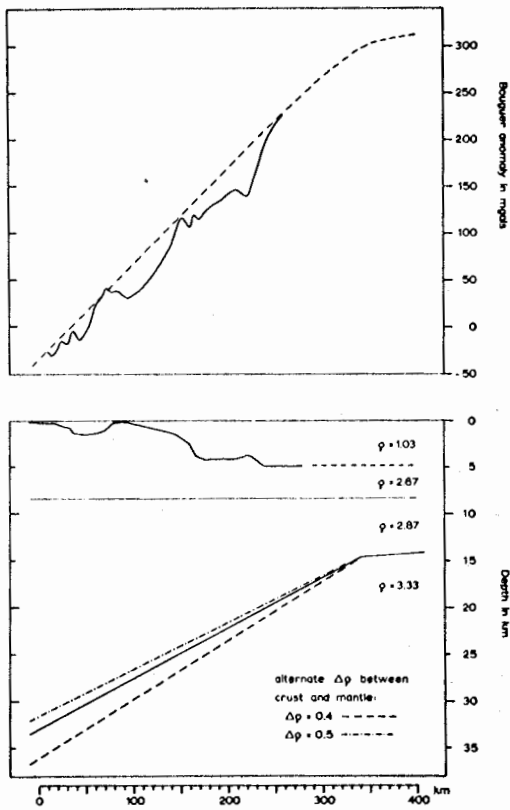


Figure 43. Crustal thickness profile of the Venezuelan continental margin. Upper half: solid line = two-dimensional Bouguer anomaly profile; dashed line = regional Bouguer anomaly profile. Lower half: bathymetric profile and crust-mantle interfaces, as computed using three different density-contrast values.

the mantle without any contribution from crustal and mantle density variations, a contour map can be prepared showing the depth below sea level to the top of the mantle (fig. 44).

Based on the crustal section (fig. 43), the deviation of the Bouguer anomalies (fig. 31) from the regional Bouguer anomalies (fig. 32) can be expressed in terms of depth differences (from fig. 43, a 50 mgal change of the regional Bouguer anomaly equals to a 3 km change in depth).

The mantle surface contours (fig. 44) north of $12^{\circ}30'N$ are in close agreement with those made by Edgar (1968) on the basis of refraction profiles. The sharp northward curve of the depth contours north of Blanquilla Island probably reflects the eastward plunge of the mantle under the flank of the Aves Ridge. The mantle depth below the Blanquilla platform is in agreement with the bathymetric data in that both suggest that the Blanquilla platform is a southwestern extension of the Aves Ridge.

The 2 km depression indicated over the Curacao Ridge (fig. 44), the isolated high east of Tortuga Island, and the low in the western half of the Bay of Barcelona are probably not real, since geophysical measurements suggest that density changes within the crust cause the

Bouguer anomaly variations in these areas. The depression below the Los Roques Trench, on the other hand, is most likely real because the seismic measurements in this area do not indicate low crustal densities that could account for the Bouguer anomalies (Edgar, 1968).

4.5 Tectonic Elements of the Island Arc

The major tectonic elements associated with the southern half of the Lesser Antilles Island Arc are: (1) The Barbados Ridge; (2) the Tobago Trough; (3) the volcanic island arc; (4) the Grenada Trough; and (5) the Aves Ridge (Bunce *et al.*, 1970; Weeks *et al.*, 1971). As each of these features approach the shelf of the South American continent, they become indistinguishable and can be followed only through the geophysical anomalies associated with them.

The Barbados Ridge, the easternmost element of the island arc (see fig. 3), is characterized by a major negative free-air anomaly belt that has been traced southwestward into Trinidad and then into the Eastern Venezuelan Basin (Talwani, 1966; Bush and Bush, 1969; Bassinger *et al.*, 1971).

The southwestward extension of the Tobago Trough is manifested in a shallow depression of the Trinidad-Venezuela shelf and a second belt of negative free-air anomalies. This belt is separated from the negative gravity anomalies of the Barbados Ridge by a weak positive trend associated with the North Tobago anticline (Bassinger *et al.*, 1971; Lattimore *et al.*, 1971).

Lattimore *et al.* (1971) suggest that the Tobago Trough is a graben bounded on the south by the coast-line fault system, that extends westward to at least 63°W. If the depression between the islands of Margarita and Los Testigos, the Carupano Sea Valley (Maloney, 1967), is the westward continuation of this same trend, then the depressions and negative free-air anomalies southwest of Margarita Island and north of the Araya block could represent its westward extension into the study area. The trend ends at 64°40'W where the presence of a cross-fault was suggested on the basis of seismic reflection results.

The volcanic arc of the Lesser Antilles has been traced southwestward from Grenada Island into Los Testigos and Margarita islands through a zone of short-wavelength magnetic anomalies and a positive free-air gravity anomaly belt (Talwani, 1966; Lattimore *et al.*, 1971). The Tortuga-Margarita Bank, characterized by positive free-air and Bouguer gravity anomalies, could represent the westward continuation of this tectonic element across the study area; however, there is a major distinction in that the short-wavelength, high-amplitude magnetic anomalies that seem to characterize this tectonic belt to the east are completely missing from this area.

The lack of the magnetic anomalies may be caused by gradual petrologic changes that might be expected as the island arc crosses from the oceanic crust into the continental crust and becomes an alpine-type mountain system (Hess, 1960a). Such petrologic changes along this

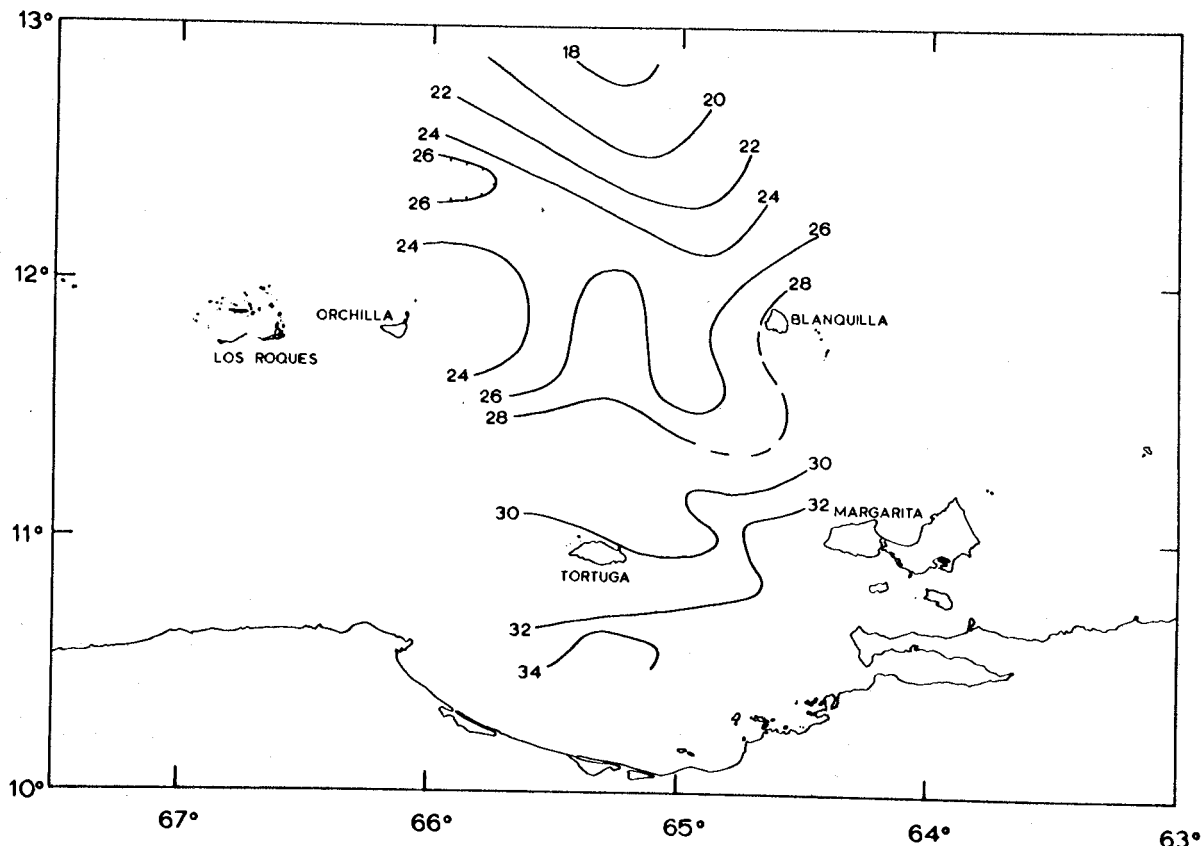


Figure 44. Contour map of the depth below sea level to the top of the mantle. Contour interval 2 km.

tectonic element were noted by Nagle (1971), who, in fact, questions the southwest extension of the volcanic arc on the basis of dissimilarity between the rock types of Grenada (unmetamorphosed Tertiary sediments, basalts, and andesites) and Margarita (highly metamorphosed Jurassic-Cretaceous sediments and intrusives).

Another explanation for the absence of the magnetic anomalies is that the igneous rocks associated with this tectonic belt may have been downfaulted along the numerous northwest-southeast trending cross-faults of the area. The writer proposes that petrologic changes and cross-faulting are both responsible for the different character of this tectonic belt along the Tortuga-Margarita Bank.

The Grenada Trough is characterized by a negative free-air anomaly belt that extends southwestward to the shelf north of Margarita Island. Talwani (1966) extends this belt farther to the southwest and joins it with the -38 mgal low southwest of Margarita. The writer believes that the positive free-air anomalies (up to 40 mgals) measured along the western coastline of Margarita (Ball *et al.*, 1971) suggest an alternative interpretation (fig. 30), namely that the positive free-air anomaly band is uninterrupted between Tortuga and Margarita, although largely reduced in width and amplitude as a result of structural collapses along cross-faults.

The positive free-air anomaly belt of the Aves Ridge extends into the Blanquilla platform where it joins the positive values associated with the Tortuga-Margarita Bank (Talwani, 1966). East of the Blanquilla platform, the large negative free-air anomaly values of the Los Roques Canyon interrupt this belt, but west of the canyon the same belt appears to follow the islands of the Aruba-Orchilla chain (Talwani, 1966; Lagaay, 1969).

4.6 Regional History and Development

4.6.1 Origin of the Caribbean Sea

Any interpretation of the geologic development of the recent continental margin of Venezuela is dependent on the interpretation adopted for the evolution of the entire Caribbean region. Before the advent of the sea floor spreading hypothesis (Hess, 1960b, 1962; Dietz, 1961, 1962) the Caribbean Sea generally was considered to be either a subsided former continental area (Eardley, 1954), or an ancient, relict ocean basin (Schuchert, 1935). Menard (1967) thinks that the development of the Caribbean Sea is typical of small ocean basins in which the oceanic crust is modified as a result of the accumulation of a thick sequence of sediments.

Dietz and Holden (1970) suggest that the Caribbean Sea was formed during the Triassic and Jurassic periods by a mid-oceanic rift system that broke up the universal continent of Pangaea (fig. 45), and carried North America away from Africa and South America.

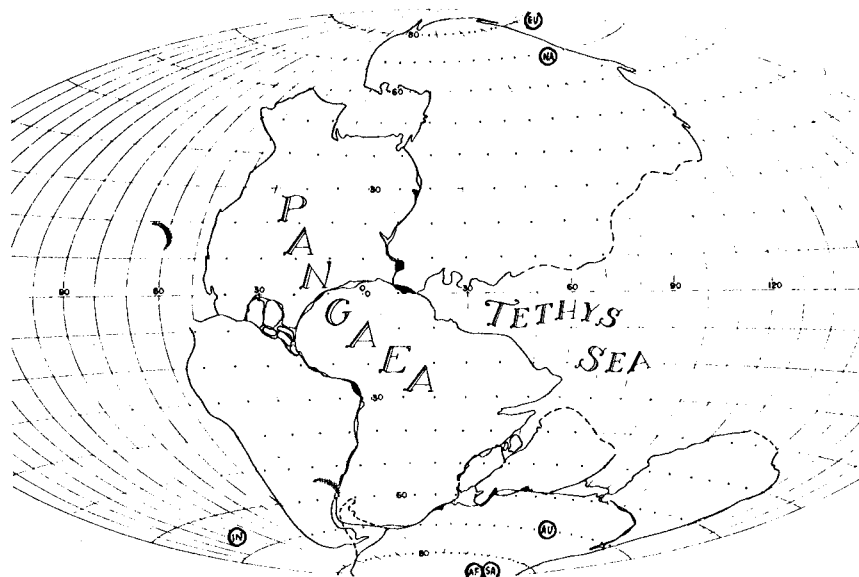


Figure 45. Reconstruction of the universal landmass of Pangaea at the end of Permian, 225 m.y. ago. Cross-hachures indicate the present position of the Lesser Antilles Island Arc at 15°N , 60°W (from Dietz and Holden, 1970).

Carey (1958), Funnel and Smith (1968), and Ball and Harrison (1969) describe the Gulf of Mexico and the Caribbean Sea as an area formed by north-south extension accompanied by east-west shearing.

Based on the wide distribution of the undisturbed B" seismic reflector, which is tentatively dated as Upper Jurassic, Edgar (1968) proposed that the Caribbean Sea must have existed prior to the earliest sea floor spreading episodes. As he believed that sea floor spreading did not commence in the Atlantic until the mid-Mesozoic, he suggested that the Caribbean crust is either a relict primitive oceanic crust or a continental crust that subsided very early in geologic time.

The writer accepts Edgar's (1968) interpretation that the basins of the Caribbean Sea must have formed prior to mid-Mesozoic, but prefers Carey's (1958) explanation that the basins developed between the small continental fragments that were left behind as North America drifted northwestward away from South America in Early Mesozoic time.

Utilizing these concepts of continental drift, knowledge of regional geology, and the results of this investigation, the following brief history is proposed for the development of the continental margin of northeastern Venezuela.

4.6.2 Paleozoic

The reconstruction of the continents into an universal Paleozoic landmass (fig. 45) (Carey, 1958; Bullard *et al.*, 1965; Dietz and Holden, 1970) appears to support the contention of Eardley (1954) and Carey (1958) that the Paleozoic tectonic belt of eastern North America may be continuous with a similar belt in western South America. The oldest known rocks in north-central Venezuela, the Tinaco, Sebastopol, and Peña de Mora gneiss complexes, may represent the easternmost vestiges of this belt, or they may be continuous with the Guayana shield.

In northeastern Venezuela the end of the Paleozoic and the beginning of the Mesozoic was essentially a period of erosion (Bucher, 1952; Mencher, 1963). The initial breakup of the continents probably started in the Permian with the development of depressions and grabens, along which the continents fragmented as the separation intensified.

4.6.3 Mesozoic

The separation of North America from South America, and the breaking off, rotation, and shearing of continental fragments probably continued throughout the Triassic and Lower Jurassic periods (Carey, 1958; Dietz and Holden, 1970). According to the sediment record (Edgar, 1968), the separation of the individual continental fragments must have ceased, allowing the development of uniform conditions for sedimentation within the Caribbean basins by Upper Jurassic.

During Middle and Upper Jurassic times a volcanic island arc developed on the eastern margin of the primordial Caribbean Sea (Fink, 1968), and this ancestral Lesser Antilles Arc probably extended southwestward and westward into the area north of Venezuela. Volcanics and

sediments filled a geosyncline that developed between the South American craton and the volcanic arc during Upper Jurassic and Lower Cretaceous; metamorphism, emplacement of batholiths, and uplift of these rocks occurred during the Upper Cretaceous and Paleocene.

Large scale east-west shearing probably accompanied the separation of the continents along the El Pilar and the coast line fault systems, but the dominant shearing motion most likely stopped during the Upper Cretaceous when the welding of the Caribbean and South American crustal plates took place. This conclusion appears to be supported by the studies of Metz (1968a) along the El Pilar fault by the extension of the tectonic elements of the Lesser Antilles Island Arc into the Venezuelan shelf and by the alignment of the Urica and San Francisco faults with the faults bordering the Los Roques Canyon.

4.6.4 Cenozoic

The Cenozoic was essentially an era of vertical adjustments, which caused folding, thrusting, and large scale erosion and sediment deposition in the area of the continental margin of Venezuela. The elements of the former volcanic arc off the Venezuelan shelf underwent considerable uplift and erosion, and their plutonic core became exposed. Probably in Late Cenozoic, the island platforms started to subside, and to the north the Curacao Ridge was uplifted. Vertical adjustments on the shelf caused the formation of the basins in which there are indications of Recent normal faulting.

The writer does not believe that a major transform fault boundary was active along the southern margin of the Caribbean Sea in the Cenozoic. The relatively few earthquakes along the southern border of the Caribbean Sea with right-lateral motion (Molnar and Sykes, 1969) in comparison to the northern margin may be related to comparatively minor tectonic adjustments; however, if the seismicity gap is only apparent and strike-slip motions are indeed predominate, then one may assume that the South American-Caribbean weld is weakening and may be in the process of breaking up.

5. SUMMARY

(1) The east-west trending tectonic elements of the Venezuelan continental margin are interrupted by a series of northwest-southeast trending faults bordering the Los Roques Canyon and by the seaward extension of the Urica fault.

(2) On the continental shelf, the Urica fault forms the western limit of the competent Lower Cretaceous rocks of the eastern Serranía del Interior, the El Pilar fault, the Araya horst block, and the basins that extend north of the coast line fault system of the eastern Cordillera de la Costa.

(3) Geophysical measurements indicate that west of the Urica fault the Bay of Barcelona is underlain by rocks that probably belong to the seaward extension of the tectonic belts of the western Serrania del Interior.

(4) The Tortuga-Margarita Bank lies along the westward continuation of a positive gravity anomaly belt that is associated with the volcanic island chain of the Lesser Antilles Island Arc. Where the southward extension of the faults along the eastern wall of the Los Roques Canyon intersect the Tortuga-Margarita Bank, the amplitude and the width of the gravity anomalies are reduced, suggesting that the igneous basement rocks are probably down-faulted. The absence of high-amplitude, short-wavelength anomalies over the Tortuga-Margarita Bank also support the proposed down-faulting of the basement, although petrologic changes along this belt could also equally account for the lack of significant magnetic anomalies.

(5) Magnetic and seismic reflection data suggest that the island platforms are underlain by igneous basement rocks. On the basis of the known geology of the islands and the sampling of a basement outcrop, it is suggested that these basement rocks are mostly Upper Cretaceous "granitic" plutons. The K-Ar age determinations on the biotites of one "granitic" sample gave 81 m.y. for the formation of the plutons on the Blanquilla platform.

(6) The Los Roques Canyon appears to be a graben, which is in alignment with two major northwest-southeast trending faults of northeastern Venezuela, the Urica and the San Francisco faults. The northwest-southeast alignment of these faults suggests that they may be related, and that no major strike-slip displacement has occurred along the east-west trending fault systems since Cretaceous time.

(7) The similarity of the reflectors on the southern slope of the Tortuga-Margarita Bank and in the western deep of the Cariaco Basin, together with the numerous faults that appear to offset the sea floor on the continental margin, suggest that Late Tertiary to Recent tectonic activity is responsible for the subsidence of the basins on the shelf, and for the formation of the present topography.

(8) Recent tectonic activity is indicated not only in the area of the shelf but also along the faults of the Los Roques Canyon and the Curacao Ridge. The presence of well-stratified sediments that cover the Curacao Ridge north of the Los Roques Canyon suggest that these may have been carried directly from the canyon into the Venezuelan Basin prior to the uplift of the ridge.

(9) Bouguer anomalies northwest to the Blanquilla platform indicate that the mantle plunges eastward beneath the Aves Ridge. A mantle depth of 32 km is indicated west of Margarita Island and south of

Tortuga Island; a 28 km depth-to-mantle below the Blanquilla platform most likely reflects the influence of the Aves Ridge.

(10) The major tectonic elements of the continental margin of northeast Venezuela were established by the Upper Cretaceous; during the Cenozoic mainly vertical adjustments occurred, which were responsible for folding, thrusting, large scale erosion, and periodic readjustment of the sedimentation pattern.

6. ACKNOWLEDGEMENTS

This publication is based on work done in partial fulfillment of the Doctor of Philosophy degree at The George Washington University, Washington, D.C. I wish to thank my dissertation advisors, Drs. J. W. Pierce and M. M. Ball, for their untiring interest, advice, criticism and encouragement during this investigation.

Special thanks go to Drs. M. M. Ball, F. Nagle, E. Bonatti, and P. Kirch of the Rosenstiel School of Marine and Atmospheric Sciences, University of Miami, for their help in the preparation and identification of the thin sections, and for making available to the author their extensive bibliography on Caribbean geology, among them several yet unpublished manuscripts.

Unpublished maps and manuscripts were received also from Dr. C. Schubert of the Instituto Venezolano de Investigaciones Cientificas, which are hereby gratefully acknowledged.

The author is indebted to I. Zietz for providing guidance during part of this investigation, and to G. H. Keller, R. K. Lattimore, H. B. Stewart, and his dissertation advisors for their suggestions and critical review of this manuscript.

The author also wishes to express his gratitude to J. I. Ewing of the Lamont-Doherty Geological Observatory, Columbia University, for providing unpublished seismic reflection data, and to G. Pardo of the Gulf Oil Company for many useful discussions during the field work and for arranging the K-Ar dating of one of the rock samples.

I also wish to thank Drs. G. Teleki and H. B. Stewart for providing the inspiration and encouragement during the past several years, that resulted in this dissertation.

This research was carried out as part of the Caribbean research project of the Marine Geology and Geophysics Laboratory of the NOAA Atlantic Oceanographic and Meteorological Laboratories. The field work was performed on the NOS Ship DISCOVERER, whose officers and crew are gratefully acknowledged for their help and cooperation.

7. REFERENCES

- Aguerrevere, S. E., and G. Zuloago (1937), Observaciones geologicas en la parte central de la Cordillera de la Costa, Venezuela, Bol. de Geol. y Min., 1, p. 3-22.
- Alberding, H. (1957), Application of principles of wrench-fault tectonics of Moody and Hill to northern South America, Geol. Soc. America Bull., 68, p. 785-790.
- Ball, M. M., and C. G. A. Harrison (1969), Origin of the Gulf and Caribbean and implications regarding ocean ridge extension, migration, and shear, Gulf Coast Assoc. Geol. Soc. Trans., 19, p. 287-294.
- Ball, M. M., C. G. A. Harrison, P. R. Supko, W. D. Bock, and N. J. Maloney (1971), Marine geophysical measurements on the southern boundary of the Caribbean Sea, Geol. Soc. America Mem. (in press).
- Bassinger, B. G., R. N. Harbison, and L. A. Weeks (1971), Marine geophysical study northeast of Trinidad-Tobago, Am. Assoc. Petroleum Geologists Bull., 55, p. 1730-1740.
- Bell, J. S. (1967), Geology of the Camatagua area Estado Aragua, Venezuela: unpublished PhD Thesis, Princeton University.
- Bucher, W. H. (1952), Geologic structure and orogenic history of Venezuela, Geol. Soc. America Mem. 49, 113 p.
- Bunce, T. E., J. D. Phillips, R. L. Chase, and C. O. Bowin (1970), The Lesser Antilles Arc and the eastern margin of the Caribbean Sea, in Maxwell A., Editor, The Sea, 4, (in press).
- Bullard, E. C., J. E. Everett, and A. G. Smith (1965), The fit of the continents around the Atlantic, Phil. Royal Soc. Trans., 258, p. 41-51.
- Bush, S. A., and P. A. Bush (1969), Isostatic gravity map of the Eastern Caribbean region, Gulf Coast Assoc. Geol. Soc. Trans., 19, p. 281-285.
- Carey, S. W. (1958), The tectonic approach to continental drift, in Carey, S. W., Editor, Continental Drift, A Symposium, Dept. Geology, Univ. Tasmania, Hobart, Tasmania, Australia, p. 177-355.
- Chase, R. L., and E. T. Bunce (1969), Underthrusting of the eastern margin of the Antilles by the floor of the western Atlantic Ocean and origin of the Barbados Ridge, Jour. Geophys. Research, 74, p. 1413-1420.
- Christensen, R. M. (1961), Geology of the Paria-Araya Peninsula, Northeastern Venezuela, unpublished PhD Thesis, University of Nebraska.
- Dengo, G. (1953), Geology of the Caracas region, Venezuela, Geol. Soc. America Bull., 64, p. 7-40.
- Dietz, R. S. (1961), Continent and ocean basin evolution by spreading of the sea floor, Nature, 190, p. 854-857.
- (1962), Ocean basin evolution by sea floor spreading, in MacDonald, G. A. and H. Kuno, Editors, The crust of the Pacific Basin, Amer. Geophys. Union, Mon. 6, p. 11-12.

- Dietz, R. S., and J. C. Holden (1970), Reconstruction of Pangea: Breakup and dispersion of continents, Permian to Present, Jour. Geophys. Research, 75, p. 4939-4956.
- Eardley, A. J. (1954), Tectonic relations of North and South America, Am. Assoc. Petroleum Geologists Bull., 38, p. 107-773.
- Edgar, N. T. (1968), Seismic refraction and reflection in the Caribbean Sea, unpublished PhD Thesis, Columbia University.
- Ewing, J., J. L. Worzel, M. Ewing, and C. Windisch (1966), Ages of Horizon A and the oldest Atlantic sediments, Science, 154, p. 1125-1132.
- Ewing, J., M. Talwani, M. Ewing, and T. Edgar (1967), Sediments of the Caribbean, Stud. Trop. Oceanography, University of Miami, 5, p. 88-102.
- Ewing, M. J. L. Worzel, and G. L. Shurbet (1957), Gravity observations at sea in U. S. submarines Barracuda, Tusk, Conger, Argonaut and Medregal, Kon. Nederlandsch Geo.-Mijn. Genootschap Ver., Geol. Ser., 18, p. 49-116.
- Ewing, M., T. Saito, J. Ewing, and L. Burckle (1966), Lower Cretaceous sediments from the northwestern Pacific Ocean, Science, 152, p. 751-755.
- Fink, K. L. (1968), Geology of the Guadeloupe region, Lesser Antilles Island Arc, unpublished PhD Thesis, University of Miami.
- Funnel, B. M., and A. G. Smith (1968), Opening of the Atlantic Ocean, Nature, 219, p. 1328-1333.
- Grim, P. J. (1970), Computer program for automatic plotting of bathymetric and magnetic anomaly profiles, ESSA Technical Memorandum, ERLTM-AOML 8, 31 p.
- Hess, H. H. (1960a), Caribbean research project - a progress report, Geol. Soc. America Bull., 71, p. 235-240.
- _____, (1960b), Evolution of ocean basins, unpublished manuscript, ONR contract 1858(10), 38 p.
- _____, (1962), History of ocean basins, in A. E. Engel et al., Editors, Petrologic studies: A volume in honor of A. F. Buddington, Geol. Soc. America, p. 599-620.
- Hess, H. H., and J. C. Maxwell (1953), Caribbean research project, Geol. Soc. America Bull., 64, p. 1-6.
- Heezen, B. C., R. J. Menzies, W. S. Broecker, and M. Ewing (1959), Date of Stagnation of the Cariaco Trench, southeast Caribbean (abs.), Geol. Soc. America Bull., 69, p. 1579.
- Isacks, B., J. Oliver, and L. R. Sykes (1968), Seismology and the New Global Tectonics, Jour. Geophys. Research, 73, p. 5855-5900.
- JOIDES Deep Sea Drilling Project, Leg 3 and Leg 4 (1969), Geotimes, 14, p. 13-16.
- Kugler, H. G. (1957), Contribution to the geology of the islands of Margarita and Cubagua, Venezuela, Geol. Soc. America Bull., 68, p. 555-566.
- Lagaay, R. A. (1969), Geophysical investigations of the Netherlands Leeward Antilles, Verh. Kon. Ned. Akad. Wetensch., Amsterdam, 25, 86 p.

- Lattimore, R. K., L. A. Weeks, and L. W. Mordock (1971), Marine geo-physical reconnaissance of the Paria shelf, Am. Assoc. Petroleum Geologists Bull., 55, p. 1719-1729.
- Le Pichon, X. (1968), Sea floor spreading and continental drift, Jour. Geophys. Research, 73, p. 3661-3697.
- Liddle, R. A. (1946), The geology of Venezuela and Trinidad: 2nd Ed. Paleon. Research Inst., Ithaca, N. Y., 890 p.
- Lidz, L., M. Ball, and W. Charm (1968), Geophysical measurements bearing on the problem of the El Pilar fault in the Northern Venezuelan offshore: Marine Science Bull., 18, p. 545-560.
- Lidz, L., W. B. Charm, M. M. Ball, and S. Valdes (1969), Marine basins off the coast of Venezuela: Marine Science Bull., 19, p. 1-17.
- Maloney, N. J. (1965), Geomorphology of the central coast of Venezuela: Bol. Inst. Oceanog., Univ. Oriente, 4, p. 246-265.
- _____, (1966), Geomorphology of continental margin of Venezuela Part I Cariaco Basin, Bol. Inst. Oceanog., Univ. Oriente, 5, p. 38-53.
- _____, (1967), Geomorphology of the continental margin of Venezuela Part II Continental terrace off Carupano, Bol. Inst. Oceanog., Univ. Oriente, 6, p. 147-155.
- _____, (1968), Geology of La Blanquilla Island with notes on Los Hermanos islands, Preprint, Fifth Carib. Geol. Conf., St. Thomas, 12 p.
- Maloney, N. J., and O. Macsotay (1967), Geology of La Tortuga Island, Venezuela, Assoc. Ven. Geol. Min. y Petroleo, Bol. Inform., 10, p. 265-285.
- Menard, H. W., (1967), Transitional types of crust under small ocean basins, Jour. Geophys. Research, 72, p. 3061-3073.
- Mencher, E., H. J. Fichter, H. H. Renz, W. E. Wallis, H. H. Renz, J. M. Patterson, and R. E. Robie (1953), Geology of Venezuela and its oil fields, Am. Assoc. Petroleum Geologists Bull., 37, p. 690-777.
- Mencher, E. (1963), Tectonic history of Venezuela, in Childs, O. E., and B. W. Beebe, Editors, Backbone of the Americas, Am. Assoc. Petroleum Geologists Mem. 2, p. 73-87.
- Menendez, A. (1962), Geology of the Tinaco area, northcentral Cojedes Venezuela, unpublished PhD Thesis, Princeton University.
- _____, (1967), Tectonics of the central part of the Western Caribbean Mountains, Venezuela, Stud. Trop. Oceanography, University of Miami, 5, p. 103-130.
- Metz, H. L. (1968a), Geology of the El Pilar fault zone States of Sucre, Venezuela: in Saunders, J. B. Editor, Fourth Carib. Geol. Conf. Trans., Caribbean Printers, Arina, Trinidad and Tobago, p. 293-298.
- _____, (1968b), Stratigraphic and geologic history of extreme north-eastern Serrania del Interior, State of Sucre, Venezuela: ibid., p. 275-292.
- Morgan, B. A. (1967), Geology of the Valencia area Carabobo, Venezuela, unpublished PhD Thesis, Princeton University.
- Morgan, J. W. (1968), Rises, trenches, great faults, and crustal blocks, Jour. Geophys. Research, 73, p. 1959-1982.

- Molnar, P., and L. R. Sykes (1969), Tectonics of the Caribbean and Middle America regions from focal mechanisms and seismicity, Geol. Soc. America Bull., 80, p. 1639-1684.
- Nafe, J. E., and C. L. Drake (1963), Physical properties of sediments, Chapter 29, p. 794-815, in Hill, M. N., Goldbert, E. D., Iselin, C. O'D., and Munk, W. H., Editors, The Sea, 3 - The earth beneath the sea: New York, John Wiley and Sons, Inc., 963 p.
- Nagle, F. (1971), Caribbean geology, 1970: Marine Science Bull., 20, (in press).
- Officer, C. B., J. I. Ewing, R. S. Edwards, and H. R. Johnson (1957), Geophysical investigations in the eastern Caribbean: Venezuelan Basin, Antilles island arc, and Puerto Rico Trench: Geol. Soc. America Bull., 68, p. 359-378.
- Oxburgh, E. R. (1966), Geology and metamorphism of Cretaceous rocks in eastern Carabobo State, Venezuelan Coast Ranges: in Hess, H. H., Editor, Caribbean Geological Investigations, Geol. Soc. America Mem. 98, p. 241-310.
- Piburn, M. D. (1967), Metamorphism and structure of the Villa de Cura group, Northeastern Venezuela, unpublished PhD Thesis, Princeton University.
- Priem, H. N. A., N. A. I. M. Boelrijk, R. H. Verschure, E. H. Hebeda, and R. A. Lagaaay (1966), Isotopic age of the quartz-diorite batholith on the island of Aruba, Netherlands Antilles, Geol. en Mijnb., 45, p. 188-190.
- Priem, H. N. A. (1967), Beknopt verslag over de werkzaamheden in het jaar van september 1966 tot september 1967: Z. W. O. Laboratorium voor isotopgeologie, Amsterdam.
- Rod, E. (1956), Strike-slip faults of northern Venezuela, Am. Assoc. Petroleum Geologists Bull., 40, p. 457-476.
- (1959), West end of Serrania del Interior, Eastern Venezuela, Am. Assoc. Petroleum Geologists Bull., 43, p. 772-789.
- Rod, E., and W. Maync (1954), Revision of Lower Cretaceous stratigraphy of Venezuela, Am. Assoc. Petroleum Geologists Bull., 38, p. 193-260.
- Rutten, L. M. R. (1931), On the rocks from the Venezuelan islands between Bonaire and Trinidad, and on some rocks from northwestern Venezuela, Proc. Kon. Ned. Akad. Wetensch., Amsterdam, 34, p. 1101-1110.
- (1939), The age of the quartz-diorite and granodioritic rocks of the West Indies, Geol. en Mijnb., 1, p. 128-133.
- (1940), New data on the smaller islands North of Venezuela, Proc. Kon. Ned. Akad. Wetensch., Amsterdam, 43, p. 828-841.
- Salvador, A., and R. M. Stainforth (1968), Clues in Venezuela to the geology of Trinidad, and vice versa, in Saunders, J. B., Editor, Fourth Carib. Geol. Conf. Trans. Caribbean Printers, Arina, Trinidad and Tobago, p. 31-40.
- Schubert, C. (1969a), Mapa geologico del Archipielago de Los Hermanos, Dependencias Federales, (map), Minist. de Min. e Hidrocarburos, Caracas.

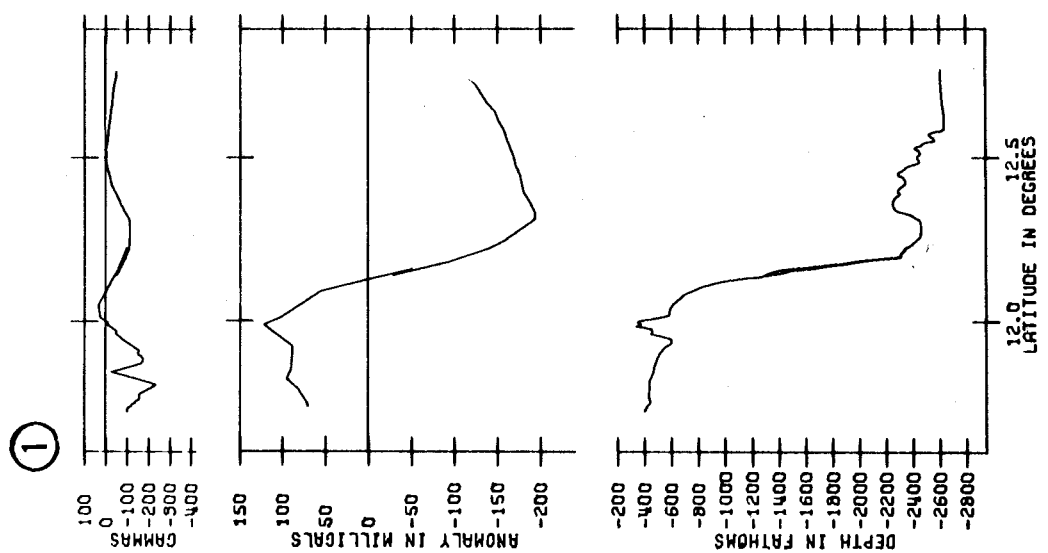
- (1969b), Mapa geologico de la isla La Blanquilla, Dependencias Federales, (map), Minist. de Min. e Hibdrocarburos, Caracas.
- (1970), Geologia de la Isla la Orchilla, Dependencias Federales: (abs.), Acta Cient. Venezolana, 21, p. 55.
- (1971), Geologia de la Peninsula de Araya, Estado, Sucre: Memorias IV Congreso Geologico Venezolano, Caracas, (in press).
- Schuchert, C. (1935), Historical geology of the Antillean - Caribbean region, John Wiley and Sons, Inc., New York, 84 p.
- Shepard, F. P., and K. O. Emery (1941), Submarine topography of the California coast: canyons and tectonic interpretation, Geol. Soc. America, Special Paper 37, 171 p.
- Smith, R. J. (1953), Geology of the Los Teques-Cua region, Venezuela, Geol. Soc. America Bull., 64, p. 41-64.
- Sykes, L. R., and M. Ewing (1965), The seismicity of the Caribbean region, Jour. Geophys. Research, 70, p. 5065-5074.
- Talwani, M. (1966), Gravity anomaly belts in the Caribbean, p. 177, in Poole, W. H., Editor, Continental margins and island arcs, Geol. Sur. Can. Paper 66-15, 486 p.
- Talwani, M., G. H. Sutton, and J. L. Worzel (1959), A crustal section across the Puerto Rico Trench, Jour. Geophys. Research, 64, p. 1545-1555.
- Taylor, G. C. (1960), Geology of the island of Margarita, unpublished PhD Thesis, Princeton University.
- Von der Osten, E. (1955), Geologia de la Bahia Santa Fe (Estado Sucre), Bol. de Geol., Caracas, 3, p. 123-201.
- (1957), Lower Cretaceous Barranquin Formation of northeastern Venezuela, Am. Assoc. Petroleum Geologist Bull., 41, p. 679-708.
- Weeks, L. A., R. K. Lattimore, R. N. Harbison, B. G. Bassinger, and G. F. Merrill (1969), Structural relationships between Lesser Antilles, Venezuela, and Trinidad-Tobago, Gulf Coast Assoc. Geol. Soc. Trans., 19, p. 321
- (1971), Structural relationships between Lesser Antilles, Venezuela, and Trinidad-Tobago, Am. Assoc. Petroleum Geologists Bull., 54, (in press).
- Woollard, G. P. (1959), Crustal structure from gravity and seismic measurements, Jour. Geophys. Research, 64, p. 1521-1544.
- Woollard, G. P., and J. C. Rose (1963), International gravity measurements, George Bantha Co., Inc., Menasha, Wisconsin, 518 p.
- Zuloaga, G. (1953), La Blanquilla y Los Hermanos, Bol. Acad. Cient. Venezolana, 49, p. 1-46.

APPENDIX I

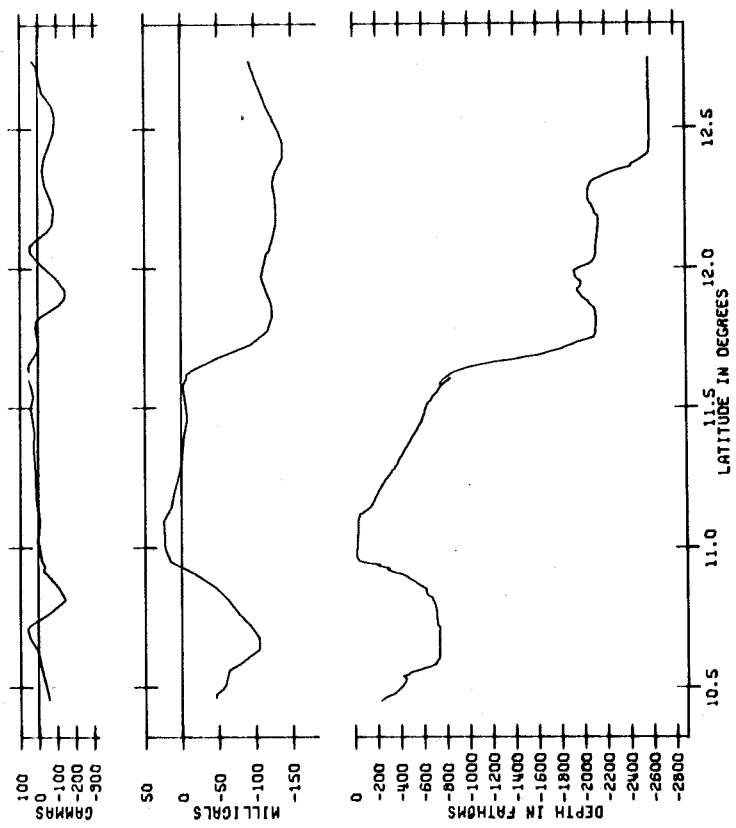
The following pages contain the combined computer plotted profiles of the bathymetry, magnetic anomaly, and gravity free-air anomaly.

These profiles represent the key geophysical survey crossings of the study area. Locations of these profiles are shown in figure 7 and figure 13; these figures are also included here for quick reference. Profile 8 was too short to include as an independent illustration.

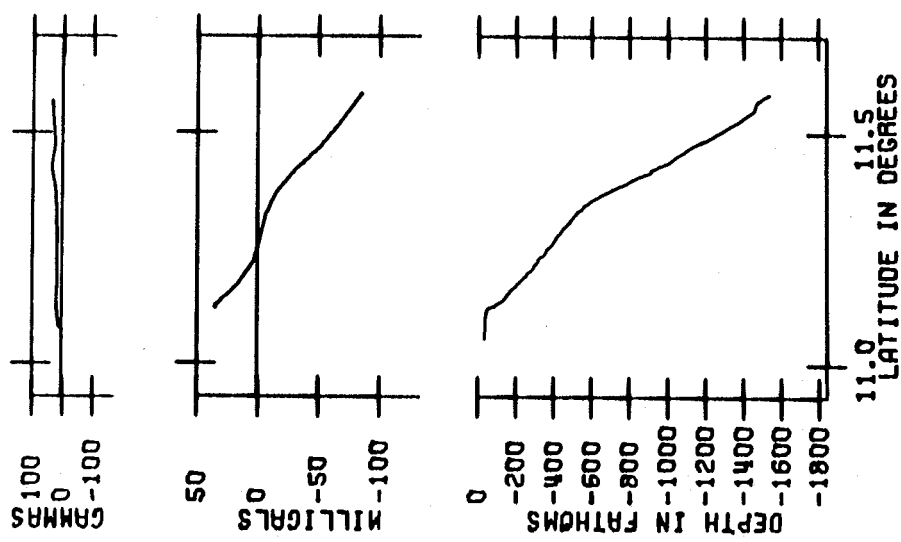
Description of the data and methods used to obtain these profiles are discussed in the Introduction (Bathymetric Survey, Magnetic Survey, Gravity Survey).



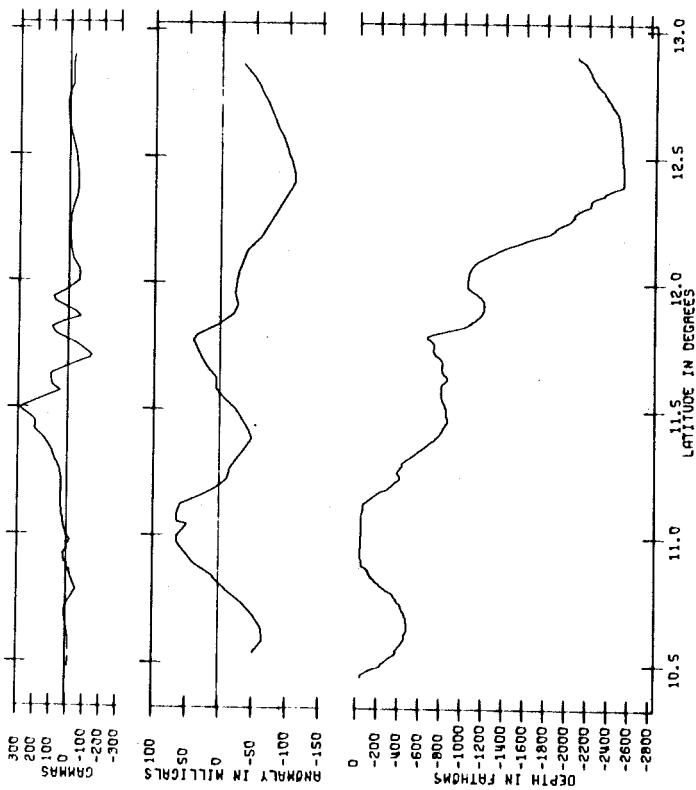
(2)



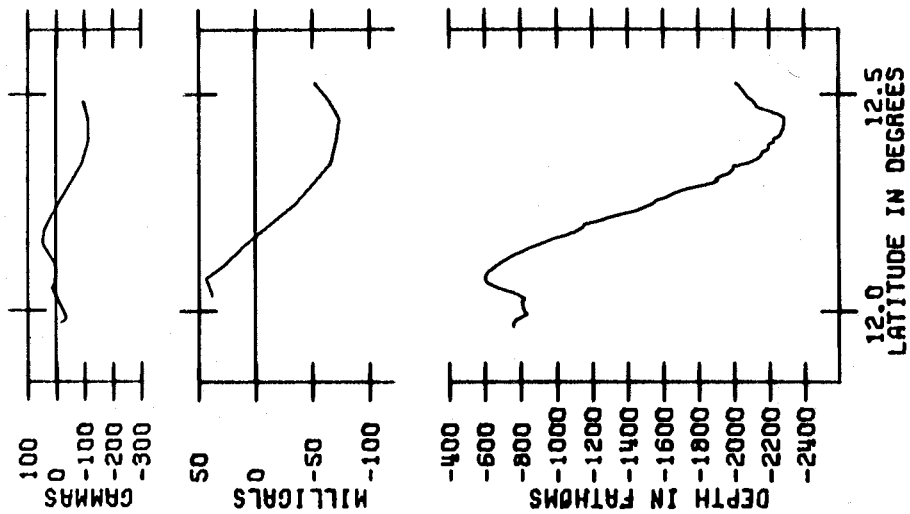
(4)



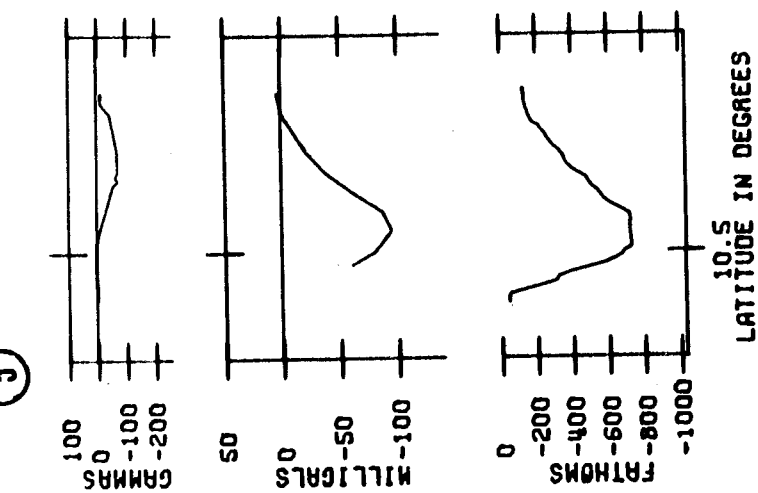
(3)



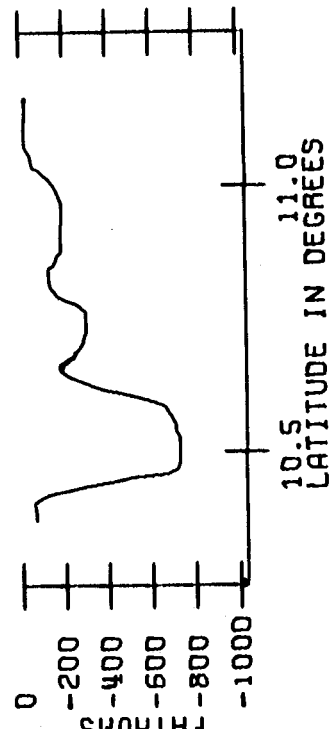
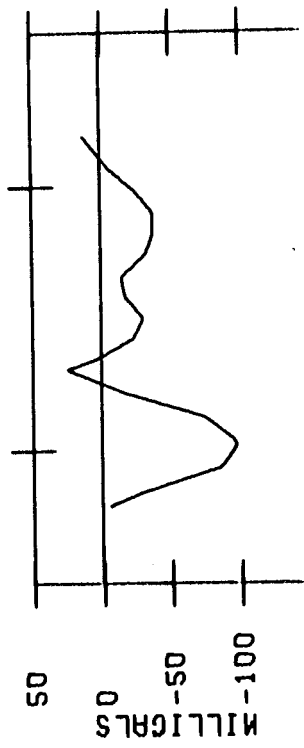
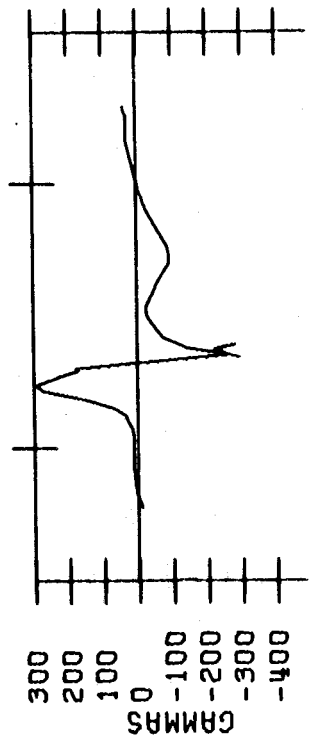
(6)



(5)

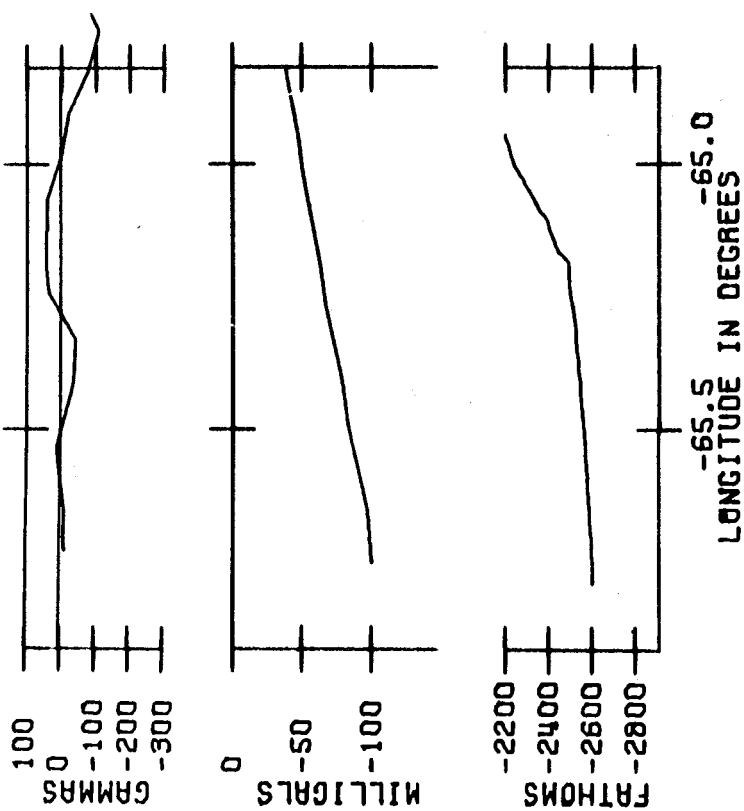


①

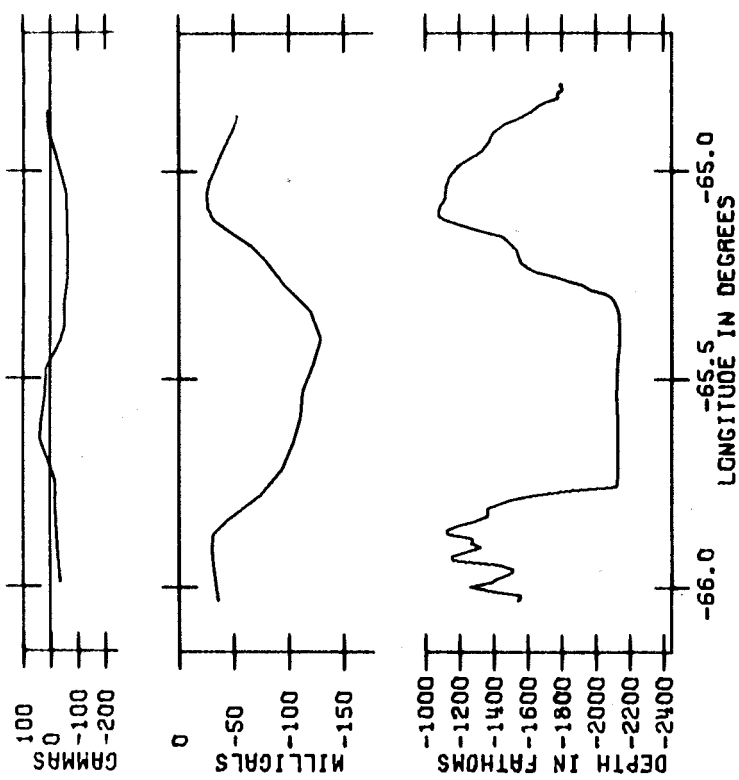


10^5 LATITUDE IN DEGREES

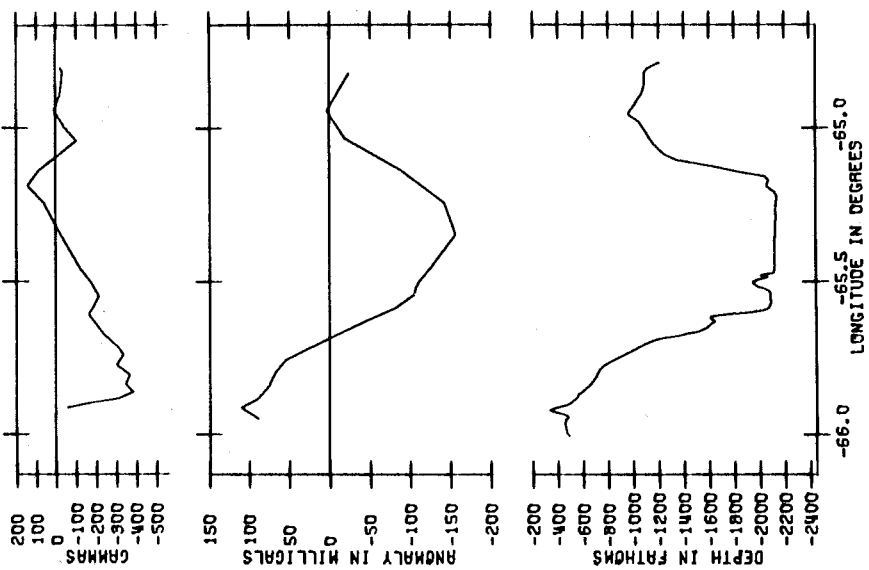
(9)



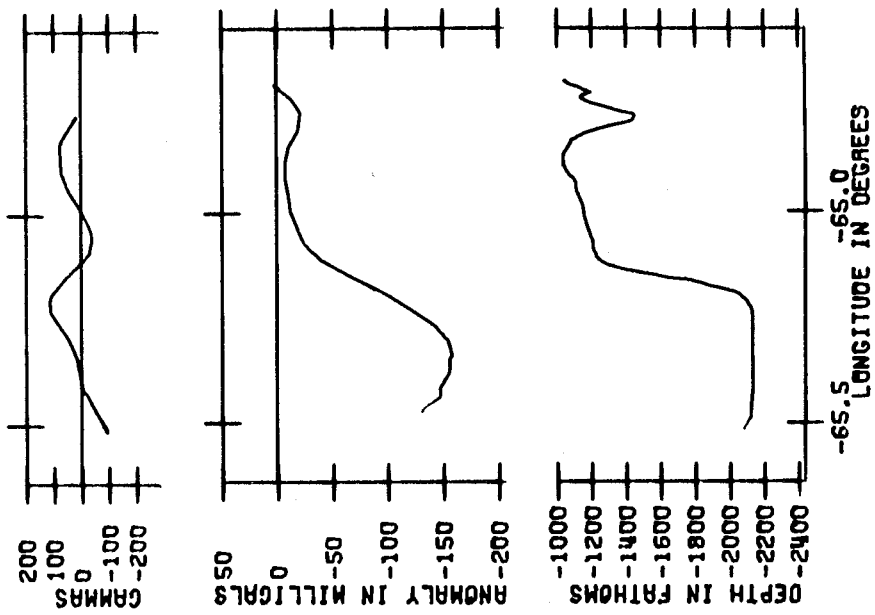
(10)



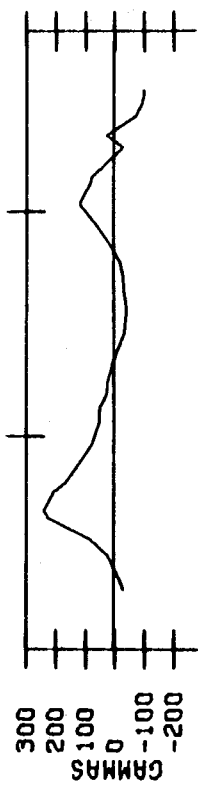
(11)



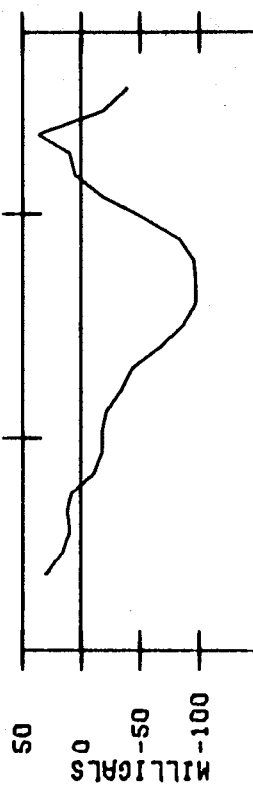
(12)



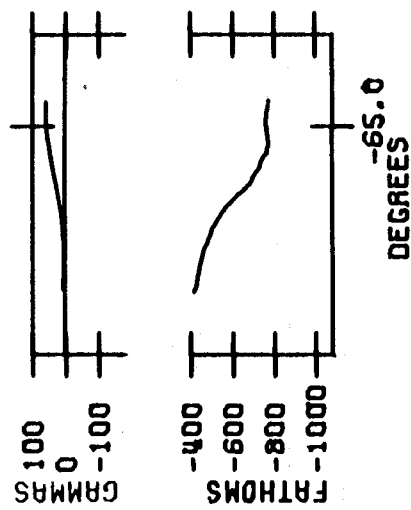
(13)



50



(14)



DEGREES
-65.0

LONGITUDE IN DEGREES
-65.5

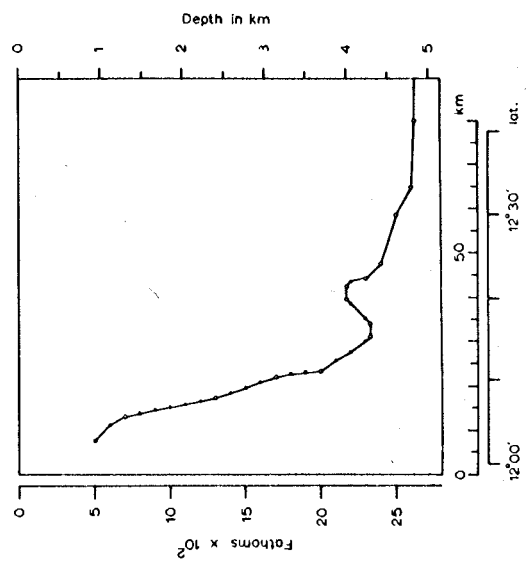
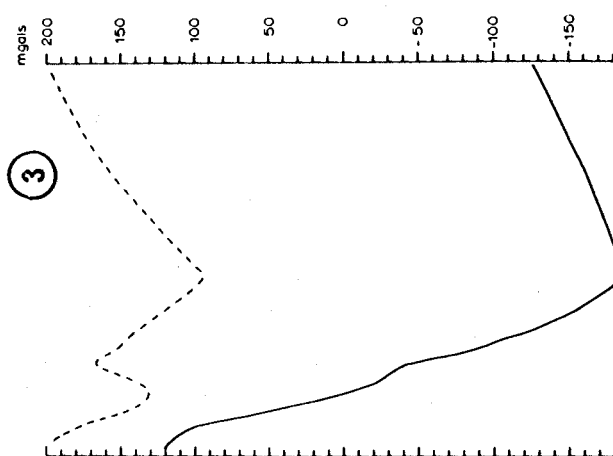
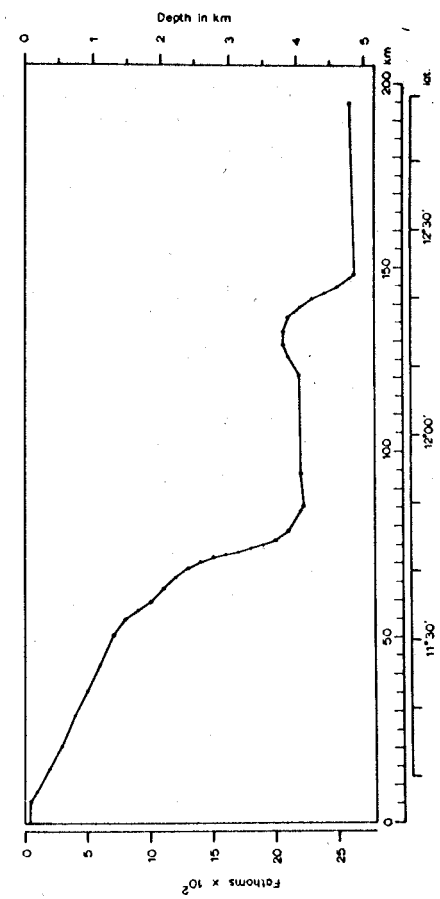
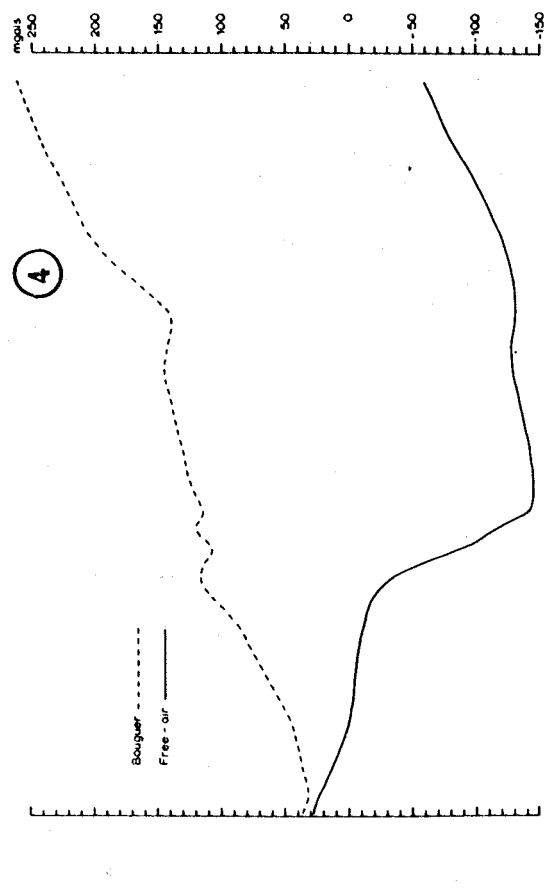
APPENDIX II

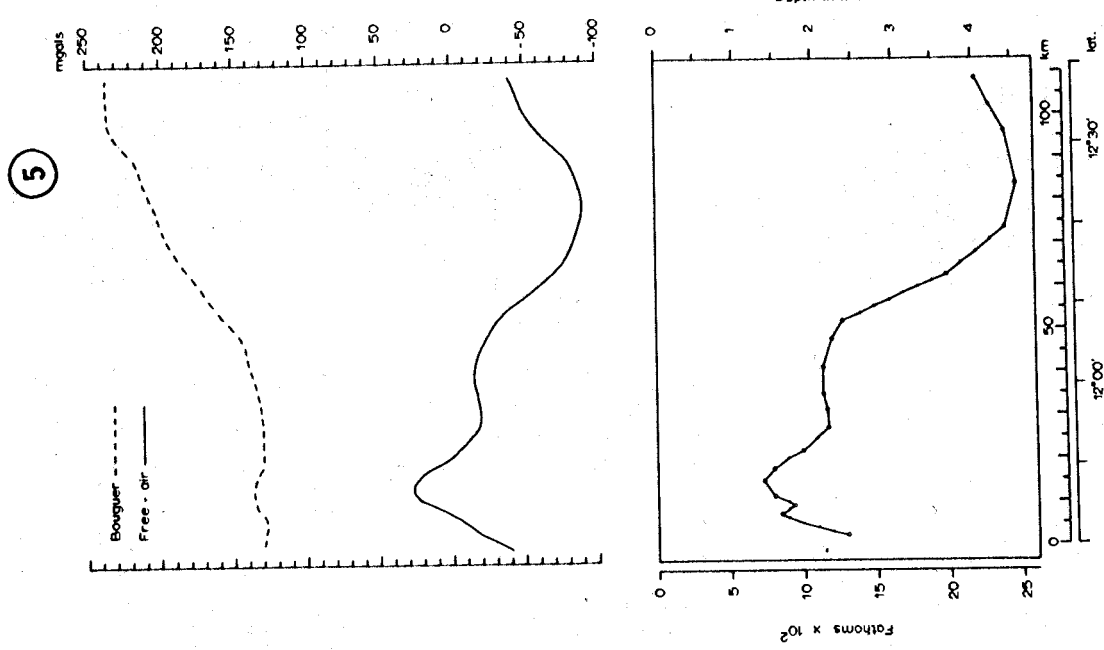
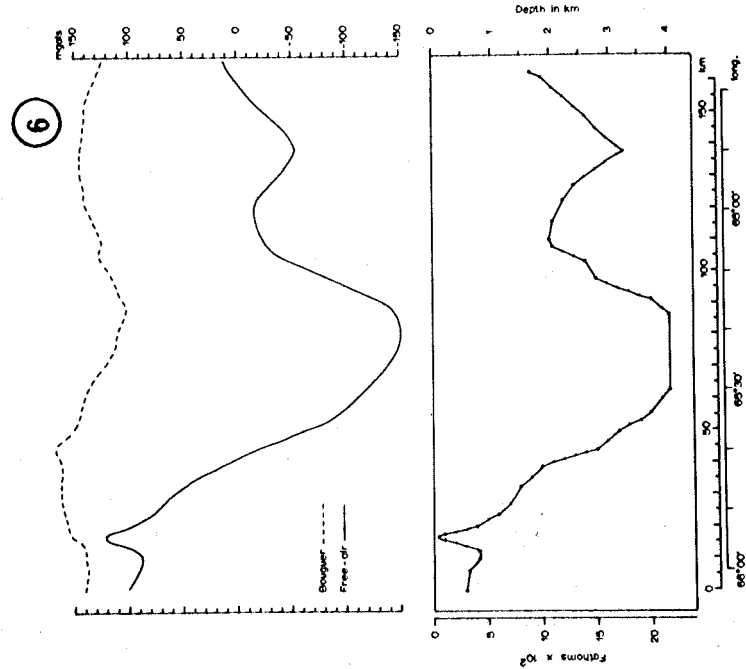
The following pages contain eight two-dimensional Bouguer anomaly profiles used to construct the Bouguer anomaly map, figure 31 in the main part of the text.

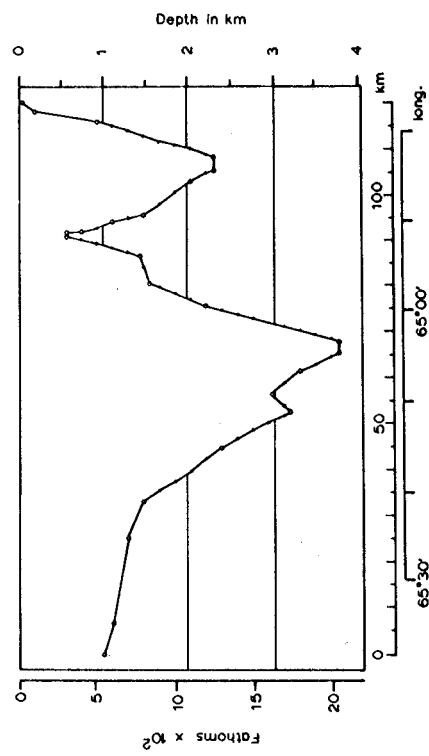
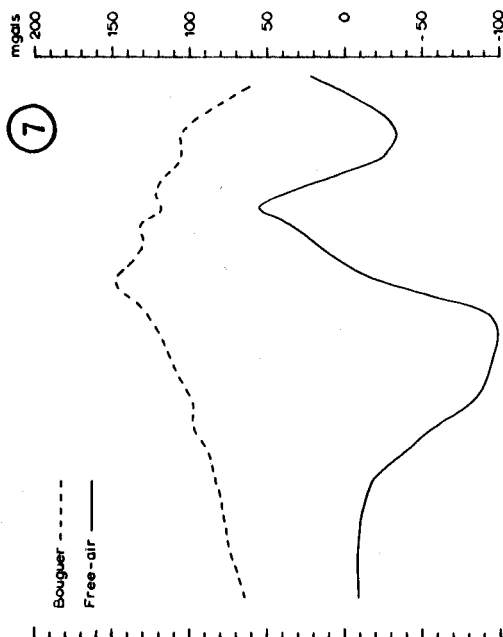
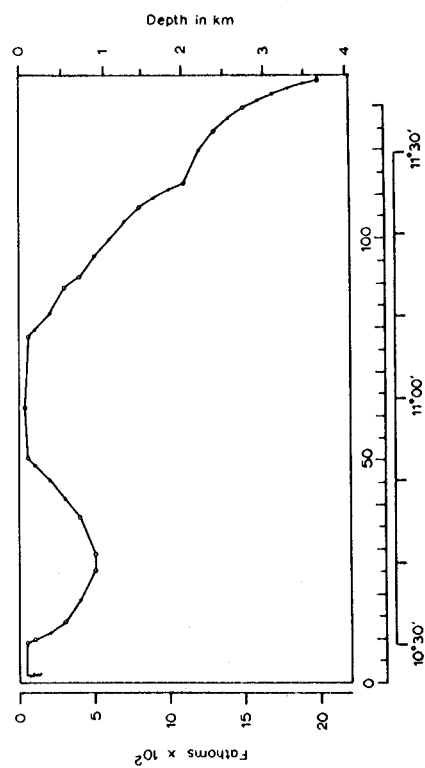
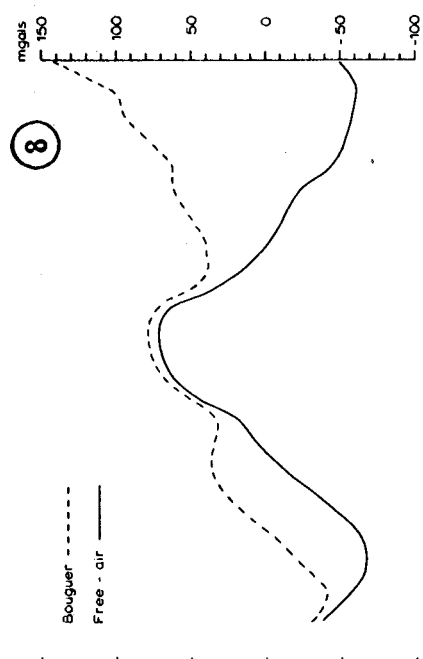
The free-air anomalies are also shown together with Bouguer anomaly profiles to illustrate that the selection of density for the Bouguer correction (2.67 g/cm^3) is essentially correct.

In the lower half of each profile a simplified bottom topography is shown. The large circles represent the major gradient changes in the topography, which were used in the computation of the two-dimensional Bouguer correction.

Locations of the profiles are shown in figure 32, but included here also for quick reference. The discussion of the methods used is contained in the section: GEOPHYSICAL OBSERVATIONS, Gravity measurements.







APPENDIX III

The location and description of the rocks recovered in the two successful dredge-hauls on the Blanquilla platform follow (Microscopic description is summarized from P. Kirch):

Dredge No. 1

Location: $11^{\circ}00.7'N$, $64^{\circ}41.6'W$, of the southwest tip of Blanquilla Island. The rocks were recovered from the lower slope of the island.

Depth: Approximate depth between 700 and 500 fm.

Field description: The dredge brought up about 10 lbs of mostly cobble-size (15 cm x 10 cm x 5 cm) rocks, apparently from the talus material covering the slope. Most of the rocks we were deeply weathered, but the larger pieces had fresh interiors.

The samples were divided into four types of rocks:

- 1) medium to fine grained, light grey, intrusive rock, with some indication of parallelism among the mafic minerals;
- 2) medium grained, dark grey intrusive rocks;
- 3) fine grained, dark grey, massive effusive or metamorphic rock; some samples porphyritic, and contain light green alteration (?) zones;
- 4) Microcrystalline limestone or marble.

Microscopic description:

Dredge # 1/1

Quartz diorite

Quartz, 2-5 mm, 10%,
undulatory extinction in most grains;
K-spar, .5-2 mm, 30%,
poorly defined zoning, minor sericitization along fractures;
Plagioclase, An(variable), .5-2 mm, 55%(?),
zoned xls perhaps as high as An₈₅? in centers
and An₃₀₋₄₅ on rims;
Hornblende, 1-3 mm, 1/2 - 1%,
random distribution;
Biotite, 1-3 mm, 2%,
sub-parallel alignment, contains small inclusions
of apatite;

Opaque, 1/2-2 mm, 1/2-1%,
contains small inclusions of apatite.

Dredge # 1/2

Quartz monzonite

Quartz, 1-2 mm, 5% or less;
K-spar, 1-3 mm, 45%,
untwinned, partially sericitized;
Plagioclase, An , 1-2 mm, 45%,
continuous, normal zoning, interiors (calcic) are
more altered than rims, extensive alteration
along cleavages and fractures.
Hornblend, 1-4 mm, 4-5%;
Biotite, 1-3 mm, 1%,
abundant apatite inclusions;
Sphene, .5-1 mm, <1%,
associated with mafics in clots;
Opaque, .5-1 mm, 1%;
Chlorite, .5-1 mm, <1%,
as alteration along fractures in hornblende, and
alteration from biotite.

Dredge # 1/3

Meta-basalt

Plagioclase, An , 40-45%,
(?)
normally zoned, centers almost completely altered
to clays, Epidotized in places;
Amphibole (?), 40%,
intermediate birefringence, fibrous, pleochroism
green - colorless;
Epidote, in aggregates, varies in samples 3-20%,
occurs in veins, no relict mineral is seen to
produce the Epidote;
Opaque, variable up to 10%.

Dredge # 1/4

Marble

Calcite, .1-.5 mm, 99.5%,
irregular shape, random orientation, complete
lack of twinning, possible serpentine inclusions.

Dredge No. 2

Location: $11^{\circ}41.5'N$, $64^{\circ}53.8'W$, from the western slope of a ridge southwest of Blanquilla Island.

Depth: Approximate depth between 600 and 400 fm.

Field description: The dredge brought up approximately 150 lbs of rock. Most of the rocks were of large cobble size (30 cm x 20 cm x 15 cm), with one boulder size rock (90 cm x 40 cm x 25 cm). Many of the smaller rocks were weathered talus material, but the boulder was freshly broken off the slope.

The samples were divided into three types of rocks:

- 1) very coarse grained (pegmatitic), light brown intrusive rock;
- 2) medium grained, orange yellow, intrusive rock;
- 3) medium grained, light grey, intrusive rock.

Microscopic description:

Dredge # 2/1

Graphic granite

Quartz, 1/2-3 mm, 25%,
random distribution, local patches of quartz
intergrown with microcline;
Microcline, 5-30 mm, 74%;
Opaque, .5 mm, 1%,
Chlorite, trace;
Muscovite, trace.

Dredge # 2/2

Quartz diorite (highly altered)

Quartz, 1-3 mm, 15%,
random, highly fractured;
K-spar, 3-4 mm, 10%(?),
highly sericitized and fractured;
Plagioclase, An₃₀(?), 1-6 mm, 60-70%,
deformed (curved) twin planes, highly fractured,
very intense sausseritization, extensively
epidotized;
Epidote, 1-2 mm, 4%,
in vein fillings and cross-cutting through
plagioclase;

Chlorite (?), 1-2 mm, 1-2%;
Apatite, .5-1 mm, <1%,
associated with mafics;
Opaque, 2-3 mm, 1%,
fractured and altered to chlorite (?);
Sphene, .5 mm, trace,
associated with mafics.

Dredge # 2/3

Granodiorite

Quartz, 1-3 mm, 20-30%;
K-spar, 1-3 mm, 20-30%,
untwinned, undulatory extinction;
Plagioclase, An₍₃₀₋₄₀₎, 1-4 mm, 40-50%,
multiple normal zoning;
Hornblende, 1-4 mm, 1-2%,
small apatite inclusions;
Biotite, .5-2 mm, 1-2%,
small apatite inclusions;
Sphene, .5-1 mm, <1%;
Magnetite, .2 mm, <1/2%.

Dredge No. 2, Sample 2/3 was sent for age determination (courtesy of G. Pardo).

Petrographic description:

The rock sample is a medium grained, unaltered granite, with a following mineral composition:

Plagioclase, fresh crystals to 3 mm dia.; 40%;
Orthoclase, irregular fresh crystals to 3 mm dia.;
some zoning; 30%;
Quartz, very irregular patches to 3 mm dia.; 20%;
Hornblende, elongate crystals to 3 mm in length; partly altered to
chlorite; 5%;
Biotite, associated with hornblende; to 3 mm dia.; 5%.

Tabulation of data pertinent to geochronometry:

A 30 - 50 mesh biotite separate was used for the K-Ar age determinations.

Potassium content = 7.29%;

Radiogenic Argon content = 3.981×10^{-8} g/gram biotite;

Radiogenic character of extracted argon gas = 69.4%;

$\text{Ar}^{40}/\text{K}^{40} = 4.45 \times 10^3$; Age = 81×10^6 years.